Available online at www.sciencedirect.com
SCIENCE DIRECT®
Coordination Chemistry Reviews 243 (2003) 143–190
COORDINATION CHEMISTRY REVIEWS
www.elsevier.com/locate/ccr

Homo- and hetero-polymetallic exchange coupled metal-oximates

Phalguni Chaudhuri *

Max-Planck-Institut für Strahlenchemie, Stiftstrasse 34-36, D-45470 Mülheim an der Ruhr, Germany

Received 7 June 2002; accepted 24 April 2003

Contents

Abstract

The strategy of using 'metal oximates' building blocks as ligands to synthesize various homo- and hetero-metal paramagnetic complexes is reviewed. The modular approach with 'metal-complexes', in this case 'metal-oximates', as ligands enables the synthesis of symmetrical, asymmetrical, and linear complexes, viz. M_AM_B, $M_AM_BM_A$, $M_AM_BM_BM_A$ (M_A, M_B being two different metal ions). Even the synthesis of asymmetric heterotrinuclear complexes with $M_AM_BM_C$ cores and of $M_A(\mu_3\text{-}O)_2M_B$ butterfly cores has been achieved. This article is focused on such exchange coupled polymetallic, both homo- and hetero-metallic, systems containing the bridging core M–N–O–M′ with an aim to delineate the exchange mechanism through the bridging oximates. The uniqueness of oximates providing diatomic NO-bridging is demonstrated by several series of isostructural complexes with different terminal metal ions like Fe(III), Mn(III), Mn(IV) and Cr(III). Such isostructural series are not available for any other bridging ligands. A qualitative rationale for the trend and nature of exchange interactions between the spin carriers has been provided. This article confirms the essentially σ nature of the exchange interaction transmitted through the diatomic NO-bridging ligand and the applicability of Goodenough–Kanamori rules, in general, to predict the nature of exchange interactions for different heterometal compounds. The π-conjugated system of the oxime ligand, delocalized over the whole bridging groups and perpendicular to the plane of the oxime ligand, appears to play an important role in the antiferromagnetic interaction between the terminal metal ions, separated by as much as ∼7 Å. A comparison of the complexes $M_AM_BM_A$ containing a diamagnetic central ion (M_B) clearly indicates the participation of the central metal ion in the transmission of the antiferromagnetic exchange interaction between the

* Tel.: +49-208-306-3662; fax: +49-208-306-3951.
E-mail address: chaudh@mpi-muelheim.mpg.de (P. Chaudhuri).

doi:10.1016/S0010-8545(03)00081-X

terminal paramagnetic M_A ions. Competing exchange interactions, or spin frustration in the general sense of the term, in polynuclear complexes may lead to ground-state variability. This type of variable ground-state has been observed for several complexes. The strategy of irregular spin-state structure resulting from a particular spin topology has been found to be more effective, as expected, in obtaining 'high spin' molecules than the common strategy of obtaining ferromagnetically coupled systems through involvement of symmetry-related strict orthogonality of the magnetic orbitals of the interacting metal centers. Of particular interest for molecular magnetism is the small but significant effect of bridging ligands like carboxylato anions for cooperation with the ancillary ligand, viz. the oxime ligands, to build up high-nuclearity metal clusters.

Keywords: Metal oximates; Heteropolymetallic complexes; Modular synthesis; Exchange coupling; Spin frustration

1. Introduction

Exchange coupled polymetallic complexes [1–7], in which spin coupling between paramagnetic metals is propagated via bridging atoms, are of special interest to researchers seeking new molecule-based magnetic materials displaying interesting electronic properties and to bioinorganic chemists investigating the structure and function of polynuclear metal centers in proteins. There is an impressive diversity of spin coupled structures in biology [1]. The intimate relationship between spin coupling and molecular structure has fostered, on the other hand, the emergence of molecular magnetism [2–4] as a multidisciplinary field. The fundamental understanding regarding the factors that determine the spin states of polynuclear transition metal complexes owes much to the study of model compounds where magnetostructural correlations can be established in a systematic way. Thus, during the last two decades polynuclear systems have drawn the attention particularly of inorganic chemists, as they constitute a common ground for symbiosis of two apparently different subjects viz. molecular magnetism and metal sites in biology. Of particular concern in this context is the development of synthetic routes that can provide metal complexes with high nuclearity [5–7], particularly heterometallic systems, in a controlled fashion. Amongst the variety of methodologies applied to synthesize polymetallic coordination compounds, the use of 'metalloligands', i.e. metal complexes as ligands [4,8–10], in which the ligands already bound to one metal have free coordination sites that can bind a second metal of the same or different kind, has proven to be very successful; this route involving multinucleating ligands offers many potential advantages over the self-assembly route in that it enables more stringent control over the course of the reaction and upon the products that are formed. This approach of using metalloligands containing polynucleating ligands proceeds step by step and provides a route to gain control of the nuclearity in addition to the preparation of species containing different metal ions, i.e. heterometallic complexes. We and others [9–15] have favored the strategy of using 'metal oximate' building blocks as ligands to synthesize various homo- and hetero-metal complexes. This review article is focussed on such exchange coupled polymetallic complexes containing the bridging core M–N–O–M′ originating only from metal oximates.

2. Background

Since 1905, when Tschugaeff [16] first introduced dimethylglyoxime as a reagent for nickel, oximes as ligands have played an important role for the continuing progress in coordination chemistry. A vast amount of fascinating chemistry has thus accumulated with fundamental bearing on areas such as structure, stability and reactivity of molecules, biochemical models, analytical and organometallic chemistry and noticeably synthesis of molecules with unusual electronic properties. This progress has been documented in a significant number of review articles. We refer the reader to some of these excellent treatises covering these areas [17–22].

3. Scope of the review with respect to magnetism

In the present review we wish to focus on the publications since 1970, describing paramagnetic transition metal oximates of nuclearity two and higher. We wish to emphasize that it is not the purpose of this article to discuss mononuclear oxime complexes. Structurally characterized paramagnetic polymetal (both homo- and hetero-metal) complexes of the first transition series are mostly discussed in relation to the bridging oximates as the exchange-coupling medium. The main objective of the review would be to delineate the progress in the field of exchange coupling through oximate ($-C{=}N-\bar{O}I^{\theta}$) groups by reviewing the relevant

literature of the past 30 years together with the unpublished results of the author and coworkers. As rationalization of the magnetic properties of the compounds in terms of their structural parameters is one of the major aims, compounds with reported structural and magnetochemical data are mainly the subject of this review. Complexes characterized even competently on the basis of indirect spectroscopic, magnetic and other data are not generally discussed. In other words, no claim is made for this review to be of an exhaustive nature. Discussion in detail is concentrated on a few selected systems where considerable structural and magnetochemical work have already been reported or where such work will be worth-doing.

The nature of the spin–spin interactions can be described in terms of the sign of the exchange parameter J. The Heisenberg–Dirac–van Vleck exchange Hamiltonian for a cluster is given by $H_{ex} = -2J \Sigma_{ij} J_{ij} S_i S_j$, the eigenvalues of which are descriptions of the energies of the different spin states thus yielding the spin ladders. Hence, if the spins are paired antiparallel (i.e. S_i and S_j are of opposite sign) in the ground state the system will have $J_{ij} < 0$, but if the spins are parallel in the ground state $J_{ij} > 0$ is the result. Hence, antiferromagnetic systems have singlet ground states for even numbered paramagnetic centers and negative exchange parameter J, while ferromagnetic systems have positive J values and nondiamagnetic ground states.

The mechanisms of exchange coupling have been described by Goodenough and Kanamori [23,24] in terms of the overlap of the d orbitals on one metal ion with the s and p orbitals on a bridging ligand and with the d orbitals on the other metal. This concept of 'super exchange' is used throughout this review; we refer the reader to the book by Goodenough [25] and to the excellent treatises by Ginsberg [26] and later by Kahn [4] for detailed theoretical treatment. The exchange interactions between the spin carriers will be described in the corresponding sections for each exchange coupled system later by considering the symmetry of the molecule within the framework of localized spins.

Concepts like 'spin frustration', 'irregular spin-state structure' are widely used in this review. These ideas are well-known in the literature [4,5,7]. Hence, to avoid repeatation we are refraining from describing them here again and the readers are referred to these articles.

4. Modular synthesis

The strategy of using 'metal complexes as ligands' has been applied frequently to solve the problem of low

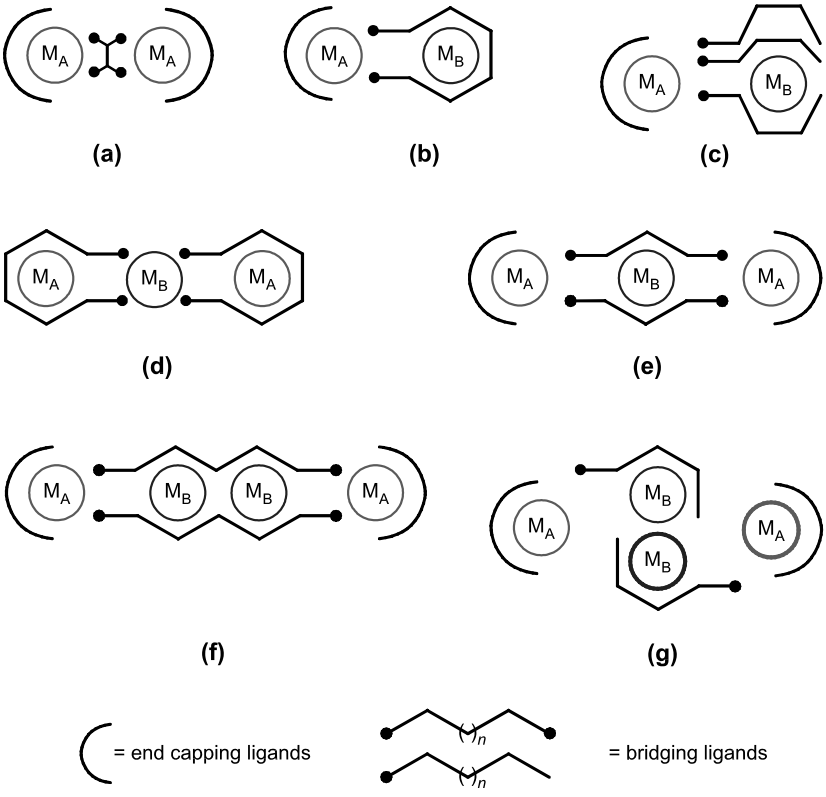

Fig. 1. Schematical drawings of dinuclear (a–c), trinuclear (d, e) and tetranuclear (f, g) homo- and heterometal complexes.

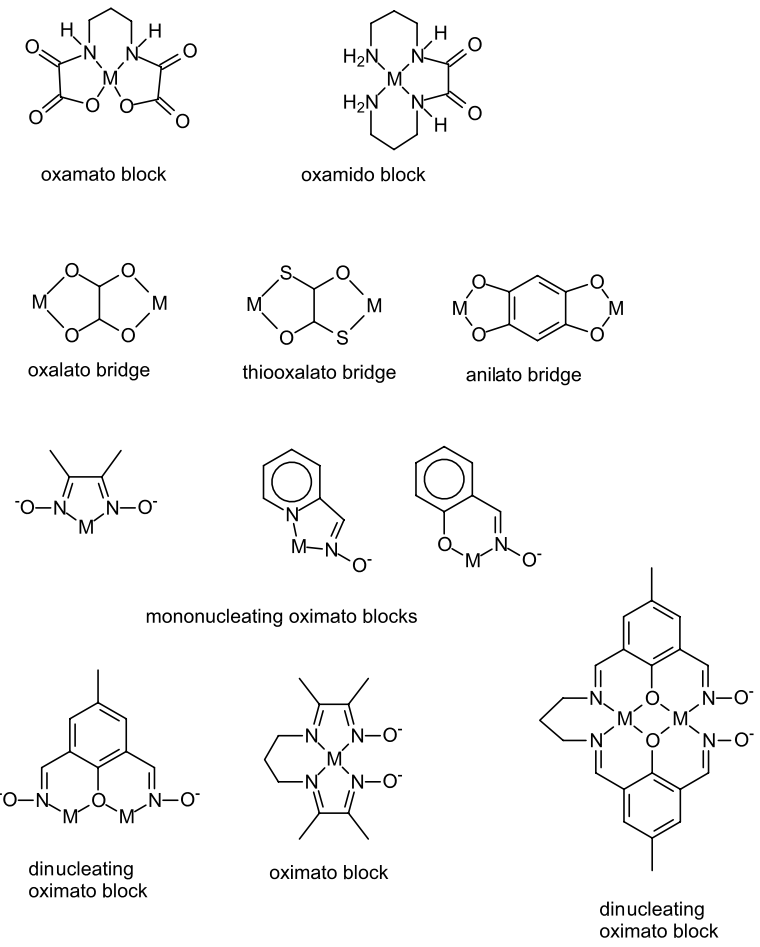

Fig. 2. A few building blocks and bridges used for modular synthesis of polynuclear complexes.

nuclearity and to achieve heteronuclearity [4,5,27]. Different *modules* (i.e. complexes containing one or more metal centers) are able to react further with other modules through available appropriate donor atoms. This 'Baukasten' or modular approach allows the synthesis of larger molecules by reaction of mono or binuclear complexes of appropriate ligands, which are able to coordinate to different metal centers or to other complexes. Fig. 1 shows a few easily visualized schematical representations for different kinds of modular homo- and heteropolynuclear complexes.

Certain complexes such as in Fig. 1(a) involve an organic bridging ligand between two similar or dissimilar modules. In Fig. 1(b and c) two mononuclear dissimilar modules generate heterobinuclear entities, (d) shows a metallic ion bridging two similar modules; (e) and (f) illustrate the connection of a mono or binuclear module with two other modules generating tri- or tetranuclear complexes. Case (g) demonstrates the schematical representation of two modules connected in a butterfly-fashion.

The ligands bonded to the terminal ions are called *end-caps*, whereas the intermediate ones are referred to as *bridging ligands*. The most frequently encountered building blocks for modular synthesis are listed in Fig. 2.

Metal-oximates have proven to be versatile for this approach as will be evident from the compounds described later. The modular preparation with oximate ligands enables the synthesis of linear symmetrical and asymmetrical cores M_AM_A, M_AM_B [28], $M_AM_BM_A$ [29], $M_AM_BM_BM_A$ [30] (M_A, M_B being two different metal ions). The synthesis of asymmetric heterotrinuclear complexes with cores $M_AM_BM_C$ [31] and of $M_A(\mu_3\text{-}O)_2M_B$ [32] butterfly cores has also been achieved. The uniqueness of oximates providing diatomic N,O-bridging is demonstrated by several series of isostructural complexes with different metal ions like Cr(III), Mn(III), Mn(IV), Fe(III), Co(III). Thus, linear heterotrinuclear complexes [29] of general formula **A** and asymmetric dinuclear complexes [28] of general formula **B** have been synthesized. Such isostructural series are not available for any other bridging ligands.

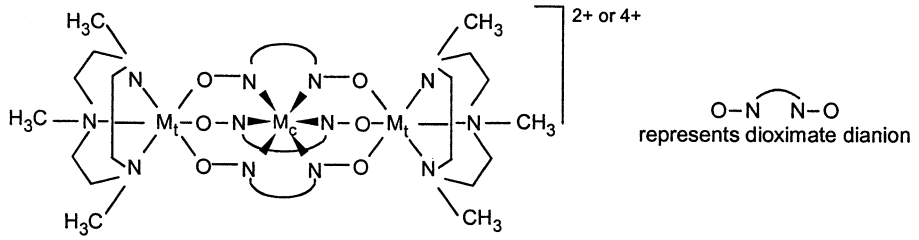

General formula **A**: M_t = Fe(III), Mn(III), Mn(IV), Cr(III) or Co(III)
M_c = Zn(II), Cu(II), Ni(II), Fe(II), Mn(II).

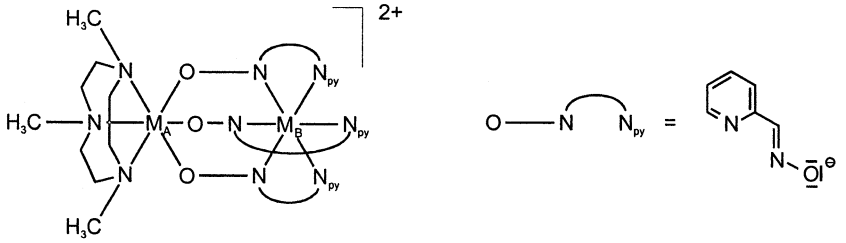

General formula **B**: M_A = Fe(III), Mn(III), Mn(IV), Cr(III) or Co(III) and
M_B = Zn(II), Cu(II), Ni(II), Fe(II), Mn(II).

Several different end-cap ligands (**1**–**7**) have been reported. The function of such ligands is to prevent undesired oligomerization processes. Many acyclic polyamines including di-, tri- and tetra-amines, bipyridine, phenanthroline have been used as end-cap ligands due to their ready commercial availability.

End-Cap Ligands

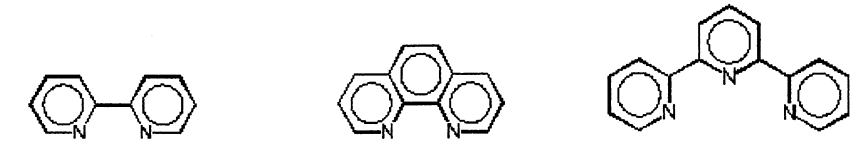

2,2' - Bipyridine (Bipy) **1**

1,10 - Phenanthroline (Phen) **2**

2,2':6',2" - Terpyridine **3**

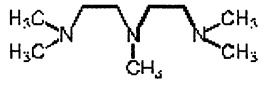

Pentamethyldiethylenetriamine (Pmdt)
4

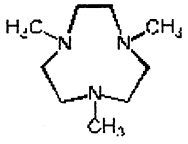

1,4,7 - Trimethyl - 1,4,7 - triazacyclononane (Me_3L) **5**

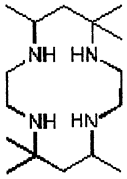

CTH **6**
(d,l - 5,5,7,12,12,14 - hexamethyl-1,4,8,11 - tetraazacyclotetradecane)

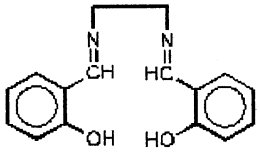

H_2Salen
7

Although not so readily available and obtainable only by a lengthy multistep synthesis, a very versatile end-cap ligand is the cyclic tridentate amine **5**. This amine is a facially coordinating tridentate nitrogen ligand and a significant number of, both thermodynamically and kinetically, stable complexes of this ligand is known [33].

Thus, the problem of scrambling in the product complexes has been avoided by the judicious choice of **5**. Additionally, **5** is apparently too bulky to form the bis(ligand)metal^{n+} ion, a species expected to be the major side product encountered during attempts to synthesize the desired polymetallic centers with other end-cap ligands.

5. Oxime ligands and their abbreviations

Different oxime-ligands which have been used for synthesizing polynuclear complexes are listed below:

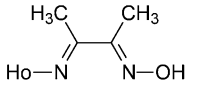

H_2L^1 (H_2dmg)

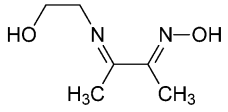

H_2L^2

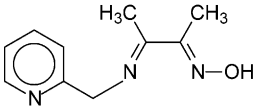

HL^3

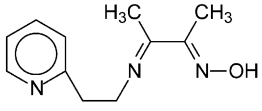

HL^4

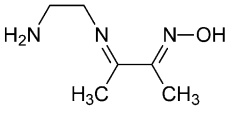

HL^5

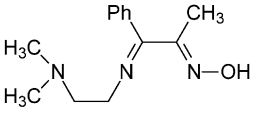

HL^6

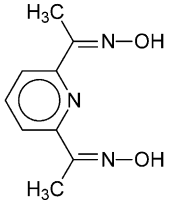

H_2L^7

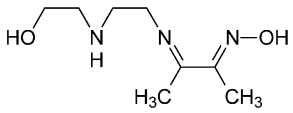

H_2L^8

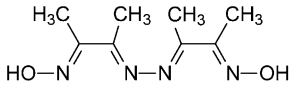

H_2L^9

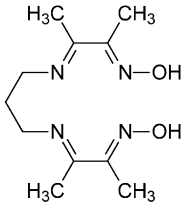

H_2L^{10} (H_2Dopn)

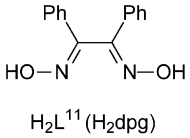

H_2L^{11} (H_2dpg)

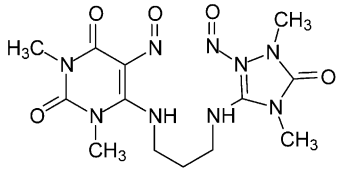

H_2L^{12}

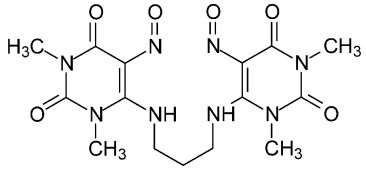

H_2L^{13}

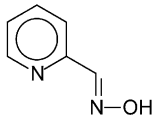

HL^{14}(HPyA)

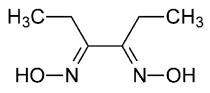

H_2L^{15} (H_2dieg)

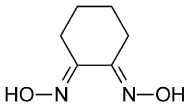

H_2L^{16} (H_2niox)

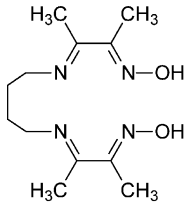

H_2L^{17}

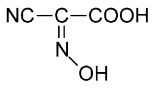

H_2L^{18}

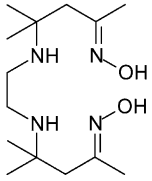

H_2L^{19}

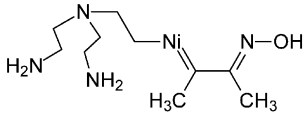

HL^{20}

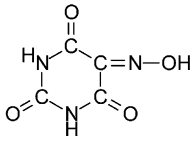

H_3L^{21}
(Violuric acid)

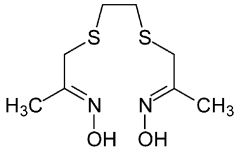

H_2L^{22}

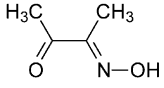

HL^{23}

H_3L^{21}

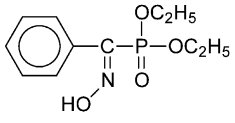

HL^{24}
Diethyl 1-hydroxyimino-
benzylphosphonate

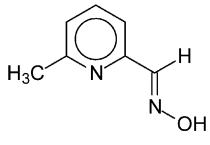

HL^{25}

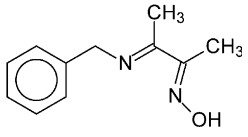

HL^{26}

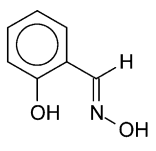

H_2L^{27}

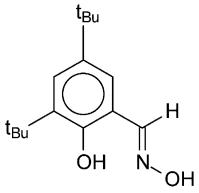

H_2L^{28}

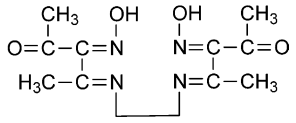

H_2L^{29}

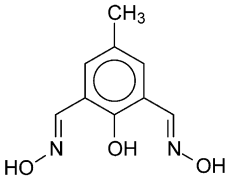

H_3L^{30}

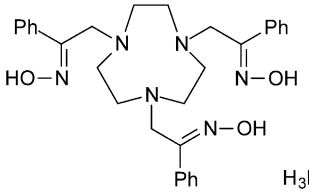

H_3L^{31}

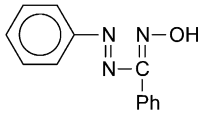

HL^{32}

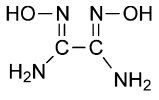

H_2L^{33}

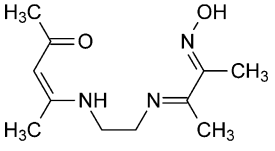

HL^{34}

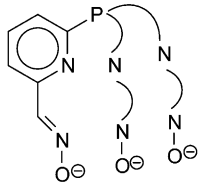

$[P(PyA)_3]^{3-} = [L^{35}]^{3-}$

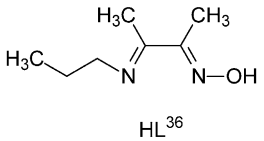

HL^{36}

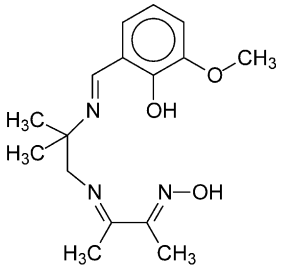

H_2L^{37}

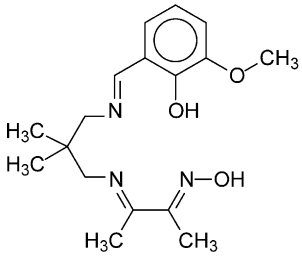

H_2L^{38}

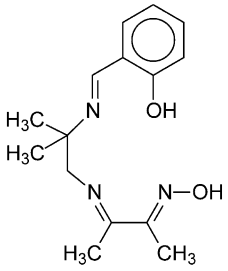

H_2L^{39}

6. Homometal complexes

6.1. Copper(II) complexes

That oximate ligands generally mediate very strong antiferromagnetic exchange interactions between two d^9 Cu(II) centers to provide, in some cases, a nearly complete spin-pairing at room temperature was first authenticated in a trinuclear copper(II) complex of pyridine-2-aldoxime (HL^{14}, HPyA). The compound $[Cu_3(L^{14})_3(OH)SO_4]$ (**8**) contains a planar unit with a μ_3-sulfate group below the plane [34].

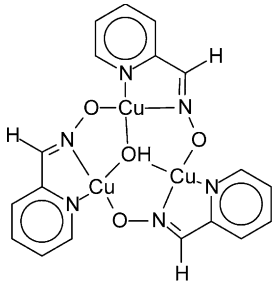

8

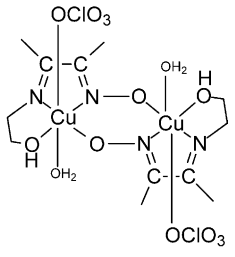

9

The coordination about each copper(II) is square-pyramidal with a sulfate–oxygen in the axial position. Two of the three electrons of the Cu_3-core are completely paired and only the doublet spin state ($S_t = 1/2$) is populated at room temperature ($\mu_{eff} = 1.0$ μ_B per Cu (80–300 K)), which is evidence for strong antiferromagnetic coupling. The first diamagnetic copper(II) dimer, thus historically worthmentioning and ascribable to superexchange through the oxime bridges, was described by Bertrand et al. [35] with the centrosymmetric nearly planar six-membered ring formed by two copper atoms and two oxime (NO) groups, $[Cu_2(HL^2)_2(H_2O)_2(ClO_4)_2]$ (**9**).

Numerous examples of polynuclear copper(II) complexes with oxime ligands have been reported; many of them have magnetic moments much below the spin-only value and they are listed in Table 1.

The structure of $[\{Cu_2(L^1)(HL^1)(H_2L^1)\}_2(\mu_4\text{-}O_4S)]$ consists of two monocationic dinuclear $[Cu_2(L^1)(HL^1)(H_2L^1)]^+$ units bridged by a sulfate anion, leading to a neutral tetrameric entity [48,49]. In this monocation an oxime group acts as a bridging ligand only through the oxygen atom, which is schematically shown in Fig. 3. Strong antiferromagnetic coupling between copper(II) ions ($J \approx -475$ cm^{-1}) was observed, revealing that the NO-group has a remarkable ability to mediate strong antiparallel spin coupling when it acts as a bridging ligand either through the nitrogen and oxygen atoms or only through the oxygen atom.

In a modular approach by using the bridging module $[Cu(L^1)_2]^{2-}$, two trinuclear compounds, $[Cu_3(L^1)_2(\mathbf{1})_2(CH_3OH)_2](NO_3)_2$ [12] and $[Cu_3(L^1)_2(\mathbf{5})_2Br](ClO_4)$ [11], were synthesized. The basal planes of the copper(II) ions in the **1**-containing compound (Fig. 4(a)) are nearly planar, whereas the three basal planes containing the copper(II) ions in the **5**-compound (Fig. 4(b)) are not coplanar, which should diminish the overlap between the magnetic orbitals. But the spin exchange interactions in these two compounds are strongly antiferromagnetic ($J < -300$ cm^{-1} for **1**; $J \approx -448$ cm^{-1} for **5**) suggesting that the unusually large spin exchange interaction in these trinuclear copper(II) complexes is not the result of any special geometrical feature but is related to the electronic structure of the bridging dioximato ions. The structures of these two cations are shown in Fig. 4.

Inspection of Table 1 together with the structural parameters [9–15,34–59] of the oximato-bridged copper(II) complexes reveal that exchange interactions (J values) show no correlation either with the distances Cu···Cu, Cu–N_{oxime}, Cu–O_{oxime} and N_{oxime}–O_{oxime}, or with the nature of the basal skeleton $Cu(NO)_2Cu$ i.e. the magnitude of exchange coupling is independent of the degree of deviation from planarity, or deviation of copper from the mean basal plane (range 0.003–0.463 Å). Recently, MO extended Hückel calculations [54] using the CACAO program have shown that a considerable deviation from the planarity of the $Cu(NO)_2Cu$ core has an insignificant influence on the overlap between the interacting orbitals. These calculations also show that 'the HOMO–LUMO energy gap is practically not affected by the apical coordination to

Table 1
Comparison of magnetostructural parameters in different oximato-bridged copper(II) complexes

Complex	Nature of the $Cu_2(NO)_2$ ring and/or bridging mode	Spin interaction ($H = -2JS_1 \cdot S_2$)	Reference
$Cu_2(HL^1)_4$	Chair-conformation: out-of-plane Oximato bridging	$J = +4.5\ cm^{-1}$ $J = +20\ cm^{-1}$	[36–38]
$Cu_2(HL^{15})_4$	Chair conformation: out-of-plane Oximato bridging	$J = 0.5\ cm^{-1}$	[38]
$Cu_2(HL^{16})_4$	Chair conformation: out-of-plane Oximato bridging	$J = +1.6\ cm^{-1}$	[38]
$[Cu_2(HL^{17})_2](ClO_4)_2$	Chair conformation: out-of-plane Oximato bridging	$J = -1.0\ cm^{-1}$	[38,39]
$[Cu_2(HL^2)_2(H_2O)_2(ClO_4)_2]$	Planar; in-plane oximato bridging	Diamagnetic	[35]
$[Cu_2(L^3)_2(NO_3)_2]$	Planar	$J = -410\ cm^{-1}$	[40]
$[Cu_2(L^4)_2](ClO_4)_2$	Nonplanar; twisted-boat configuration	$J = -275\ cm^{-1}$	[40]
$[Cu_2(L^4)_2(H_2O)_2](ClO_4)_2$	Nonplanar; twisted-boat configuration	$J = -255\ cm^{-1}$	[40]
$[Cu_2(L^4)_2(CH_3CN)_2](ClO_4)_2$	Planar; in-plane bridging	$\mu_{eff} = 1.04\ \mu_B$ at 298 K	[41]
$[Cu_4(L^5)_4(ClO_4)_2](ClO_4)_2$ **	In-plane and out-of-plane bridging	Not reported**	[41]
$[Cu_2(L^6)_2(CH_3OH)_2](ClO_4)_2$	Planar; in-plane bridging	$J < -500\ cm^{-1}$	[42]
$[Cu_2(HL^7)_2(H_2O)_2](BF_4)_2$	Planar	$\mu_{eff} = 0.6\ \mu_B$ at 298 K	[43]
$[Cu_2(HL^8)_2](ClO_4)_2$	Nonplanar chair conformation: in-plane Oximato bridging	$\mu_{eff} = 1.07\ \mu_B$ at 298 K $J = -273\ cm^{-1}$	[44]
$[Cu_2(HL^9)_2(C_2H_5OH)_2](ClO_4)_2$	Planar	Strongly coupled (EPR)	[45]
$[Cu_3(L^1)_2(\mathbf{1})_2(CH_3OH)_2](NO_3)_2$	Planar	$\mu_{eff} = 1.85\ \mu_B$ (80–300 K) strongly antiferromagnetically coupled, $J < -300\ cm^{-1}$	[12]
$[Cu_2(L^{10})(\mathbf{2})(CH_3OH)_2](ClO_4)_2$	Nonplanar; in-plane bridging	$\mu_{eff} = 0.69\ \mu_B$ (296 K) $J = -433\ cm^{-1}$	[46]
$[Cu_3(L^{11})_2(\mathbf{1})_2(CH_3OH)_2](NO_3)_2$	Planar; in-plane bridging	$\mu_{eff} = 1.81\ \mu_B$ (85–298 K) $J < -300\ cm^{-1}$	[13]
$[Cu_3(L^{10})_2](ClO_4)_2$	Nonplanar; a butterfly-shaped trinuclear cation	$\mu_{eff} = 1.80\ \mu_B$ (170 K) $J = -291\ cm^{-1}$	[9]
$[Cu_3(L^1)_2(\mathbf{5})_2Br](ClO_4)$	Nonplanar; basal bridging	$J = -448\ cm^{-1}$	[11]
$[Cu_2(L^4)(\mathbf{1})(1,1\text{-}N_3)](ClO_4)_2$	Coplanar	$J = -260\ cm^{-1}$	[47]
$[Cu_2(L^4)(\mathbf{4})(1,1\text{-}N_3)](ClO_4)_2$	Basal oximato bridging axial-basal azido bridging	$J = -148\ cm^{-1}$	[47]
$[Cu_2(HL^1)_2(H_2L^1)(H_2O)_2](ClO_4)_2$	Boat conformation basal oximato bridging	Diamagnetic	[48]
$[\{Cu_2(L^1)(HL^1)(H_2L^1)\}_2(\mu_4\text{-}SO_4)]$	Nonplanar; basal bridging	$J \approx -475\ cm^{-1}$	[49]
$[Cu_2(L^{10})(\mathbf{5})(H_2O)](ClO_4)_2$	–	$J = -298\ cm^{-1}$	[50]
$[Cu_3(HL^{13})(L^{13})(H_2O)(\mu\text{-}Cl)](ClO_4)_2$	Nonplanar	$J = -189\ cm^{-1}$	[15]
$[Cu_2(L^{10})(\mathbf{1})(H_2O)_2](ClO_4)_2$	Boat conformation	$J = -337\ cm^{-1}$	[14]
$[Cu_2(L^{14})_2(\mathbf{5})I]ClO_4$	Boat conformation	$J = -460\ cm^{-1}$	[52]
$[Cu_2(L^{14})_2(\mathbf{5})Cl]ClO_4$	Boat conformation	$J = -390\ cm^{-1}$	[53]
$[Cu_2(L^{14})_2(\mathbf{5})(CH_3COO)]ClO_4$	Boat conformation	$J = 358\ cm^{-1}$	[53]
$[Cu_2(L^{13})(\mathbf{1})(C_2H_5OH)](ClO_4)_2$	Planar	Diamagnetic	[54]
$[Cu_2(L^{12})(\mathbf{1})(H_2O)](ClO_4)_2$	Planar	Diamagnetic	[54]
$[Cu_3(L^4)_2(1,1\text{-}N_3)(H_2O)_2(CH_3OH)_2](NO_3)_2$	Planar	$J = -266\ cm^{-1}$	[55]
$[Cu_2(L^{18})_2]$	Nonplanar	Not reported	[56]
$[Cu_4(L^1)_2(HL^1)_2(\mathbf{3})](ClO_4)_2$	Parallel-planar basal plane like $Cu_2(HL^1)_4$	$J = -98.5\ cm^{-1}$, $J' = +14\ cm^{-1}$	[57]
$[Cu_2(L^4)(\mathbf{1})(OCH_3)(ClO_4)]ClO_4$	Presence of only Cu(NO)Cu-core	$\mu_{eff} = 0.4\ \mu_B$ (298 K) nearly diamagnetic	[58]
$[Cu_2(L^4)(\mathbf{1})(CH_3COO)_2]ClO_4$	Presence of only Cu(NO)Cu-core	$J = -130\ cm^{-1}$	[58]
$[Cu_2(HL^{19})_2]Br_2$	Boat conformation	Probably uncoupled	[59]
$[Cu_3(L^{14})_3(OH)SO_4]$	Trinuclear cation is planar	$\mu_{eff} = 1.85\ \mu_B$ (80–290 K) strongly antiferromagnetically coupled	[34]
$[Cu_3(L^{36})_3(H_2O)_3(OH)](ClO_4)_3$	Copper atoms are arranged in an equatorial triangle	$\sim 1\ \mu_B$ (78–366 K)	[130]

** We have measured and simulated the susceptibility data (2–290 K) of the compound described in Ref. [41]. The following parameters: $J_{12} = J_{23} = J_{34} = J_{14} = -45.0\ cm^{-1}$, $J_{24} = 0$ (fixed), $g = 2.0$ (fixed), $TIP = 240 \times 10^{-6}\ cm^3\ mol^{-1}$ have been evaluated [51].

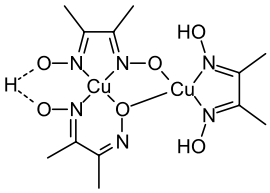

Fig. 3. Structure of the dinuclear unit present in the tetranuclear $[Cu_4(L^1)_2(HL^1)_2(H_2L^1)_2(\mu_4\text{-}O_4S)]$. Reproduced with permission from Ref. [49].

copper(II)', which is not in accord with the magnetic results of the compounds described in Refs. [52,53] (Table 1) and discussed below.

Based on the results reported in the literature it was envisaged that a suitable choice of ligand and axial group can give rise to series of complexes which, in spite of slight conformational differences in the $Cu_2(NO)_2$ ring, might exhibit large variations in the strength of the exchange coupling. Accordingly, we have synthesized a series of compounds with the compositions $[(\mathbf{5})Cu^{II}(L^{14})_2Cu^{II}X](ClO_4)$, where $X = Cl^-$, I^- or CH_3COO^-, whose structures are depicted in Fig. 5 [52,53].

For the chloro-compound (Fig. 5a), the angle between the basal planes containing the Cu(1) and Cu(2) is 67.7°, whereas the corresponding angle for the acetato-compound (Fig. 5b) is 56°. It is to be noted that acetate ion bridges the copper centers rendering them five-coordinate; on the other hand the chloro-compound contains four- and a five-coordinate copper centers. The Cu(1)···Cl(1) distance is too long, 3.128 Å. The Cu(1)···Cu(2) distances are 3.370 and 3.467 Å for the chloro- and acetato-compounds, respectively. The structure of the iodo-compound is very similar [52]. Indeed, the magnitude of J varies depending on the nature of the axial ligand: CH_3COO^- ($J = -358\ cm^{-1}$), Cl^- ($J = -390\ cm^{-1}$) and I ($J = -460\ cm^{-1}$). Interestingly, the strength of the spin interaction is not related to the N–O and C=N bond distances, suggesting that *π exchange mechanism via the ring system is not the major pathway*.

Oximato-bridged copper(II) complexes, based on the magnetic results, can thus be divided mainly into two groups: (i) strong antiferromagnetically coupled dicopper(II) compounds, which in some cases may even exhibit diamagnetism at room temperature, irrespective of the in-plane bonding via a planar or a nonplanar $Cu_2(NO)_2$ ring; (ii) very weak ferro- or antiferromagne-

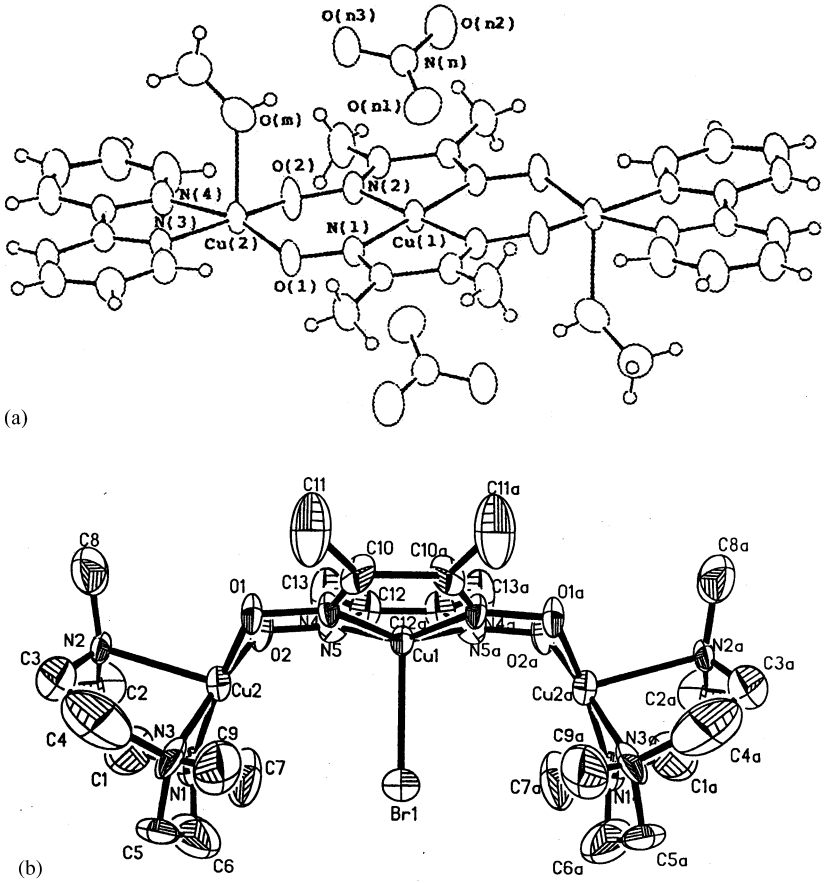

Fig. 4. Solid state structures of: (a) the dication $[Cu_3(L^1)_2(\mathbf{1})_2(CH_3OH)_2]^{2+}$ [12]; and (b) the monocation $[Cu_3(L^1)_2(\mathbf{5})_2Br]^+$. Reproduced with permission from Ref. [11].

tically coupled complexes, which are the result of out-of-plane bonding via the N–O moiety, the axial-basal bridging. The analysis of the exchange pathway through the out-of-plane oximato bond in this family has been substantiated by Extended-Hückel calculations and a correlation between the value of J and the angle at the $Cu–O_{ox}–N_{ox}$ has been proposed [38].

Although no simple magnetostructural correlation has been established and a more clear picture can be expected with the availability of more structural data for closely related complexes displaying suitable variation over only one of the structural parameters, a qualitative rationale for the strongly coupled complexes can be provided. Despite the significant distortion from co-planarity of the copper(II) centers, as is evident from the structural parameters [9–15,34–59] of the compounds listed in Table 1, the antiferromagnetic interaction is quite strong. This independence of the angles between the basal planes of the copper(II) complexes is in accord with the earlier suggestion [11] of the dominance of the σ-pathway over the π-pathway for the antiferromagnetic exchange mechanism in oximato-bridged copper(II) complexes. The π-pathway is expected to lead to exchange interactions whose magnitudes should be dependent on the angles between the copper basal planes, in which unpaired spins are located. The environment around the copper(II) ions is square pyramidal/planar with $d_{x^2-y^2}$ ground states. Thus the magnetic orbitals of the copper(II) ions, $d_{x^2-y^2}$, point from the metal toward the four nearest neighbors and overlap on either side of the bridging oximate. Because of the symmetry properties of the σ-interaction, the $d_{x^2-y^2}$ orbitals on the copper(II) ions and σ orbitals on the bridging oxygen and nitrogen atoms (sp^2-hybridization of the NO moiety) are involved in the exchange pathway for the unpaired spin density. Thus the strong antiferromagnetic interaction can be interpreted as the symmetry allowed $d_{x^2-y^2}||\sigma_{sp2}(NO)||d'_{x^2-y^2}$ (using Ginsberg's symbols) [26] σ-superexchange pathway. Scheme 1 shows the orientation of the relevant orbitals for the mechanism.

In summary, oximato-bridges in *syn*, *anti* or *o-monoatomic* form are able to transmit, in general, strong antiferromagnetic exchange interactions.

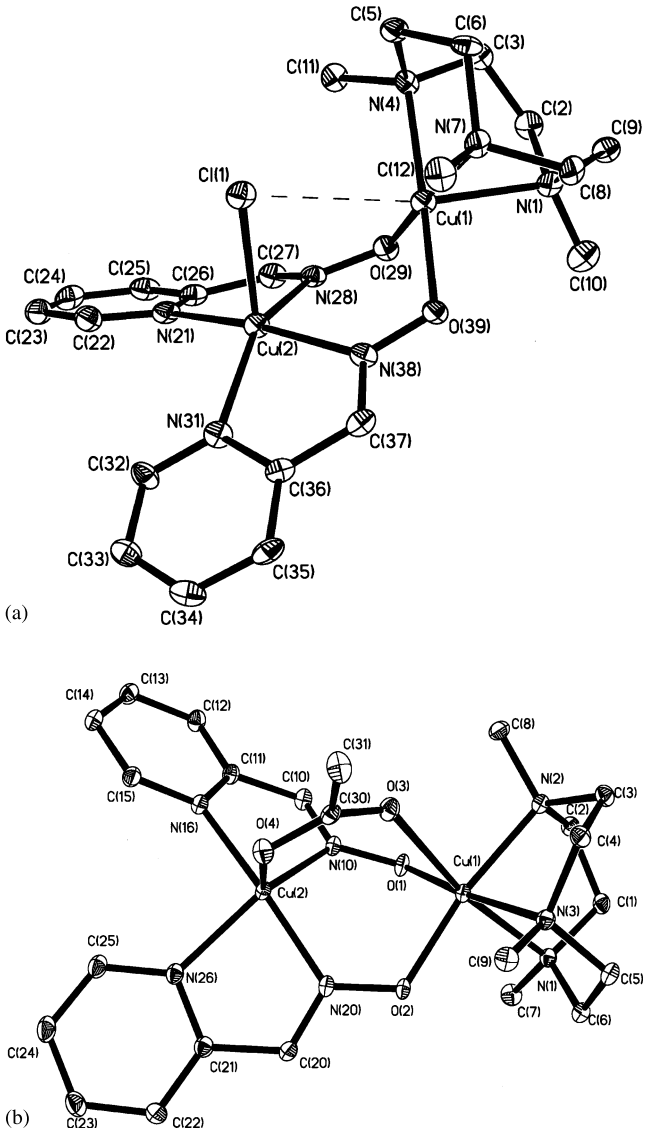

Fig. 5. Molecular structures of: (a) $[(\mathbf{5})Cu(L^{14})_2Cu(Cl)]^+$; and of (b) $[(\mathbf{5})Cu(L^{14})_2Cu(OOC{\cdot}CH_3)]^+$. Reproduced with permission from Ref. [53].

6.2. Nickel(II) complexes

On changing copper(II) with the $(d_{x^2-y^2})^1$ magnetic orbital to nickel(II) with $S_{Ni}=1$ and singly occupied $(d_{x^2-y^2})^1$ and $(d_{z^2})^1$ orbitals, a different situation arises. The dominant interactions prevailing are

$d_{x^2-y^2}||\sigma_{sp2}(NO)||d'_{x^2-y^2}$ antiferromagnetic

$d_{z^2}||\sigma_{sp2}(NO)||d'^2_z$ weak antiferromagnetic

$d_{x^2-y^2}||\sigma_{sp2}(NO)||\perp d'^2_z$ ferromagnetic

which lead to reduction in the strength of the overall exchange interaction in comparison to that for copper(II). As will be shown below, all reported oximate-bridged nickel(II) complexes accordingly exhibit moderate to weak antiferromagnetic interactions.

The structure of dark red crystals of $[Ni_2(L^{20})_2](ClO_4)_2$ [60] consisting of discrete dinuclear nickel(II) cations is shown in Fig. 6.

The two octahedral nickel(II) centers are bridged by two oxime(NO) ligands. The central six-membered ring $Ni_2N_2O_2$ adopts a twist boat conformation, as is known for oximate-bridged dicopper(II) complexes. The Ni···Ni distance of 3.706(1) Å excludes any direct metal–metal interactions. A remarkably strong antiferromagnetic coupling ($J=-79\ cm^{-1}$) has been reported

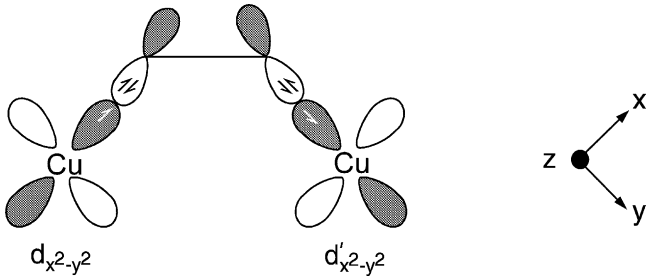

Scheme 1.

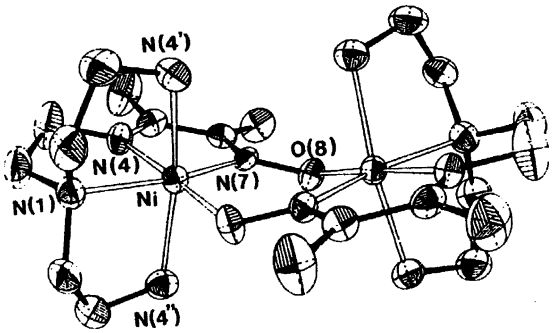

Fig. 6. An ORTEP drawing of $[Ni_2(L^{20})_2]^{2+}$. Reproduced with permission from Ref. [60].

without stating the spin-Hamiltonian used. Comparison with the J-values for similar bisoximato-bridged dicopper(II) complexes helps us to come to the conclusion that the authors used the $(-2JS_1 \cdot S_2)$-form of the Hamiltonian. For d^8Ni(II) with two unpaired electrons in the antibonding e_g^* level, the strength of coupling is remarkably strong. For the superexchange mechanism a σ-pathway has been proposed.

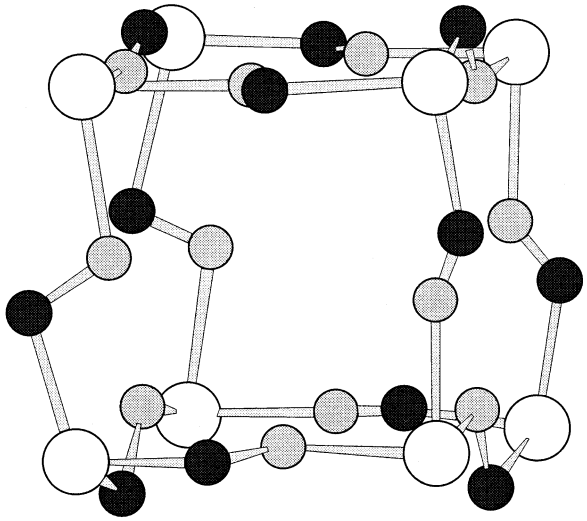

Fig. 7. The hexahedro-Ni_8 unit present in the anion of $K_4[Ni(H_2O)_6][Ni_8(HL^{21})_{10}(H_2L^{21})_2]\cdot 20H_2O$. Ni···Ni = 4.83–4.85, Ni–O = 1.97–2.22, Ni–N = 2.01–2.30 Å. Reproduced with permission from Ref. [61].

The octanuclear nickel(II) anionic complex, $[Ni_8(HL^{21})_{10}(H_2L^{21})_2]^{6-}$, can be considered as a nickel(II) analogue of cubane C_8H_8. In Fig. 7 only the $Ni_8(NO)_{12}$ core containing the oximate groups (NO) of the violurate ligand (H_3L^{21}) is depicted. Variable-temperature (4–298 K) magnetic data were simulated to provide $J = -30$ cm^{-1} and $g = 2.27$, showing that *trans*-μ-oximate group is also able to transmit strong antiferromagnetic coupling between Ni(II) centers, which are at a distance of ~4.85 Å [61].

A trinuclear complex, $[Ni_3(L^{22})(HL^{22})_2](ClO_4)_2$ has been described with a thioether sulfur-containing dioxime ligand (H_2L^{22}) [62]. The pseudo-octahedrally coordinated three nickel(II) centers are disposed in an isosceles triangle, in which Ni(2) is directly bridged to each of Ni(1) and Ni(3) by a single-atom oximate bridge, whereas four other bridges that link Ni(1) to Ni(2) and Ni(3) and additionally Ni(3) to Ni(2) and Ni(1) are two-atom N–O linkages, shown as **10**.

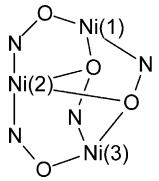

10

Magnetic data were analyzed by a 'two-J' model for an isosceles triangle with $J_{12} = J_{23} = -14.4 + 0.6$ cm^{-1}, $J_{13} = -7.6 + 1.1$ cm^{-1}, $g = 2.166$, confirming the antiferromagnetic interactions transmitted through the single atom oxygen and two atom N–O bridges of the oxime functionality.

The structure of brown $[Ni(Dien)]_2(\mu_3\text{-}OH)_2\{Ni_2(L^{23})_4\}(ClO_4)_2$ [63] is shown schematically in Fig. 8.

The coordination core of the tetranuclear nickel(II) complex containing the Ni_4O_2 core has been described as an 'out-of-phase butterfly', in which the spin coupling would be transmitted through the bridging (NO) and OH groups. The Ni(2)–OH–Ni(2a) angles are 97.73°. Like other structurally related complexes $[Fe_4(\mu_3\text{-}O)_2]^{8+}$ [64,68], $[Mn_4(\mu_3\text{-}O)_2]^{8+}$ [65,79], $[Cr_4(\mu_3\text{-}O)_2]^{8+}$ [66], $[V_4(\mu_3\text{-}O)_2]^{8+}$ [67], $[Cr_2(\mu_3\text{-}O)_2Fe_2]^{8+}$ [69], $[Cr_2(\mu_3$-

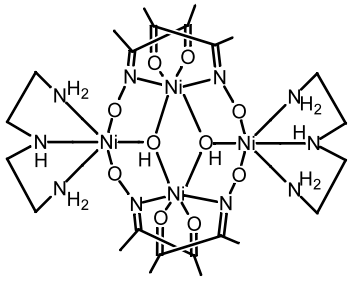

Fig. 8. Atom connectivity as obtained from the X-ray structure of $[Ni(Dien)]_2(\mu_3\text{-}OH)_2[Ni_2(L^{23})_4]^{2+}$. Reproduced with permission from Ref. [63].

$O)_2Mn]^{8+}$ [70] and $[Fe_2(\mu_3\text{-}O)_2Mn]^{8+}$ [79,122] the magnetic properties were analyzed by using a 'two-J' model, $J_{wing-body}$ (J_{wb}) and $J_{body-body}$ (J_{bb}) (Fig. 9). Simulation of the susceptibility data (2–300 K), which indicate a diamagnetic ground state $|0, 2, 2\rangle$, yielded the parameters $J_{wb} = -20.3$ cm^{-1}, $J_{bb} = +10$ cm^{-1} and $g = 2.32$. Additionally an error-surface plot indicated that any estimate of $J_{bb} > 0$ is rendered exceedingly imprecise. This is in accord with the earlier observation that J_{bb} cannot be precisely determined from the susceptibility data in the temperature range 2–300 K, but J_{wb} can be evaluated with a reasonable accuracy (see later: tetranuclear Fe(III) complexes in Section 6.3).

The structure of the nickel(II) complex of pyridine-2-aldoxime (HL^{14}), a neutral tris-complex was found in the solid state to consist of two monomeric $Ni(HL^{14})(L^{14})_2$ units held together by two O···O hydrogen bridges between the oxygen atoms [71]. If instead of pyridine-2-aldoxime (HL^{14}), 6-methylpyridine-2-aldoxime (HL^{25}) is used, a nonanickel(II) complex, $[Ni_9(L^{25})_{10}(OH)_6((OH)_2)_6]^{2+}$ is formed [72]. The structure contains an octahedral NiO_6 central core, and four different NiN_4O_2 and NiN_2O_4 environments. All of the oximate groups are deprotonated, and the nine nickel atoms are linked together via several bi- or trifurcated oximato and hydroxo bridges. Diethyl-1-hydroxyiminobenzylphosphonate (HL^{24}) forms a tetrameric nickel(II) complex, $Ni_4(L^{24})_6(H_2O)_2(\mu_3\text{-}OH)_2$ [73], in which nickel(II) atoms are disposed in a butterfly arrangement with a $Ni_4(\mu_3\text{-}OH)_2$ core. Unfortunately, none of the above three reported nickel(II) complexes have been magnetochemically investigated.

A series of mixed-ligand nickel(II)-metallacrowns containing ligands like phenoxyacetic acid, salicylhydroxamic acid and di-(2-pyridyl)ketone oxime has been reported [74]. As several exchange pathways are available between the paramagnetic and diamagnetic nickel(II) ions present in the molecules, it is difficult to provide a quantitative assessment of the exchange interactions. Variable-temperature magnetic susceptibility data indicate that the paramagnetic nickel(II) centers are antiferromagnetically coupled.

The ligand 1,4,7-tris(acetophenoneoxime)-1,4,7-triazacyclononane (H_3L^{31}) with nickel(II) yields a tetranuclear planar trigonal-shaped species $[Ni_4(HL^{31})_3](ClO_4)_2$ [90], whose structure is shown in Fig. 10. The complex can be described as three $[Ni(HL^{31})]^0$-units acting as bidentate ligands for the central Ni(2) yielding a NiO_6 core. A monoatomic oximato-O, 0(6), bridge present in the complex with an angle Ni(1)–O(6)–Ni(2) 113.5° probably constitutes the main path for the antiferromagnetic exchange interaction.

This tetranuclear Ni(II) complex with local spins $S_{Ni} = 1.0$ exhibits antiferromagnetic exchange interactions ($J = -13.4$ cm^{-1}) yielding the ground state $S_t = 2.0$ owing to the topology of spin-carriers, as shown in Fig. 11. The magnetization measurements at different applied magnetic fields of 1, 4 and 7 T confirmed the ground state to be $S_t = 2.0$ (Fig. 11). The simulated parameters are $S = 2.0$ (fixed), $g = 2.0$, $D = 0.65$ cm^{-1}.

The μ_{eff} versus T-plot (Fig. 12) shows a broad minimum at 30–50 K indicating an irregular spin-level structure (Fig. 12) for the compound. Simulation of the experimental data yielded $J = -13.4$ cm^{-1}, g_{Ni} (central) = 2.271, g(peripheral) = 2.055. The compound belongs to the class, due to the molecular topology of the paramagnetic centers [131], where it is possible to stabilize a high spin ground state, in spite of antiferromagnetic interactions prevailing between the spin carriers.

Summarizing the results of the exchange-coupled oximate-bridged nickel(II) complexes reported in the last ~30 years, there are only eight structurally characterized complexes, only five of which have been subjected to magnetic susceptibility measurements. So no correlation between structural and magnetic properties for such complexes has been obtained, and hence

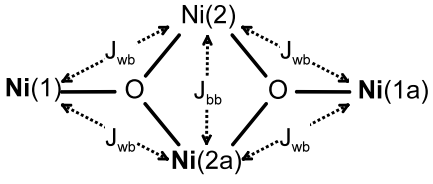

Fig. 9. Coupling model for the $Ni_4(OH)_4$ core.

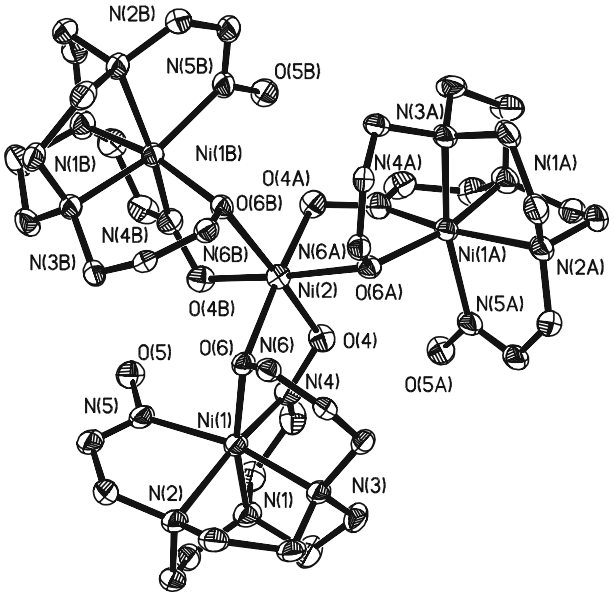

Fig. 10. Solid state structure of $[Ni_4(HL^{31})_3]^{2+}$. The phenyl groups attached to C(12), C(22) and C(32) are omitted for clarity. Reproduced with permission from Ref. [90].

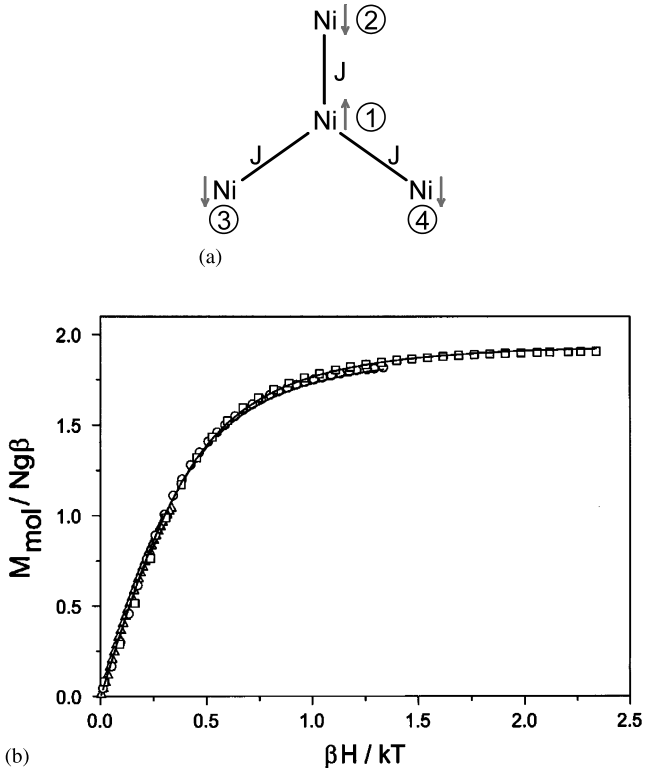

Fig. 11. Topology of the spin-carriers and the VT-magnetization measurements at magnetic fields of 1, 4 and 7 T. Reproduced with permission from Ref. [90].

more oximate-bridged paramagnetic complexes of nickel(II) are warranted.

6.3. Iron complexes

Based on the structural and magnetic results available until now iron-containing oxime ligands can mainly be divided into two groups: (i) most of the oxime ligands stabilize iron in the Fe(II) l.s.-state. The exceptions are the phenol-containing oximes; (ii) the phenol-containing oximes like salicylaldoximes (H_2L^{27}, H_2L^{28}), 2,6-diformyl-4-methylphenoldioxime (H_2L^{30}) yield both ferrous and ferric complexes in high-spin states. Additionally, a reductive deoxygenation of the oxime by the metal ion might occur to yield the novel core $[M_3^{III}(\mu_3\text{-O})(\mu_2\text{-OPh})]^{6+}$, where M(III) = Ti, V, Cr, Mn and Fe.

This generalization is documented below by the data from the literature and our own results. We have tried to narrow the gap prevailing so long in the area of coordination chemistry of salicylaldoxime with trivalent transition metal ions. Of particular interest is the dramatic effect of bridging carboxylato ligand anions for cooperation with the ancillary ligand, viz. salicylaldoxime, to build up high-nuclearity metal clusters.

A linear trinuclear species Fe^{II}(l.s.)Fe^{III}(h.s.)Fe^{II}(l.s.) containing the phenylazoaldoxime, PhC(=NOH)N=NPh was structurally characterized [75]. As the compound contains only one paramagnetic center, Fe(III) ($S = 5/2$), we are refraining from discussing it further. Similarly, the localized mixed-valence cation $[(\mathbf{5})Fe^{III}(L^{14})_3Fe^{II}]^{2+}$ containing a l.s.Fe(II), behaves magnetically as a mononuclear complex, $\mu_{eff} = 5.83 \pm 0.02\ \mu_B$ (10–290 K) [76].

By adopting a modular approach dark red solids of diiron(III) complexes, $[(\mathbf{5})Fe(L^{27})_3Fe]$ and $[(\mathbf{5})Fe(L^{28})_3Fe]$ were prepared by the reaction of $FeCl_3$ with either salicylaldoxime (H_2L^{27}) or its di-tertiary-butyl derivative (H_2L^{28}), respectively, in dry methanol, followed by addition of $[(\mathbf{5})FeCl_3]$ and triethylamine [77]. As expected the structures are identical with respect to the atom connectivity and the coordination geometry of the iron(III) centers. An ORTEP for the tertiary-butyl derivative is shown in Fig. 13.

Each iron center is hexacoordinated with FeN_3O_3 cores. The iron centers are held together by three N–O groups. The binuclear skeleton is not coplanar, but is bent with a Fe(1)···Fe(2) separation of 3.49 Å, which is slightly shorter than that in the complex with the ligand L^{27} (3.57 Å). The +III oxidation state and the high spin electronic configuration of the iron centers in both

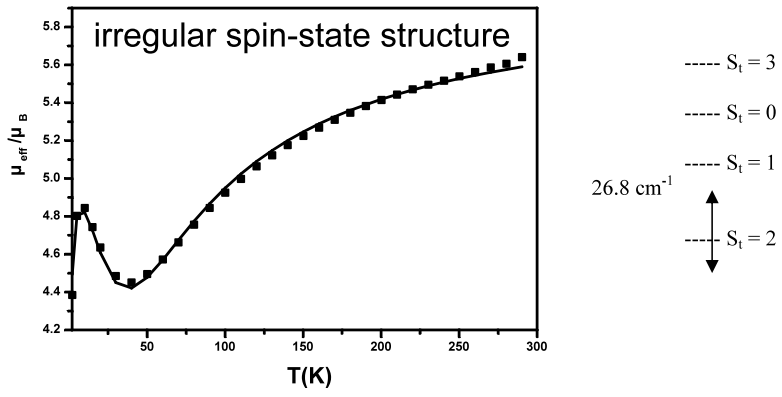

Fig. 12. A plot of μ_{eff} vs. T for $[Ni_4(HL^{31})_3]^{2+}$ and the low-lying spin-ladders. Reproduced with permission from Ref. [90].

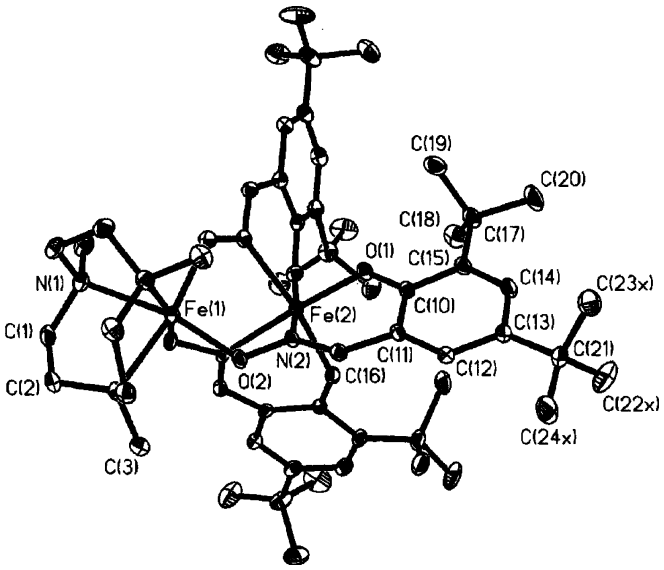

Fig. 13. An ORTEP of $[(\mathbf{5})Fe^{III}(L^{28})_3Fe^{III}]$. Reproduced with permission from Ref. [77].

complexes were in accord not only with the structural parameters but also confirmed by Mössbauer spectroscopy. By using the Hamiltonian $H = 2J\hat{S}_1 \cdot \hat{S}_2$ ($S_1 = S_2 = 5/2$), the susceptibility data were simulated yielding similar exchange coupling constants, $J(L^{27}) = -11.8$ cm^{-1} and $J(L^{28}) = -12.6$ cm^{-1}. The small increase in the strength of antiferromagnetic coupling for the substituted ligand (L^{28}) might be due to the effect of the electron donor *t*-Bu groups.

The tetranuclear iron(III) $Fe_4(L^{27})_4(HL^{27})_4$ species is formed from the reaction of iron(III) chloride with salicylaldoxime (H_2L^{27}) [78]. Magnetic data for this compound have yet to appear in the literature.

Reaction of ferrous acetate with salicylaldoxime (H_2L^{27}) in methanol, followed by addition of (**5**)$FeCl_3$ and NEt_3 gives a brown precipitate and deep red–violet solution. The brown precipitate has been characterized as $[(\mathbf{5})Fe^{III}(L^{27})_3Fe^{III}]$, whose structure is shown in Fig. 13. Addition of a perchlorate salt to the red–violet solution yields dark brown crystals containing $[(\mathbf{5})_2Fe_4(L^{27})_2(\mu_3\text{-}O)_2(\mu_2\text{-}CH_3COO)_3](ClO_4)$ which has been structurally characterized [68]. Similar structural data have been obtained also for diphenylglycolate as the bridging carboxylate, $[(\mathbf{5})_2Fe_4(\mu_3\text{-}O)_2(\mu_2\text{-}OOC{\cdot}C(OH)Ph_2)_3(L^{27})_2]ClO_4$ [79].

The structure of the cations is based on the $[Fe_4(\mu_3\text{-}O)_2]^{8+}$ core with a butterfly arrangement of iron atoms based on two edge sharing $Fe_3(\mu_3\text{-}O)$ units (Scheme 2). There are three bridging carboxylates and two bridging –NO groups from the deprotonated oximes. Two central iron centers are in a distorted octahedral environment with the two chelated by phenolate oxygens having NO_5 coordination while the two coordinated to the macrocycle **5** have N_3O_3 coordination spheres.

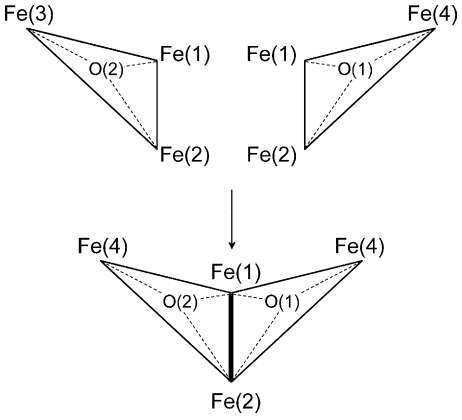

Scheme 2.

The Mössbauer spectra for both of these compounds confirm not only the high-spin electron configuration for the iron ions ($S = 5/2$), but also show two iron sites with different coordination spheres, in agreement with the molecular structures and are thus called 'body' and 'wing-tip' pairs of Fe(III) ions.

A 'two-*J*' model (Scheme 3) was applied to analyze the magnetic properties of these butterfly complexes and the bis-μ_3-oxo-core is represented below, where J_{wb} is the wing-tip/body and J_{bb} is the body/body interactions,

$$\hat{H} = -2J_{wb}(\hat{S}_1 \cdot \hat{S}_3 + \hat{S}_2 \cdot \hat{S}_3 + \hat{S}_1 \cdot \hat{S}_4 + \hat{S}_2 \cdot \hat{S}_4) - 2J_{bb}(\hat{S}_1 \cdot \hat{S}_2)$$

where S_i $(i = 1, 2, 3, 4) = 5/2$

It was noted earlier [64] that J_{bb} cannot be determined precisely from the susceptibility data, but J_{wb} can be evaluated with a reasonable accuracy. Additionally, the quality of the fit is negligibly dependent on J_{bb}; J_{bb} was therefore kept fixed at 0. Selective fitting parameters obtained are: $J_{wb} = -46.1$ cm^{-1}, $J_{bb} = 0$ (fixed) for the acetate complex and $J_{wb} = -41.4$ cm^{-1}, $J_{bb} = 0$ (fixed) for the glycolate complex and compare well with those reported in the literature [64]. The 'body–body' Fe(1)···Fe(2) interaction, J_{bb}, is dominated by the 'wing–body' Fe(3)···Fe(1) exchange interactions, J_{wb}, resulting in the overall favoured spin alignment, represented in Scheme 4.

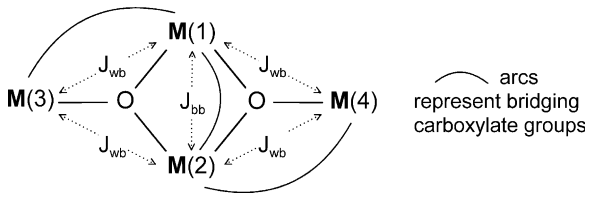

Scheme 3.

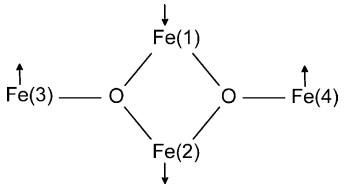

Scheme 4.

The intrinsic character (i.e. antiparallel coupling) of the Fe(1)···Fe(2) interaction, J_{bb}, can thus be ignored resulting in spin frustration in the general sense of the term or more accurately competing spin interactions [80]. This type of spin frustration in polynuclear manganese and iron complexes has been elaborately discussed by Hendrickson [81] and hence we refrain from discussing this further and refer the reader to this treatise.

Ferrous chloride with salicylaldoxime H_2L^{27} and triethylamine in methanol under argon yielded a dark solution, which in the air afforded red–brown crystals of $[(C_2H_5)_3NH][Fe_3O(Salmp)(HL^{27})(L^{27})_2]\cdot 2H_2O$ [82] where H_3Salmp is a new ligand [2-(bis(salicylidenamino)-methyl)phenol], which is generated in situ in the course of the reaction. The generation of H_3Salmp was explained on the basis of a reductive hydrolysis reaction pathway, involving deoxygenation of the oxime by the metal center, as outlined in Scheme 5

The trinuclear iron complex is based on an asymmetric $[Fe_3^{III}(\mu_3\text{-}O)(\mu_2\text{-}OPh)]^{6+}$ core. The core $[M_3^{III}(\mu_3\text{-}O)(\mu_2\text{-}OPh)]^{6+}$ is ubiquitous [83] and can be obtained for Ti(III), V(III), Cr(III), Mn(III), Fe(III) with the general composition

$$[(C_2H_5)_3NH][M_3^{III}(\mu_3\text{-}O)(Salmp)(HL^{27})(L^{27})_2]$$

Except for the corresponding Ti(III) complex, all the complexes are characterized crystallographically. As the complexes are isostructural, we will deal with all these compounds together in this Section 6.3 on iron. The structures of the trinuclear iron [82] and vanadium [83] were described earlier [22b], the manganese- and chromium structures belonging to yet unpublished results are described here. The molecular structures of the anion $[M_3(\mu_3\text{-}O)(Salmp)(HL^{27})(L^{27})_2]^-$, [M = Mn(III) or Cr(III)] together with a view of the first coordination spheres of the M(III) ions [84] are shown in Fig. 14.

The structure is an archetype of the trinuclear complexes containing the structural unit $[M_3^{III}(\mu_3\text{-}O)(\mu_2\text{-}OPh)]^{6+}$. The manganese atoms Mn(1) and Mn(2) have pseudo octahedral N_2O_4 coordination, while Mn(3) is in a trigonal pyramidal NO_4 environment. The uninegative charge of the anion leads us to conclude that the oxygen O(32) of the hydroxy group in the salicylaldoxime, bonded only to Mn(3), is protonated. The disposition of the μ_3-oxide O(1) is not symmetrical, the differences being significant, Mn(1)–O(1) 1.964(8) Å, Mn(2)–O(1) 1.977(8) Å and Mn(3)–O(1) 1.905(7) Å. One metal center in the trinuclear unit is always *five coordinate*, *even in the Cr(III) compound*.

The exchange coupling model used, shown in Scheme 6, to analyze the variable-temperature magnetic suscept-

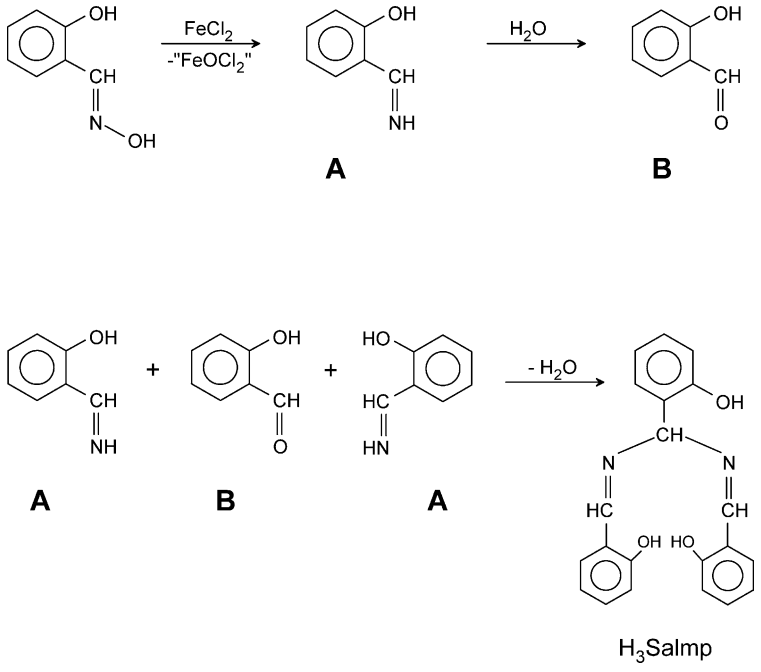

Scheme 5.

ibility data contains two J's, $J_{13} = J_{23} = J$ describing the interaction of M(3) with M(1) and M(2), $J_{12} = J'$ the interaction between the M(1) and M(2) ions, as the trinuclear M(III) framework forms an isosceles triangle.

The simulation of the experimental magnetic data by using a computer program with a full-matrix diagonalization approach using the $H = -2JS_i \cdot S_j$ convention has been performed for the V_3^{III}, Cr_3^{III}, Mn_3^{III} and Fe_3^{III}

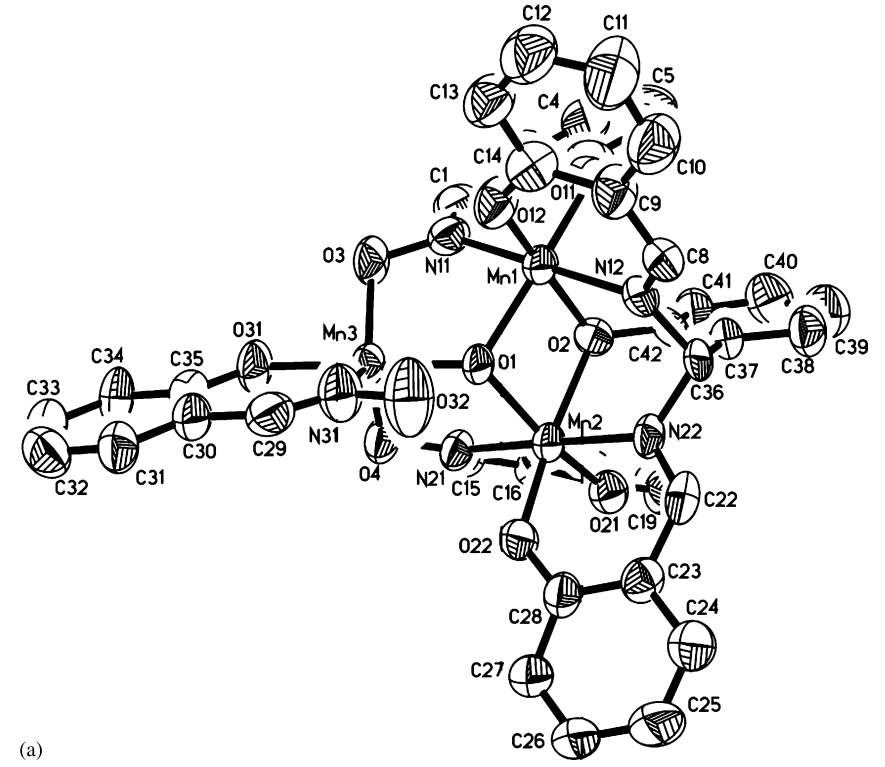

(a)

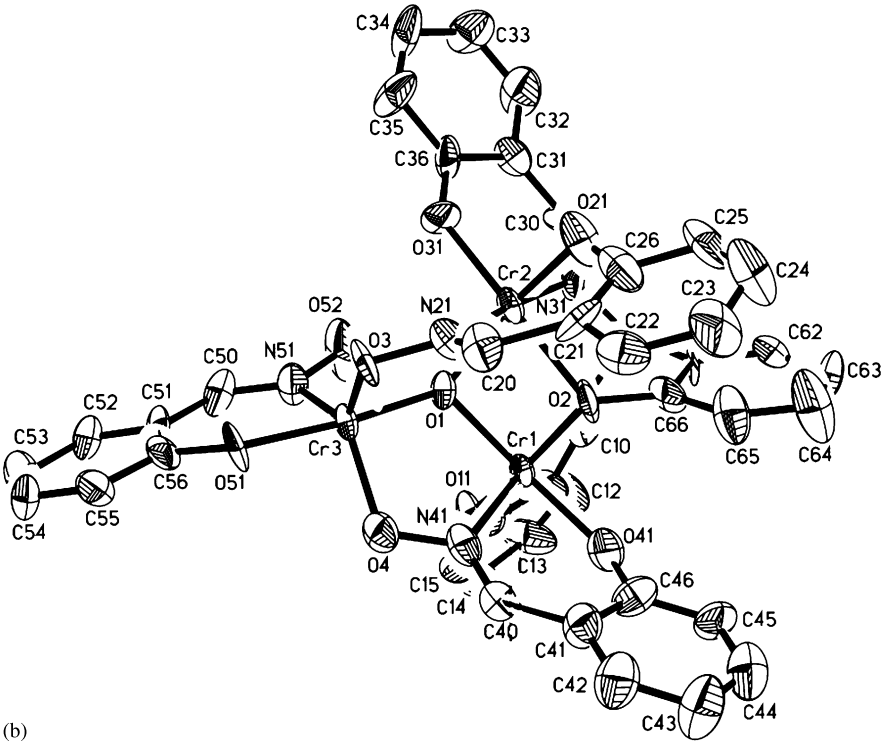

(b)

Fig. 14. Molecular structures of the anions: (a) $[Mn_3(\mu_3\text{-O})(Salmp)(HL^{27})(L^{27})_2]^-$ and (b) $[Cr_3(\mu_3\text{-O})(Salmp)(HL^{27})(L^{27})_2]^-$ together with (c) the metal(III) coordination spheres. Reproduced with permission from Ref. [84].

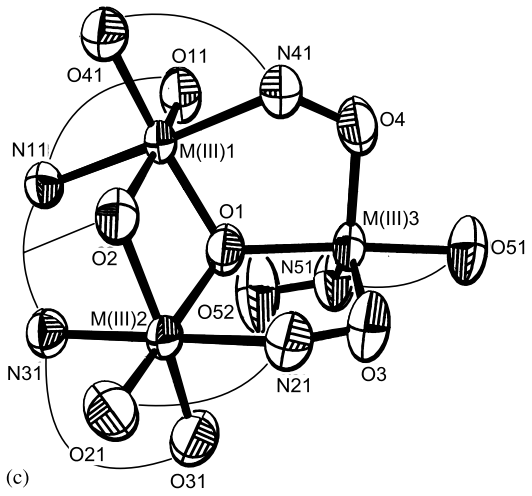

Fig. 14 (*Continued*)

complexes. For comparison purpose only the exchange coupling constants are reported below:

	$J_{13}=J_{23}$ (cm^{-1})	J_{12} (cm^{-1})
$[V_3(\mu_3\text{-O})(\mu_2\text{-OPh})]^{6+}$	+4.0	−26.9
$[Cr_3(\mu_3\text{-O})(\mu_2\text{-OPh})]^{6+}$	−10.8	−5.3
$[Mn_3(\mu_3\text{-O})(\mu_2\text{-OPh})]^{6+}$	+0.23	−0.15
$[Fe_3(\mu_3\text{-O})(\mu_2\text{-OPh})]^{6+}$	−34.3	−4.7

In contrast to the antiferromagnetic coupling between the V(III) centers reported in the literature for $[V_3O]^{7+}$ cores [85,86], the exchange $J_{13}=J_{23}=J$ in the V(III)-trimer is of weak ferromagnetic nature. A butterfly complex with $[V_4O_2]^{8+}$ core has recently been reported [87] with a ferromagnetic spin coupling between the wing-tip and body V(III) ions. On the other hand, the J_{12} interaction describing the exchange paths through the phenoxide and μ_3-oxide groups is antiferromagnetic, indicating substantial antiferromagnetic contribution by the μ_2-OPh bridge. In other words, the oximate groups probably transmit ferromagnetic exchange between the V(III) ions.

The $[M_3(\mu_3\text{-O})(\mu_2\text{-OPh})]^{6+}$ unit can be viewed as a trinuclear $[M_3O]^{7+}$-unit to which has been added an phenoxide PhO^- moiety. Phenolate bridge formation between M(1) and M(2) increases the M(1)–μ_3-O and

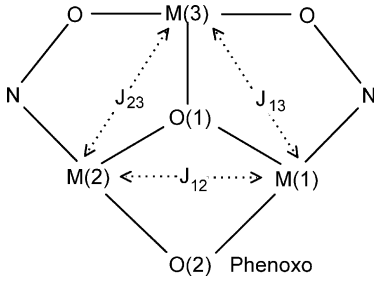

Scheme 6.

M(2)–μ_3-O bond lengths and thus diminishes the antiferromagnetic exchange coupling in a manner similar to protonation or metalation of the μ-oxo bridge. Thus the exchange interaction along the short edge of the isosceles triangle J_{12} is comparatively weaker. The occurrence of oximate bridges along the edges complicates the situation, however. For the manganese(III) compound, the antiferromagnetic contributions are balanced by the ferromagnetic contributions resulting in three manganese(III) centers being practically uncoupled(!!).

Spin frustration results naturally from the triangulated topological arrangement of metal ions. We employ the term 'spin frustration' for the general situation [81], where competing exchange interactions of comparable magnitude lead to the prevention (frustration) of preferred spin alignments, and not in the sense of 'orbital degeneracy' [80]. If all of the pairwise interactions in the M_3-triangle are antiferromagnetic, as is in most of the cases here, the origin of this frustration is easily understood. The spins on each Fe(1)/Fe(3) and Fe(3)/Fe(2) are paired, because these antiparallel interactions ($J=-34.3$ cm^{-1}) dominate the interaction between the Fe(1) and Fe(2) ions ($J'=-4.7$ cm^{-1}). This frustrates the spins on the Fe(1) and Fe(2) ions, as the intrinsic nature of the interaction (J') is antiferromagnetic. The unpaired electrons on Fe(1) and Fe(2) want to pair, but they cannot and hence are frustrated. A very similar situation prevails in the chromium(III) complex (Fig. 15).

The situation for the manganese(III) complex is more complicated and warrants further investigation.

Black crystals of $[Fe_4(L^{29})_3(NO)_3]$ contain, as seen from the X-ray analysis, three iron-nitrosyl complexes binding the fourth iron in an octahedral cavity with six oxygen donor atoms of the oximate groups [88]. A plausible stepwise formation of the mixed-valence

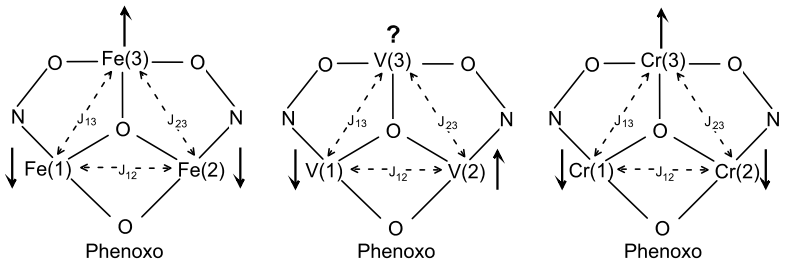

Fig. 15. Spin frustration in $[M^{III}_3(\mu_3\text{-O})(\mu_2\text{-OPh})]$-core.

tetrairon complex as suggested by the authors is shown in Scheme 7.

The coordination around the central iron FeO_6 is close to a regular octahedron whereas the three peripheral iron atoms are in a slightly distorted square-pyramid with the nitrosyl groups at the axial positions. The effective magnetic moment of 4.37 μ_B at 292 K for the tetranuclear unit does not provide any information on the electronic structure of this interesting molecule, which needs further study.

A modular approach for preparing linear tetranuclear complexes of the type $M_AM_BM_BM_A$, where the two central metal ions are embedded in a dicompartmental oxime ligand 2,6-diformyl-4-methylphenoldioxim, H_3L^{30}, as a singular building block is depicted schematically in Scheme 8.

Realization of this synthetic strategy is documented by the preparation of $[(\mathbf{5})Fe^{III}\{(L^{30})_3Fe^{II}_2\}Fe^{III}(\mathbf{5})]BPh_4$ which exhibits a diamagnetic ground state [89].

The four high-spin metal ions, two terminal Fe(III) and two central Fe(II) ions, are disposed in a linear fashion ($180 \pm 1^\circ$). The central tris(oximato)bisferroate(II) ion, $[Fe_2(L^{30})_3]^{5-}$, bridges two terminal iron(III) centers through the deprotonated oxime oxygen atoms. An intramolecular Fe(1)···Fe(4) separation of 9.885 Å was found.

Hexanuclear iron(III) complexes containing two triangular $[Fe_3(\mu_3\text{-O})]$-units linked via two oximic oxygen atoms have the following general composition $[Fe^{III}_6(\mu_3\text{-O})_2(L^{27})_6(RCOO)_2(H_2O)_2(RCN)_2]$ [96,97] and exhibit a diamagnetic ground state. Their manganese(III) and chromium(III) analogs will be described in more detail in Sections 6.4 and 6.5.

6.4. Manganese complexes

Manganese-complexes of various nuclearity, viz. dinuclear, linear trinuclear, tetranuclear and hexanuclear, with various oxime ligands are known. Like the iron complexes, oximic nitrogen (>C=N–) stabilizes in the absence of the phenolate donors the +II oxidation state. Thus the isolated dinuclear and trinuclear complexes with the ligands dimethylglyoxime (H_2L^1) and pyridine-2-aldoxime (HL^{14}) contain localized mixed-valence Mn(III)Mn(II) ions, whereas all manganese centers in the tetranuclear and hexanuclear complexes with the phenol-containing oxime, salicylaldoxime H_2L^{27}, are in the +III oxidation states (h.s. d^4). We will see in this section that the overall exchange interaction in the oximate bridged h.s. d^5–h.s. d^4 systems is of a weak ferromagnetic nature. In the linear trinuclear complexes two different coupling constants, $J = J_{12} = J_{23}$ and J_{13}

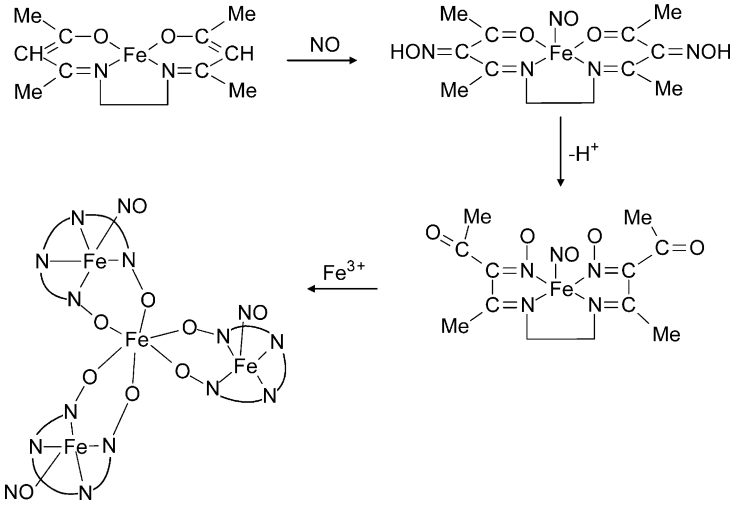

Scheme 7.

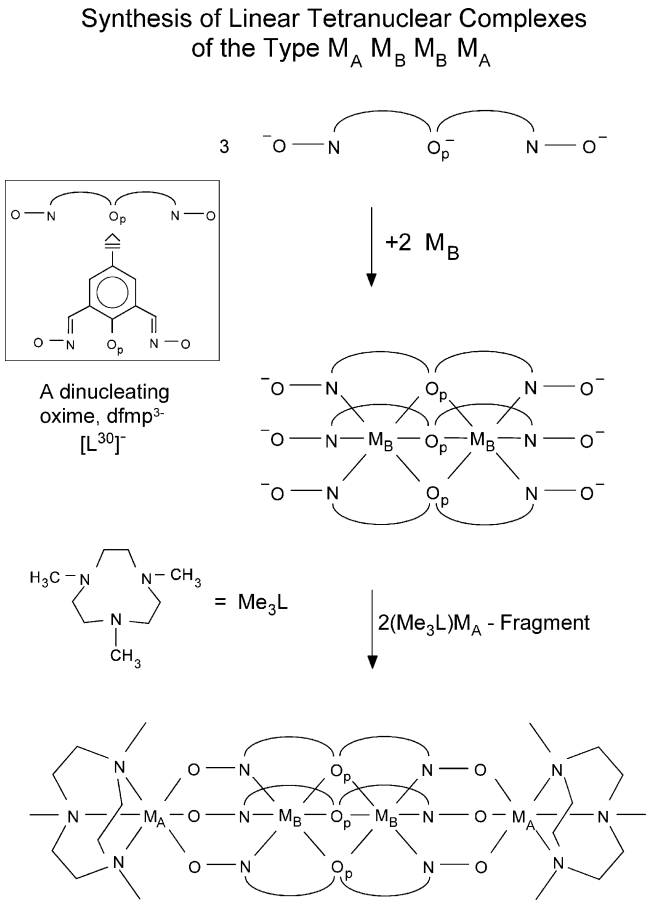

Scheme 8.

are operative. J_{13} describes the exchange interactions between two terminal paramagnetic centers separated by as large as $\sim$7 Å. Complexes of the type $M_AM_BM_A$ exhibit irregular spin-level structures, whose ordering is a result of the mutual influence of two different interactions J and J_{13}, leading in some cases to ground-state variability. These points are delineated in detail by the results described below.

A modular approach using tris(pyridine-2-aldoximato)manganese(II)anion, $[Mn^{II}(L^{14})_3]^-$ and $[Mn^{III}(\mathbf{5})]$-cores yields a localized mixed-valence $Mn^{III}Mn^{II}$ species, $[(\mathbf{5})Mn^{III}(L^{14})_3Mn^{II}]^{2+}$ [91], whose structure is shown in Fig. 16.

The two manganese centers are bridged by three –NO linkages and separated by a distance of 3.686(2) Å. The interaction between the magnetic centers was found to be ferromagnetic ($J = +1.8$ cm^{-1}) yielding a ground state of $S_t = 9/2$, which has been confirmed by the VT-magnetization measurements at different fields (1, 4 and 7 T). The net exchange interaction in a d^4(h.s.)/d^5(h.s.) system is expected to be weak resulting from both antiferromagnetic and ferromagnetic contributions. Qualitatively, the interactions between the e_g^*-type magnetic orbitals on the manganese(II) ion and t_{2g}-type magnetic orbitals on the manganese(III)-ion, as propagated by the sp^2-hybridized O and N atoms of the bridging oxime groups, will largely be orthogonal and consequently ferromagnetic in origin.

An interesting trinuclear manganese(II) complex is $Mn_3(L^{32})_6$, in which (phenylazo)benzaldoxime HL^{32} acts as the ligand in the deprotonated form [92]. The trinuclear N,O-coordinated complex contains both low-spin ($S = 1/2$) and high-spin ($S = 5/2$) manganese(II) centers. The structure of the compound has been determined by X-ray crystallography [93]. The atom connectivity is shown schematically in Fig. 17.

The effective magnetic moment of $[Mn_3(L^{32})_6]$ varies only slightly from 6.9 to 7.2 μ_B in the temperature range 10–300 K and no evidence for any large exchange interaction was obtained [92]. As a ferromagnetic interaction, albeit weak, is expected, a detailed magnetic study of this compound is worth doing.

The X-ray structure of a linear trinuclear complex (Mn(2)–Mn(1)–Mn(2a) = 179.2°) containing a central manganese(II) and two manganese(III) as terminal ions in their high-spin electronic configurations is shown in Fig. 18 [94].

The central tris(dimethylglyoximato)manganese(II) ion, $[Mn(L^1)_3]^{4-}$, bridges the two terminal manganese(III) centers through the deprotonated oxime oxygens. The terminal manganese coordination geometry is distorted octahedral with three nitrogen atoms from the facially coordinated tridentate macrocyclic amine **5** and three oxygen atoms from three bridging oximate groups. The central $Mn(II)N_6$ core is nearly trigonal prismatic (twist angle 5.7°). The nearest neighbour Mn(2)···Mn(1) distance within the trinuclear cation is 3.571 Å, whereas an intramolecular Mn(2)···Mn(2a) separation of 7.141 Å has been found. Magnetic susceptibility data were analyzed by considering a linear model with J ($= J_{12} = J_{23}$) representing the exchange interaction between the adjacent Mn(III) and Mn(II) ions, and where J_{13} describes the interaction between the terminal manganese(III) ions. The nearest-neighbour interaction between the manganese(III) and the manganese(II) centers, J, is ferromagnetic (+4.7 cm^{-1}), while J_{13} between the terminal ions is antiferromagnetic (−3.0 cm^{-1}). Because of the competing influence of J and J_{13} upon spin coupling in the $Mn^{III}Mn^{II}Mn^{III}$ species, the ground-state properties are determined by the two, practically degenerate, spin states 11/2 and 13/2. Similar ground-state variability has been found for several other systems and will be described later. J_{13} is operative between two terminal paramagnetic centers separated by as large as $\sim$7 Å.

Deep brown crystals of $[(HL^{31})_2Mn^{II}_2(\mu\text{-}OOC{\cdot}OCH_3)(CH_3OH)Mn^{III}](ClO_4)_2$ [90], contain the monoprotonated ligand 1,4,7-tris(acetophenoneoxime)-1,4,7-triazacyclononane, H_3L^{31}, with one of the oxime groups protonated and non-coordinated. Interestingly, a bridging monomethyl carbonato-ligand formation occurs

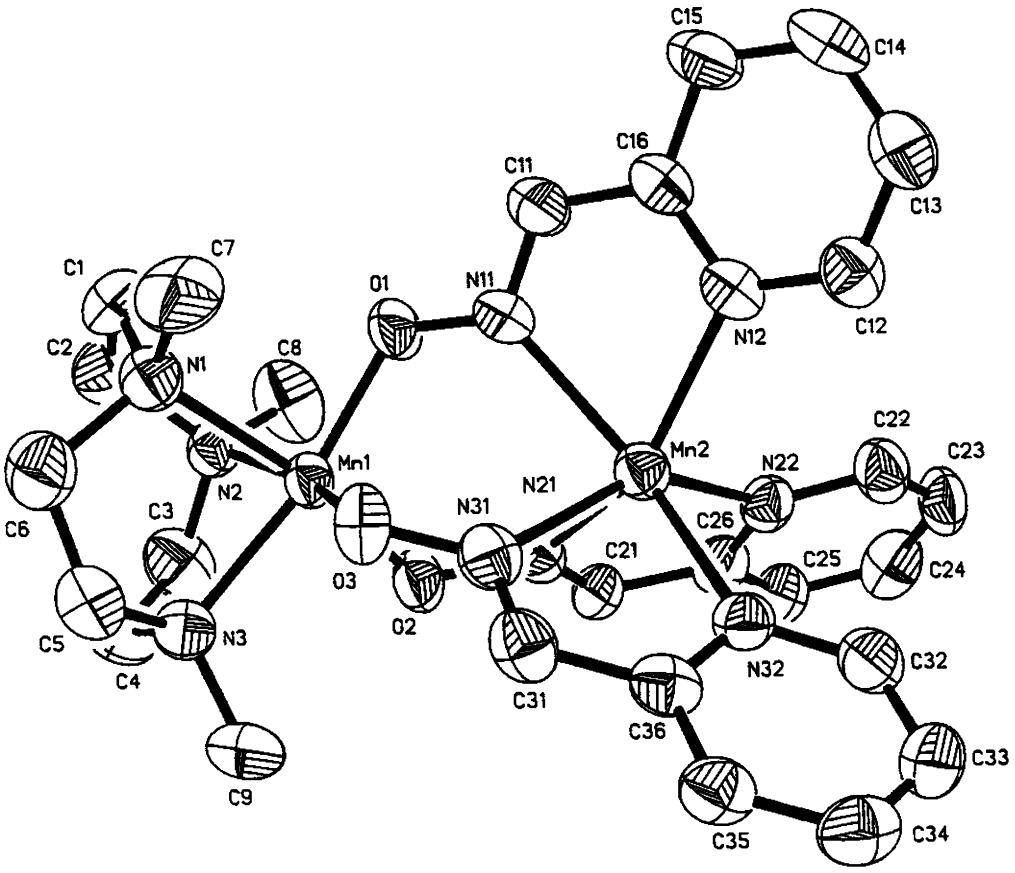

Fig. 16. Solid state structure of the dication in $[(\mathbf{5})Mn^{III}(L^{14})_3Mn^{II}](ClO_4)_2$. Reproduced with permission from Ref. [91].

through CO_2-uptake from air by the methanolic solution containing NEt_3 as a base, presumably according to the following reaction:

$$CH_3OH + CO_2 + NEt_3 \rightarrow CH_3OCO_2^- + HNEt_3^+$$

Carbon dioxide is taken up from the air spontaneously and the monomethyl carbonato complex was isolated (70%) as a single product. The coordination spheres of the manganese centers in the trinuclear $Mn^{II}Mn^{III}Mn^{II}$ complex are shown in Fig. 19.

The two terminal Mn(II) centers, Mn(1) and Mn(3), have essentially the same sevenfold coordination, MnN_5O_2, whereas the central Mn(2) is a Jahn–Teller distorted high-spin d^4Mn(III) ion with six oxygen donor atoms. Notably O(70) acts as a monoatomic bridging ligand between Mn(1) and Mn(2), whereas the second oxygen O(71) of the carbonate group is a donor atom only for Mn(3).

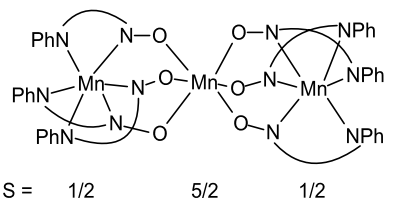

Fig. 17. Schematic representation of the atom connectivity in $Mn_3(L^{32})_6$ as determined by X-ray crystallography. Reproduced with permission from Ref. [93].

Simulation of the experimental magnetic susceptibility data for the localized mixed-valence $Mn^{II}Mn^{III}Mn^{II}$ species was performed using a full-matrix diagonalization approach of the spin Hamiltonian $H = -2J(\hat{S}_1 \cdot \hat{S}_2 + \hat{S}_2 \cdot \hat{S}_3)$ with $S_1 = S_3 = 5/2$ and $S_2 = 4/2$. Considering the large distance of ~ 6.0 Å, the spin interaction between the terminal Mn(II) ions within the trinuclear entity was neglected. An excellent fit with the following parameters was obtained: $J = +2.0\ cm^{-1}$, $g_1 = g_3 = 2.05$, $g_2 = 1.98$. The exchange interaction prevailing between the neighbouring high-spin Mn(II) and high-spin Mn(III) ions is of ferromagnetic nature leading to a ground state of $S_t = 7.0$ for the trinuclear manganese compound with the ligand H_3L^{31}. This is in complete accord with the other Mn^{III}–Mn^{II}-species described in this section. The VT-magnetization measurements at different magnetic fields (1, 4 and 7 T) also confirmed the ground state of $S_t = 7.0$ with a small zero-field splitting, $|D| = 0.6\ cm^{-1}$. Based on the smallest bridging

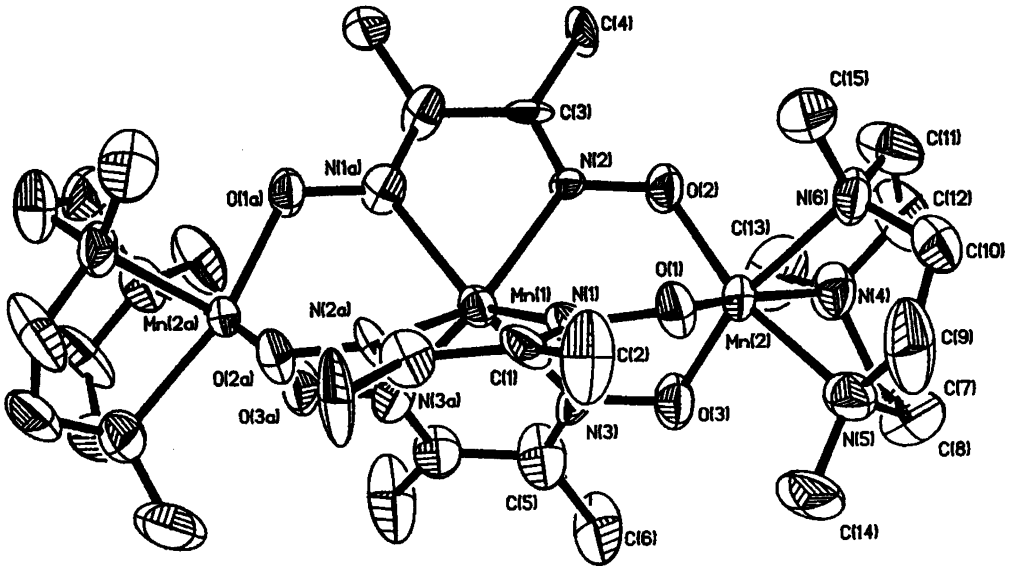

Fig. 18. An ORTEP drawing of $[(\mathbf{5})_2Mn_2^{III}\{(L^1)_3Mn^{II}\}]^{2+}$. Reproduced with permission from Ref. [94].

angle Mn(1)–O(70)–Mn(2) of 89.3° reported so far, a rationale for the parallel spin coupling has been presented [90].

An asymmetric trinuclear manganese(III) complex containing the structural unit $[Mn_3(\mu_3\text{-}O)(\mu_2\text{-}OPh)]^{6+}$, obtained by a Mn(II)-promoted reductive cleavage of salicylaldoxime, has already been described together with its other congeners [82–84] in the section on iron, Section 6.3.

Recently a trinuclear manganese(III) complex having the formula $[Mn_3(\mu_3\text{-}O)(\mu_3\text{-bamen})](ClO_4)$, in which the central planar unit $[Mn_3^{III}(\mu_3\text{-}O)]$ is coordinated to three hexadentate bridging oximate ligands, 1,2-bis(acetylmonoximeimino)ethane, H_2bamen, has been reported [132]. Each Mn(III) center is pentagonal-bipyramidal with N_4O_3 donor atoms. In contrast to antiferromagnetic interactions observed in general for the carboxylate-bridged $[Mn_3^{III}(\mu_3\text{-}O)]^{7+}$-core, this doubly oximate-bridged compound exhibits remarkably strong ferromagnetic interactions ($J = +22.3$ cm^{-1}) transmitted through the oximate groups between the manganese(III) centers.

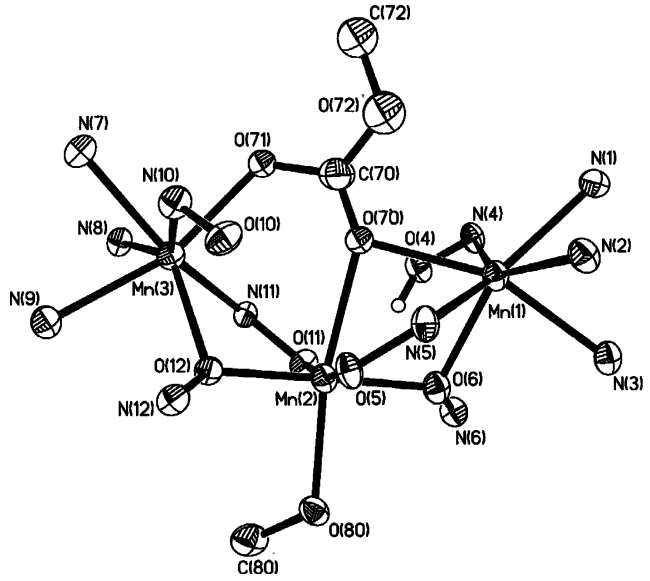

Fig. 19. The coordination spheres of the manganese centers in $[(HL^{31})_2Mn_2^{II}(CH_3OH)(\mu\text{-}OOC{\cdot}OCH_3)Mn^{III}]^{2+}$. Reproduced with permission from Ref. [90].

Similar to tetranuclear iron(III) complexes with a butterfly M_4O_2 core described in Section 6.3, manganese(III) complexes, $[Mn_4O_2]^{8+}$, in which the manganese centers are disposed in a butterfly structure were prepared by using salicylaldoxime (H_2L^{27}) and different carboxylic acids [79]. The structure of the cation in the complex $[(\mathbf{5})_2Mn_4^{III}(L^{27})_2(\mu_3\text{-}O)_2\{Ph_2C(OH)COO\}_3](ClO_4)$ is reported in Ref. [79]. The cation possesses an Mn_4O_2 core, and the structure is very similar to that in other $[Fe_4O_2]^{8+}$ and $[Mn_4O_2]^{8+}$ complexes reported in the literature [64,65,68,79,95]. Field-dependent magnetization measurements at 2 K up to 6 T and the variable-temperature susceptibility measurements at 1 T demonstrate that the ground state is $S_t = 3$ (simulation with $S = 3.0$ (fixed), $g = 2.02$, $|D| = 4.13$ cm^{-1}). The ground state is within 5 cm^{-1} of the first excited one with $S_t = 4$. As the μ_3-oxo atom provides the main super-exchange pathway and the exchange through the oximate groups is not of significant importance, and the spin interactions in these butterfly complexes have been described in detail previously [64,65,67,81], these compounds albeit oximate bridging, will not be discussed further.

We have discovered that the hexanuclear complexes with the $[M_6^{III}(\mu_3\text{-}O)_2]$-core [M = V, Cr, Mn, Fe] are not very unusual species and can be obtained through a

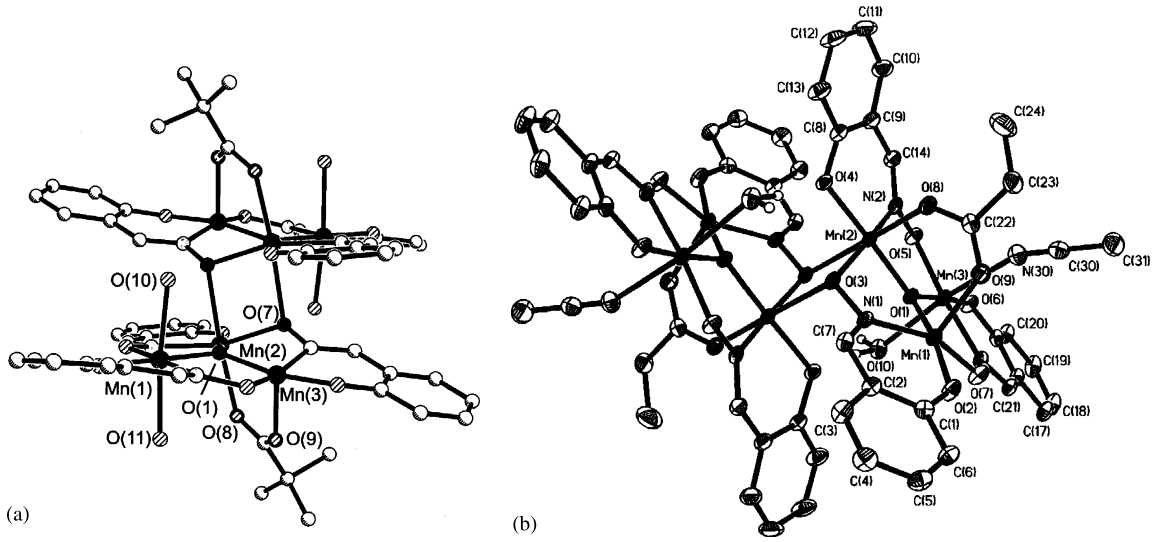

Fig. 20. Structures of: (a) $[Mn_6^{III}(pivalate)_2(L^{27})_6(OH_2)_4(\mu_3\text{-}O)_2]$; and (b) $[Mn_6^{III}(propionate)_2(L^{27})_6(OH_2)_2(CH_3CN)_2(\mu_3\text{-}O)_2]$. Reproduced with permission from Refs. [96,97].

general synthetic route [96,97]. The hexanuclear compounds with the general composition

$$[M_6^{III}(\mu_3\text{-}O)_2(L^{27})_6(\mu_2\text{-}OOCR)_2(OH_2)_2(RCN)_2]$$

or

$$[M_6^{III}(\mu_3\text{-}O)_2(L^{27})_6(\mu_2\text{-}OOCR)_2(OH_2)_4]$$

where L^{27} represents the dianion of salicylaldoxime, $RCOO^-$ carboxylate anions such as triphenylacetate, pivalate, benzilate, benzoate or propionate, and RCN a nitrile like acetonitrile, propionitrile or butyronitrile, have been synthesized and found to be structurally isotypic. As representatives of the above two types the structures of $(L^{27})Mn_6^{III}(pivalate)_2(OH_2)_4(\mu_3\text{-}O)_2$ and $(L^{27})_6Mn_6^{III}(propionate)_2(OH_2)_2(CH_3CN)_2(\mu_3\text{-}O)_2$ are shown in Fig. 20(a and b), respectively [96].

The hexanuclear complexes are built up of two identical μ_3-oxo centered trinuclear $[Mn_3(\mu_3\text{-}O)]$ units, which are bridged by two oximic oxygen atoms. In each $[M_3(\mu_3\text{-}O)]$ unit two metal ions are bridged additionally by a carboxylate group that leads to a significant distortion of the trinuclear unit. Two of the three manganese centers in each triangular unit have sixfold coordination, whereas the third manganese is five-coordinated and best described as a square-pyramidal with an NO_4 donor atoms.

No significant structural changes result from varying bridging carboxylates for the hexanuclear manganese(III) compounds. Interestingly, magnetic measurements clearly show an influence of the bridging carboxylate anions on the strength of the coupling constants. The exchange-coupling model with the Hamiltonian used is described in Scheme 9.

The parameters obtained from the simulation of the experimental susceptibility data are

Mn_6-propionate:	$J_1 = -4.8\ cm^{-1}$, $J_2 = -0.27\ cm^{-1}$
	$J_3 = +0.34\ cm^{-1}$, $g = 1.92$
Mn_6-benzilate:	$J_1 = -5.35\ cm^{-1}$, $J_2 = +0.08\ cm^{-1}$
	$J_3 = +6.5\ cm^{-1}$, $g = 1.83$
Mn_6-benzoate:	$J_1 = -3.26\ cm^{-1}$, $J_2 = -0.27\ cm^{-1}$
	$J_3 = +2.5\ cm^{-1}$, $g = 1.95$
Mn_6-triphenylacetate:	$J_1 = -5.43\ cm^{-1}$, $J_2 = +4.24\ cm^{-1}$
	$J_3 = +2.31\ cm^{-1}$, $g = 1.85$

J_3 transmitted through the monoatomic oximic oxygen is of ferromagnetic nature. As the μ_3-oxo ion and not the oximate(NO)-bridging provides the principal superexchange pathway and the coupling constants are small, we refrain from discussing the individual coupling constants.

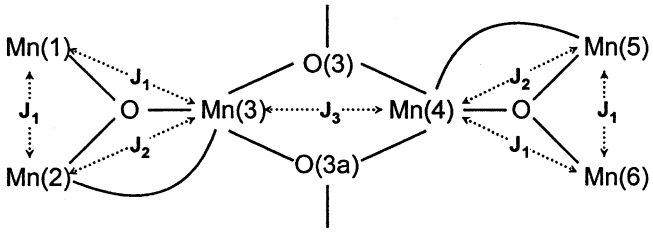

represents the bridging carboxylato-anions

$$H = 2J_1(S_1 \bullet S_2 + S_1 \bullet S_3 + S_4 \bullet S_6 + S_5 \bullet S_6) - 2J_2(S_2 \bullet S_3 + S_4 \bullet S_5) - 2J_3(S_3 \bullet S_4).$$

Scheme 9.

6.5. Chromium(III) complexes

A dinuclear mixed-valence (d^3/d^4-system) compound $[(\mathbf{5})Cr^{III}(L^{14})_3Cr^{II}](ClO_4)_2$ containing pyridine-2-aldoximato, $(L^{14})^{2-}$, as the bridging ligands has been reported [28], in which the chromium(III) and chromium(II) centers are antiferromagnetically coupled ($J = -7.9$ cm^{-1}). Unfortunately, no structural data are yet available for the compound.

A novel 14-membered metallamacrobicycle containing two chromium(III) ions as part of the ring skeleton, $[(\mathbf{5})_2Cr^{III}_2(HL^1)_2(L^1)](ClO_4)_2$ [98], has been synthesized as red prisms. The X-ray structure and a schematic view of the 14-membered metallamacrobicycle are shown in Fig. 21. The coordination geometry of the chromium ions is distorted octahedral with three nitrogen atoms from the facially coordinated tridentate macrocyclic amine **5** and three oxygen atoms from three bridging dimethylglyoximato ligands resulting in *fac*-CrN_3O_3 cores. Two significant residual electron densities at a distance of ca. 1 Å from N(1) and N(3) have been assigned to two statistically disordered protons. The presence of these protons is also in conformity with the pH-metric titration of the complex with NaOH ($pK_1 = 10.72 \pm 0.03$ and $pK_2 = 4.39 \pm 0.08$ at 25 °C, $I = 0.1$ M (KNO_3)) and the charge balance consideration, together with the chemical analysis. Noteworthy, substitution of these two protons by a divalent metal ion, e.g. Fe^{II}, is a kinetically very slow process.

The chromium(III) centers are antiferromagnetically coupled ($J = -4.7$ cm^{-1}) yielding a diamagnetic ground state ($S_t = 0$). A moderate exchange coupling is observed in a dinuclear compound, in which the Cr(III) centers are separated by the large distance 7.27 Å, showing the effectiveness of oximate groups in transmitting spin-coupling.

Leaving the trinuclear chromium(III) complex with the core $[Cr_3(\mu_3\text{-}O)(\mu_2\text{-}OPh)]^{6+}$ which has been described in Section 6.3, the only other example of a homochromium(III) complex with a reported X-ray structure is a hexanuclear species containing salicylaldoxime (H_2L^{27}) as the oxime ligand [97]. The addition of H_2L^{27} and NEt_3 to a previously prepared green solution of CrF_2 and $CaCl_2$ in methanol and propionic acid affords a brown solution, which was kept open to air to yield a brown solid. Recrystallization from propionitrile produced brown crystals of $[Cr^{III}_6(\mu_3\text{-}O)_2(L^{27})_6(\mu_2\text{-}OOC\cdot C_2H_5)_2(OH_2)_2(C_2H_5CN)_2]$, shown in Fig. 22.

The hexanuclear structure comprises two identical μ_3-oxo centred trinuclear $[Cr_3(\mu_3\text{-}O)]$ units. Two of the three chromium atoms in each triangular unit have distorted octahedral environments with coordination spheres of N_2O_4 and NO_5. The remaining *chromium Cr(1) is five-coordinated*, providing a rare example of a non-octahedral Cr(III), and is best described as square-pyramidal with an NO_4 donor set.

The exchange coupling model shown in Fig. 23 was considered for simulation of the experimental magnetic data using the irreducible tensor operator (ITO) [99] mathematical method with the Heisenberg Hamiltonian in the form $H = -2JS_i \cdot S_j$.

The best fit, shown as the solid line in Fig. 23, yields the following parameters:

$J_1 = -14.2$ cm^{-1}, $J_2 = +12.8$ cm^{-1},

$J_3 = +5.3$ cm^{-1}, $g = 2.13$.

The ground state $S_t = 3$, lying 18.4 cm^{-1} below the first excited state $S_t = 2$, is also confirmed by the field-

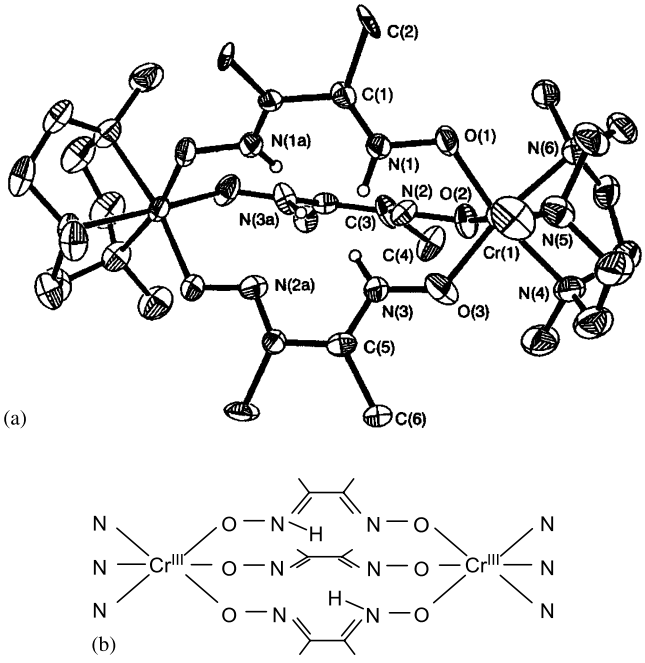

Fig. 21. Structure of the cation $[(\mathbf{5})_2Cr_2(HL^1)_2(L^1)]^{2+}$ and a schematic view of the 14-membered metallamacrobicycle. Reproduced with permission from Ref. [98].

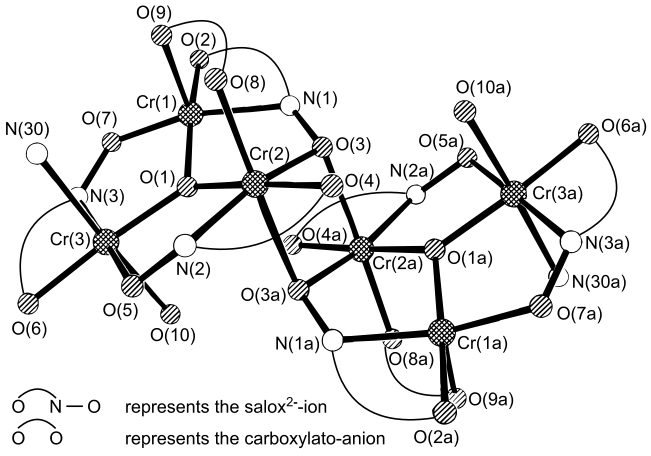

Fig. 22. A view of the first coordination spheres of the chromium(III) ions in the hexanuclear complex. Reproduced with permission from Ref. [97].

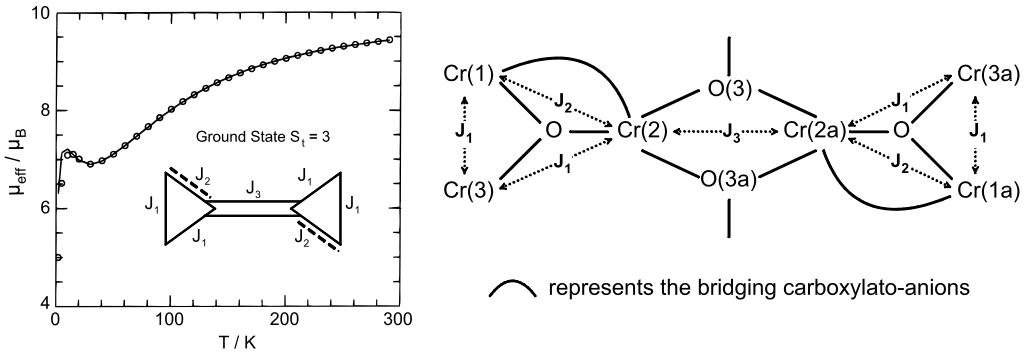

Fig. 23. A plot of μ_{eff} vs. T for the $[Cr(III)]_6$-complex. The solid line is the calculated curve. The coupling model is illustrated on the right-hand side. Reproduced with permission from Ref. [97].

dependent magnetization study at 5 K in the 0.5–6.5 T magnetic field range.

The antiferromagnetic coupling between the Cr^{III} centres reported in the literature for $[Cr_3O]^{7+}$ cores, typically $J = -9.5$ cm^{-1}, is weaker than $J_1 = -14.2$ cm^{-1} for the present complex, although it is generally accepted that in compounds of this type the μ_3-oxo ion provides the principal superexchange pathway. J_2 and J_3 are of ferromagnetic nature. As the interpretation of magnetic data for the hexanuclear Cr^{III} is difficult at the present state of knowledge, we do not discuss the individual coupling constants. Nevertheless, the coupling between the two trinuclear units $[Cr_3(\mu_3\text{-}O)]$ linked via two μ_2-bridging oximic oxygen atoms with Cr–O(3)–Cr angle of 99.3° is ferromagnetic ($J_3 = +5.3$ cm^{-1}).

6.6. Miscellaneous

Reports on the magnetochemistry of polynuclear homometal cobalt(II) complexes with oxime ligands are scarce. One reason behind the scarcity may be the orbital degeneracy of the Co(II) ion in octahedral surroundings that forbids interpretation of the low-temperature magnetic data with an isotropic spin Hamiltonian. The structure of the cobalt(II) compound with the diaminoglyoxim (H_2L^{33}) ligand was reported as early as 1977 [100] but without magnetic data. The structure of $Co(HL^{33})_2(H_2L^{33})$ consists of chains of planar $Co^{II}(HL^{33})_2$ units stacked along the b-axis, through long Co–N bonds (2.64 Å) to terminal N atoms of the adjacent molecular units. The stacked chains form sheets in the bc plane. Magnetic data [101] reveal the low-spin state of the Co(II) centers, with the unpaired electron residing in the d_{z^2} orbital. The existence of a ferromagnetic interchain interaction ($J = +9.04$ cm^{-1}) along the b-axis, accompanied by a very weak interchain antiferromagnetic interaction ($J' = -0.005$ cm^{-1}!!) in the bc-plane have been observed. Thus, the compound exhibits one-dimensional ferromagnetic interactions. The interaction of the d_{z^2} orbital of the Co(II) center with the π-systems of the adjacent molecules (the two apical N atoms) was proposed to be the principal superexchange path.

Polymeric complexes, $[Co^{II}(HL^1)_2(Pyrazine)]_n$ and $[Co^{II}(HL^{11})_2(Pyrazine)]_n$, have been reported [102]. The crystal structure shows linear chains of alternating cobalt atoms and pyrazine ligands. Perpendicular to the chain, the cobalt atoms are coordinated in a square-planar arrangement by two monoprotonated oximato ligands with remarkably short Co–N bonds, 1.89 Å. The cobalt complexes are paramagnetic with $\mu_{eff} = 1.85$ μ_B at 20 °C. A Weiss constant $\theta = -110$ K(!!) has been found.

The neutral species $[Fe^{II}(HL^7)_2Fe^{III}_2OCl_4]$ was obtained [103] from a methanolic solution of $FeCl_2 \cdot 4H_2O$ and 2,6-diacetylpyridine dioxime (H_2L^7) and its X-ray structure was determined. No magnetic data are available.

7. Heterometal complexes

Investigations of heteronuclear complexes are more informative than those of homonuclear complexes as new exchange pathways can be expected for two different spin carriers within a molecular unit, where unusual sets of magnetic orbitals can be brought in close proximity. For instance, the strict orthogonality of the magnetic orbitals resulting in the stabilization of the spin state of highest multiplicity is much easier to realize in heterometallic systems than in homometallic species. Additionally, designing molecular entities with interesting spin topologies becomes easier with spin carriers of different kinds. Since the pioneering work of Oliver Kahn in the magnetism of heterometallic systems, the field has developed tremendously, as will be evident from the following discussion on the oximato-bridged heterometallics of different nuclearity.

7.1. Dinuclear complexes

The module, $[Cu(L^{13})(H_2O)]\cdot 3H_2O$ in which the copper(II) ion occupies the N_4-central cavity of the polydentate ligand, α,ω-bis(1,3-dimethyl-5-nitrosouracil-6-yl)-amino)propane, H_2L^{13}, reacts with another module with a different ligand, $[Ni(\mathbf{6})](ClO_4)_2$ in aqueous medium to afford the compound of formula $[Cu(ClO_4)(\mu\text{-}L^{13})Ni(\mathbf{6})]ClO_4\cdot H_2O$ [104] [Fig. 24(a)]. When the copper precursor $[Cu(L^{13})(H_2O)]\cdot 3H_2O$ reacts with a different Ni(II) species, $[Ni(OH)(Me_3[12]N_3)]_2(ClO_4)_2$, in aqueous perchloric acid medium, dark-red crystals $[Cu(ClO_4)(\mu\text{-}L^{12})Ni(Me_3[12]\text{-}N_3](ClO_4)\cdot H_2O$ precipitate out [104] [Fig. 24(b)].

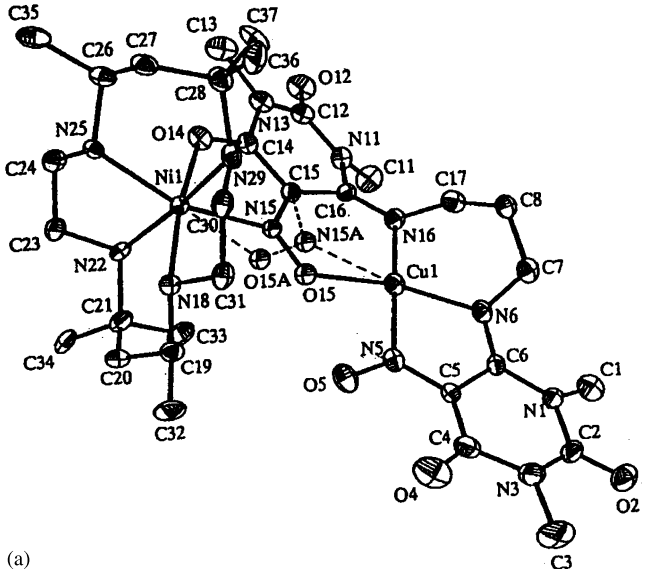

(a)

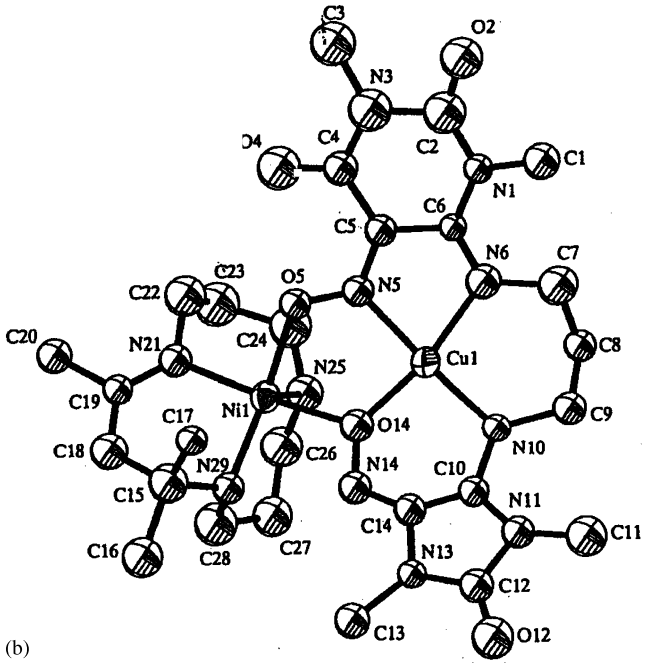

(b)

Fig. 24. (a) Structure of the cation $[Cu(ClO_4)(\mu\text{-}L^{13})Ni(\mathbf{6})]^+$ without the perchlorate ion in the coordination sphere; (b) an ORTEP view of the cation $[Cu(ClO_4)(\mu\text{-}L^{12})Ni(Me_3[12]N_3)]^+$. The perchlorate anion is omitted for clarity. Reproduced with permission from Ref. [104].

The structures of these compounds are shown in Fig. 24(a and b). The coordination of $\{CuL^{13}\}$ to the $[Ni(\mathbf{6})]^{2+}$ moiety takes place through an exocyclic oxygen atom of the uracil ring and a *syn–anti* nitroso–oximato group. The copper(II) ion occupying the inside site of the doubly deprotonated $[L^{13}]^{2-}$ ligand exhibits a distorted coordination environment. The basal plane comprises interestingly two amino and one oximate nitrogen atoms and either an oxygen (occupancy 0.78) or a nitrogen atom (occupancy 0.22) from the other oximato group. The fifth position is occupied by a disordered oxygen atom from a perchlorate anion. The nickel(II) ion is in a distorted octahedral geometry with an oxygen atom of one uracil ring and the disordered nitroso–oximato group in cis-position. The intramolecular Cu···Ni distance is 4.972 Å.

A noticeable feature of the structure containing the $Me_3[12]N_3$-unit is the elimination of one CO molecule from the pyrimidine ring of the H_2L^{13} ligand leading to H_2L^{12} with an imidazole ring. The copper(II) and nickel(II) centers are doubly bridged by one N–O in *syn–syn* fashion and one O-monoatomic oximato group from the pyrimidine and imidazole rings, respectively. The angle at the bridging oxygen is 120°, whereas the Ni···Cu separation is 3.45 Å much shorter than that in the other compound described above. The copper(II) ion is in a distorted square-pyramidal CuN_3O_2 environment with the basal plane comprising two amino, one oximato nitrogens and one oximato oxygen. The Ni(II) ion also with a square-pyramidal NiN_3O_2 coordination sphere has a basal plane defined by two oximato oxygens and two nitrogen atoms from the $Me_3[12]N_3$ ligand; the remaining nitrogen of the latter occupies the apical position.

The magnetic behavior of both complexes shows the spin doublet ($S_t = 1/2$) as the ground state separated from the excited quartet state ($S_t = 3/2$) by an energy of $3J$, thus revealing antiferromagnetically coupled oximato-bridged Cu(II)–Ni(II) pairs. Magnetic parameters evaluated for the Ni(**6**)-containing compound (Fig. 24a) are $J = -66.8\ cm^{-1}$, $g_{Cu} = 2.30$ and $g_{Ni} = 2.24$, whereas the spin interaction in the $Ni(Me_3[12]N_3)$-containing compound is presumably so strong that complete spin pairing occurs even at room temperature, i.e. $J \leq -500\ cm^{-1}$. X-band EPR spectra for both compounds below 50 K are typical of a doublet spin state. At 77 K and above a half-field signal around $g \approx 4.0$ arising from the quartet excited state is observed for the former compound containing the six-coordinated nickel(II) centre, whereas the latter compound with square-pyramidal nickel(II) does not exhibit any signal at $g \approx 4$, assignable to the $M_s = +1/2$ Kramers doublet belonging to the

quartet excited state. Based on the relatively large Cu–O–Ni bridging angle of 120° and the nature of the bridging groups, a rationalization for the complete spin-pairing even at room temperature for the second Cu(II)–Ni(II) pair has been forwarded. Complete spin pairing even at room temperature for a Cu(II)Ni(II) pair is an unexpected result and unprecedented in the literature. An alternative explanation of the presence of a diamagnetic five-coordinated nickel(II) has not been discussed, although the Ni–N and Ni–O bond lengths (average ~2.02 and 2.05 Å, respectively) are significantly shorter than the corresponding distances of 2.146 and 2.086 Å for the six-coordinated nickel(II) compound containing **6** as the capping ligand.

Ferromagnetic coupling ($J = +12.6$ cm^{-1}, $g = 1.954$) was evaluated by fitting the magnetic susceptibility data of a $Cr^{III}Cu^{II}$ species, $[(Salen)Cr^{III}(L^{10})Cu^{II}]ClO_4$, obtained by using the oximate-containing ion $Cu(HL^{10})^+$ as the ligand for the Cr^{III}(Salen)-unit, where Salen is the dianion *N*,*N*′-ethylenebis(salicylideneiminate) [105]. **11** is the proposed structure with a bis(oximato) bridge.

building blocks. Unfortunately, due to lack of suitable crystals. The X-ray structure was not determined. The structure proposed is shown as **13**. The least-squares fit with the $H = -2J \cdot S_{Cu} \cdot S_{Mn}$-convention of the experimental magnetic susceptibility data resulted in the following parameters [107]: $J = -24.9$ cm^{-1}, $g_2 = 1.88$, $g_3 = 1.98$, $|D| = 3.8$ cm^{-1}, where g_2 and g_3 are the Zeeman factors associated with the ground state $S_t = 2.0$ and the excited state $S_t = 3.0$, and D is the axial zero-field splitting parameter for the quintet ground state. The local 'g' factors g_{Mn} and g_{Cu} were calculated by the relations $g_2 = (7g_{Mn} - g_{Cu})/6$ and $g_3 = (5g_{Mn} + g_{Cu})/6$ to be $g_{Mn} = 1.95$ and $g_{Cu} = 2.31$. The strength of the antiferromagnetic exchange coupling between the high-spin Mn(II) and Cu(II) ions is moderate in comparison to a very similar, if not identical system [50] with $J = -41.9$ cm^{-1}, which will be described later.

The crystal structure of $[Cu^{II}(C_2H_5OH)(L^{10})Ni^{II}(Me_3[12]N_3)](ClO_4)_2$ [108] was determined. The $Cu^{II}L^{10}$-fragment is doubly-bridged by oximato groups in *cis* arrangement to the Ni(Me_3[12]N_3)-unit.

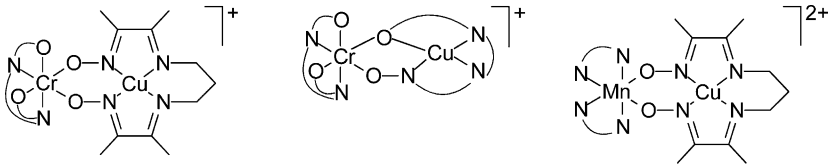

11 **12** **13**

On the contrary, an antiferromagnetic spin interaction ($J = -19.5$ cm^{-1}, $g_{Cu} = 2.06$, $g_{Cr} = 1.98$, $\theta = -2.0$ K) was evaluated for the $[Cu^{II}(L^{34})Cr(Salen)]NO_3 \cdot H_2O$ compound, for which the structure **12** with a very low symmetry has been proposed to rationalize the antiferromagnetic interaction [106]. The same paper [106] also describes an antiferromagnetically coupled ($J = -44.5$ cm^{-1}) $Cu^{II}Ni^{II}$ species with the same oxime ligand, HL^{34}.

Another related compound is $[Cu^{II}(L^{10})Ni^{II}(cyclam)](ClO_4)_2 \cdot H_2O$, where cyclam represents the macrocyclic end-capping ligand, 1,4,8,11-tetraazacyclotetradecane, in which an antiferromagnetically spin coupling, as expected, of $J = -102$ cm^{-1} transmitted through two oximato–NO linkages was observed [14]. The proposed structure is very similar to that proposed for a $Cu^{II}Mn^{II}$ species described below and depicted as **13**.

The heterodinuclear $Cu^{II}Mn^{II}$ complex of formula $[Cu^{II}(L^{10})Mn^{II}(\mathbf{2})_2](ClO_4)_2 \cdot 2.5H_2O$ [107] was obtained by a modular approach using $Cu(HL^{10})^+$ and $Mn(\mathbf{2})_2^{2+}$-

The coordination geometry around the copper ion is square pyramidal with an ethanol molecule occupying the axial position, whereas the nickel ion exhibits a trigonal-bipyramidal surrounding NiN_3O_2. The intramolecular Cu···Ni distance is 3.810 Å. In the crystal two $[Cu^{II}Ni^{II}]$ units are related through an inversion center, giving rise to a bis[CuNi] entity. Susceptibility measurements correspond to an almost isolated Cu(II)Ni(II) pair with an intramolecular antiferromagnetic interaction parameter $J = -71.8$ cm^{-1}. However, the EPR spectrum at 4.2 K is that of a triplet spin state arising from the interaction between the two doublet spin states within the $[Cu^{II}Ni^{II}]_2$ entity. In contrast, a very similar $Cu^{II}Ni^{II}$ pair with the oxime H_2L^{12} [104] containing a square pyramidal nickel with NiN_3O_2 coordination spheres is so strongly coupled that even at room temperature only the doublet ground state is populated. That the five-coordinated Ni(II) in the latter complex is paramagnetic has not been unambiguously proved.

A series of compounds with the structural motifs shown in Fig. 25 has been obtained by using the

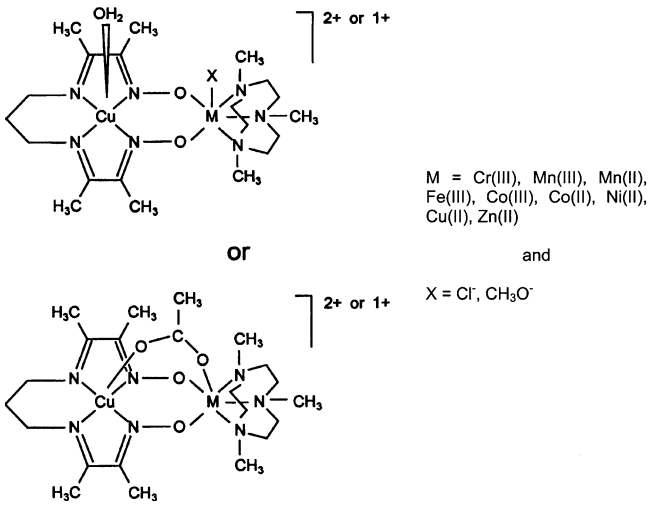

Fig. 25. The structural motifs for the heterodinuclear $[Cu^{II}(L^{10})M(x)]$ compounds.

$[Cu(L^{10})(H_2O)]^+$ cation as a ligand for the coordinative unsaturated units $M(\mathbf{5})^{n+}$ [50]. These isostructural dinuclear complexes with varying d^n-electron configurations provided more information in comparison to those comprising only of singly isolated exchange-coupled dimers. The X-band EPR spectra (3–77 K) of the compounds have been measured to establish the ground states of the heterodinuclear complexes. Well resolved EPR spectra for the systems $Cu^{II}Cr^{III}$, $Cu^{II}Mn^{II}$ and $Cu^{II}Fe^{III}$ with the $S_t = 2.0$ ground state have been observed, which reveal weak zero-field splitting within the $S = 2$ multiplets of these compounds.

Analysis of the susceptibility data yields a strong antiferromagnetic interaction ($J = -298\ cm^{-1}$) between the Cu(II) ions in the copper(II) dimer, showing once again that bridging oximes are good mediators for exchange interactions. The strength of the effective antiferromagnetic interaction decreases with increasing number of unpaired electrons in the series $Cu^{II}Cu^{II} > Cu^{II}Ni^{II} > Cu^{II}Co^{II} > Cu^{II}Mn^{II} \sim Cu^{II}Fe^{III}$. The ferromagnetic interaction observed for $Cu^{II}Mn^{III}$ ($J = +54.4\ cm^{-1}$) is stronger than that in $Cu^{II}Cr^{III}$ ($J = +18.5\ cm^{-1}$). A qualitative rationale for the trend and nature of exchange interactions between two spin carriers Cu(II) and M has been provided. This paper confirms the essentially σ nature of the $Cu^{II}(L^{10})$–M interaction and the applicability of Goodenough–Kanamori rules, in general, to predict the nature of exchange interactions for different heterometal compounds.

The exchange coupling constants for the oximato bridged dinuclear complexes and their ground spin states including the above series are summarized in Table 2.

Model calculations based on density functional theory [109] were performed to investigate theoretically the influence of the electronic configurations of the paramagnetic metal ions on the exchange interactions for the above series of heterobinuclear bis(oximato)-bridged $Cu^{II}(L^{10})M$ compounds. The results are very promising and the calculated exchange coupling constants for the model complexes are in good agreement with the experimental ones reported in Ref. [50], which are listed in Table 3.

According to these authors the nature of the terminal ligand is as important as the structural distortions in determining the magnetic behavior for the $Cu^{II}(L^{10})M$-series. Irrespective of the sign of the coupling constant, these calculations show an inverse dependence of the N–O distance and the strength of the exchange interaction. Indeed, $Cu^{II}(L^{10})Cr^{III}(OCH_3)$ with an average N–O distance of 1.40 Å exhibits a weaker ferromagnetic coupling ($J = +18.5\ cm^{-1}$) than that in $Cu^{II}(L^{10})M^{III}(OAc)$ ($J = +54.4\ cm^{-1}$) with N–O bond lengths of av. 1.37 Å [50].

Recently it has been reported [28] that tris(pyridine-2-aldoximato)metalates, $[M^{II}(L^{14})_3]^-$, are capable of acting as ligands to give rise to various asymmetric dinuclear complexes $[(\mathbf{5})M^{III}(L^{14})_3M^{II}]^{2+}$ [M^{III} = Cr(III), Mn(III), or Fe(III) and M^{II} = Cr(II), Mn(II), Fe(II), Ni(II), Cu(II), Zn(II)] containing three oximato groups (=N–O) as bridging ligands, which can mediate exchange interactions of varying range. Reference [28] contains a detailed description of the $(\mathbf{5})Cr^{III}$-containing compounds, viz. the following pairs $Cr^{III}Cr^{II}$, $Cr^{III}Mn^{II}$, $Cr^{III}Fe^{II}$(l.s.), $Cr^{III}Ni^{II}$, $Cr^{III}Cu^{II}$ and $Cr^{III}Zn^{II}$. A second $Cr^{III}Ni^{II}$ species containing the hexadentate ligand with the identical donor atoms, tris(2-aldoximato-6-pyridyl)phosphine, $P(PyA)_3^{3-}$, $[L^{35}]^{3-}$, has also been structurally and magnetically investigated. The structures consist of mixed-metal $Cr^{III}M^{II}$ complexes with a geometry in which two pseudo-octahedral polyhedra are joined by three oximato ($=N-O^-$) groups, with an intramolecular Cr···M distance in the range 3.51–3.71 Å. The compounds are isostructural in the sense that they all contain a terminal Cr(III) ion in a distorted octahedral environment, CrN_3O_3, and a second six-coordinated metal ion M in a mostly trigonal prismatic MN_6 geometry. The structural element Cr(O–N)M is not linear. Analysis of the susceptibility data indicates the presence of weak exchange interactions (Table 2), both ferro- and antiferromagnetic, between the paramagnetic centers. A notable outcome of this investigation is the observation that the spin coupling between the ions Cr(III) and Ni(II) (d^3d^8 system) can be antiferromagnetic in nature, in contrast to the generally expected ferromagnetic coupling between the said spin carriers in a six-coordinated environment. Intramolecular antiferromagnetic spin coupling ($J = -9.2\ cm^{-1}$) has been evaluated both by susceptibility and EPR measurements. The common strategy of obtaining ferromagnetically coupled bimetallic systems through involvement of symmetry-related strict orthogonality of the magnetic orbitals of the interacting metal centers,

Table 2
Oximato-bridged dinuclear heterometallic systems

Complex	Remarks	J and spin ground state(s) ($H = -2JS_1 \cdot S_2$)	Reference
$[Cu^{II}(ClO_4)(\mu\text{-}L^{13})Ni^{II}(\mathbf{6})]ClO_4$	X-ray structure; monooximato (*syn–anti*) and a keto-oxygen bridging	-61.8 cm^{-1}, $S_t = 1/2$	[104]
$[Cu^{II}(ClO_4)(\mu\text{-}L^{12})Ni^{II}(Me_3[12]N_3)]ClO_4$	X-ray structure; one N–O oximato (*syn–syn*) and one *o*-oximato bridging	Strongly coupled $J < -500$ cm^{-1}, $S_t = 1/2$	[104]
$[Cu^{II}(L^{10})Mn^{II}(\mathbf{2})_2](ClO_4)_2$	Proposed bis(oximato) bridge	$J = -25.1$ cm^{-1}, $S_t = 2.0$	[107]
$\{[Cu^{II}(L^{10})Mn^{II}(\mathbf{1})_2](ClO_4)_2 \cdot H_2O\}_2$	Proposed bis(oximato) bridge	$J = -25.5$ cm^{-1}, $J = +0.75$ cm^{-1}, $S_t = 4$	[108]
$[Cu^{II}(L^{10})Ni^{II}(Cyclam)](ClO_4)_2$	No structure; two N–O linkages proposed	$J = -102$ cm^{-1}, $S_t = 1/2$	[14]
$[Cu^{II}(C_2H_5OH)(L^{10})Ni^{II}(Me_3[12]N_3)](ClO_4)_2$	X-ray structure; $Cu(N–O)_2Ni$ unit	$J = -71.8$ cm^{-1}	[108]
$[Cu^{II}(L^{10})Cr^{III}(Salen)]ClO_4$	Proposed bis(oximato) bridge	$J = +12.6$ cm^{-1}, $S_t = 2.0$	[105]
$[Cu^{II}(L^{34})Cr^{III}(Salen)]NO_3$	Mono-keto, mono-oximato bridge proposed	$J = -19.5$ cm^{-1}, $S_t = 1.0$	[106]
$[Cu^{II}(L^{34})Ni^{II}(O,N,N)]ClO_4$	No structure	$J = -44.5$ cm^{-1}, $S_t = 1/2$	[106]
$[Cu^{II}(L^{10})Ni^{II}(\mathbf{5})(OAc)]ClO_4$	Bis(oximato) bridge proposed	$J = -99.2$ cm^{-1}, $S_t = 1/2$	[50]
$[Cu^{II}(L^{10})Co^{II}(\mathbf{5})(OAc)]ClO_4$	Bis(oximato) bridge proposed	$J = -53.8$ cm^{-1}	[50]
$[Cu^{II}(L^{10})Fe^{III}(\mathbf{5})(OAc)](ClO_4)_2$	Proposed bis(oximato) bridge	$J = -44.9$ cm^{-1}, $S_t = 2.0$	[50]
$[Cu^{II}(L^{10})Mn^{II}(\mathbf{5})(OAc)](ClO_4)_2$	Proposed bis(oximato) bridge	$J = -41.4$ cm^{-1}, $S_t = 2.0$	[50]
$[Cu^{II}(L^{10})Mn^{III}(\mathbf{5})(OAc)](ClO_4)_2$	X-ray structure; bis(oximato)mono-acetato-bridging	$J = +54.4$ cm^{-1}, $S_t = 5/2$	[50]
$[Cu^{II}(L^{10})Cr^{III}(\mathbf{5})(OCH_3)](ClO_4)_2$	X-ray structure; bis(oximato) bridging	$J = +18.5$ cm^{-1}, $S_t = 2.0$	[50]
$[(\mathbf{5})Cr^{III}(L^{14})_3Cr^{II}](ClO_4)_2$	Tris(oximato) bridging proposed	$J = -7.9$ cm^{-1}, $S_t = 1/2$	[28]
$[(\mathbf{5})Cr^{III}(L^{14})_3Mn^{II}](ClO_4)_2$	X-ray structure; tris(oximato) bridging	$J = +1.5$ cm^{-1}, $S_t = 4.0$	[28]
$[(\mathbf{5})Cr^{III}(L^{14})_3Ni^{II}](ClO_4)_2$	X-ray structure; tris(oximato) bridging	$J = -9.2$ cm^{-1}, $S_t = 1/2$	[28]
$[(\mathbf{5})Cr^{III}(L^{14})_3Cu^{II}](ClO_4)_2$	X-ray structure; tris(oximato) bridging	$J = +1.8$ cm^{-1}, $S_t = 2.0$	[28]
$[(\mathbf{5})Cr^{III}(L^{35})Ni^{II}](ClO_4)_2$	X-ray structure; tris(oximato) bridging; trigonal prismatic Ni(II) center	$J = 0$, $S_{Cr} = 3/2$; $S_{Ni} = 1$	[28]
$[(\mathbf{5})Mn^{III}(L^{14})_3Mn^{II}](ClO_4)_2$	X-ray structure; tris(oximato) bridging	$J = +1.6$ cm^{-1}, $S_t = 9/2$	[28,91]
$[(\mathbf{5})Mn^{III}(L^{14})_3Ni^{II}](ClO_4)_2$	Tris(oximato) bridging proposed	$J = -9.9$ cm^{-1}, $S_t = 1.0$	[28,91]
$[(\mathbf{5})Mn^{III}(L^{14})_3Cu^{II}](ClO_4)_2$	Tris(oximato) bridging proposed	$J = +14.8$ cm^{-1}, $S_t = 5/2$	[28,91]
$[(\mathbf{5})Fe^{III}(L^{14})_3Mn^{II}](ClO_4)_2$	X-ray structure; tris(oximato) bridging	$J = -6$ cm^{-1}, $S_t = 0$	[28,91]
$[(\mathbf{5})Fe^{III}(L^{14})_3Ni^{II}](ClO_4)_2$	X-ray structure; tris(oximato) bridging	$J = -30.0$ cm^{-1}, $S_t = 3/2$	[28,91]
$[(\mathbf{5})Fe^{III}(L^{14})_3Cu^{II}](ClO_4)_2$	Proposed tris(oximato) bridging	$J = -53$ cm^{-1}, $S_t = 2.0$	[28,91]

viz. the $t_{2g}^3(Cr) \perp e_g^2(Ni)$ interactions, does not lead to the expected results for the triply bridged $Cr^{III}Ni^{II}$ systems, presumably due to the mixing of five metal d orbitals in trigonal symmetry, which provide several exchange components opposite in nature; thus weak to negligible spin interactions result.

Considering the O and N atoms of the bridging oxime groups as sp^2 hybridized in the network $Cr(O–N)_3M$, the different possible interactions of the sp^2 orbitals on either side of the bridging oximate ligands with the different metal orbitals in idealized C_3 symmetry have been analyzed. The five metal d orbitals with the threefold axis as the z-axis along the Cr···M vector transform in C_3 symmetry as $a(d_{z^2})$, $1e(d_{x^2-y^2}, d_{xy})$ and $2e(d_{yz}, d_{xz})$, where orthogonality prevails only between a and 1e, and a and 2e. For complex $Cr^{III}Cr^{II}$ with the d^3d^4(hs) electronic configuration, it is evident from the exchange coupling constant J of -7.9 cm^{-1} that the dominant exchange pathways are the symmetry-allowed $a||sp^2||a$ and $1e||sp^2||1e$ (using Ginsberg's symbols) σ-superexchange pathway. Now, on going to the $Cr^{III}Mn^{II}$ species in which the fifth electron of Mn^{II} occupies an empty 2e orbital, the overall interaction changes its nature from antiferromagnetic to weak ferromagnetic ($J = +1.5$ cm^{-1}). Thus the contribution of the path $2e||sp^2||2e$ to the overall interaction becomes very important, since the 2e orbitals centered on chromium and manganese are empty or half-filled, respectively, leading to ferromagnetic interactions.

For the d^3d^8 case, $Cr^{III}Ni^{II}$, the antiferromagnetic contribution provided by the $1e||sp^2||1e$ exchange path now exceeds those from all other ferromagnetic interactions, leading to an effective antiparallel spin coupling. Interestingly, the second Cr(III)Ni(II) species

Table 3
Comparison of the calculated [109] and the experimental [50] exchange coupling constants as obtained for the bis(oximato)-bridged $Cu^{II}(L^{10})M(X)$-compounds

Complex	$H = -2JS_1 \cdot S_2$	
	J/cm^{-1} (Expt)	J/cm^{-1} (Calc.)
$Cu^{II}(L^{10})Cu^{II}$	-298	-324
$Cu^{II}(L^{10})Ni^{II}(OAc)$	-99.2	-100.5
$Cu^{II}(L^{10})Mn^{II}(OAc)$	-41.4	-33.5
$Cu^{II}(L^{10})Mn^{III}(OAc)$	$+54.4$	$+63.5$
$Cu^{II}(L^{10})Cr^{III}(OCH_3)$	$+18.5$	$+21.5$

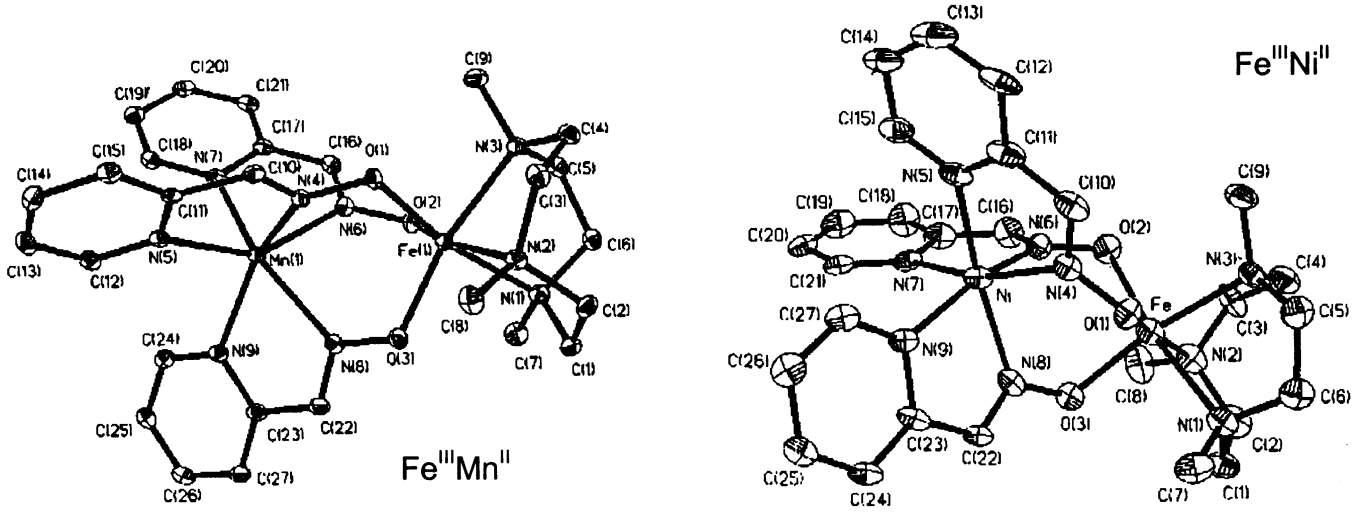

Fig. 26. ORTEP views of $[(\mathbf{5})Fe^{III}(L^{14})_3Mn^{II}]^{2+}$ and $[(\mathbf{5})Fe^{III}(L^{14})_3Ni^{II}]^{2+}$. Reproduced with permission from Ref. [91].

$CrNiP(PyA)_3$ exhibits no exchange interaction ($J=0$). The crystallographic data of $CrNiP(PyA)_3$ indicate that both twist angle ϕ and dihedral angle θ, are more toward trigonal prismatic in comparison to those for $CrNi(L^{14})_3$. Hence, the nature of the exchange interaction and its magnitude in triply-bridged $Cr^{III}Ni^{II}$ pair is expected to be a function of both ϕ and θ. A triply-oxime bridged $Cr^{III}Ni^{II}Cr^{III}$ species [29] with a twist angle of 24°, (described in the next section on trinuclear complexes) which is in-between those for these dinuclear complexes exhibits a very weak antiparallel interaction ($J=-0.7\ cm^{-1}$). Interestingly, occupancy of the 2e orbital of Cu(II) by one more single electron, thus reducing the number of unpaired electrons to one in the 2e orbital, results in weakening of the antiparallel coupling thus yielding an overall parallel spin coupling for $Cr^{III}Cu^{II}$. The description above of the orbital pathways is based on a very simplified model. The network Cr–O–N–M is not linear and oriented in different ways for structurally characterized pairs, thus leading to mixing-up of the metal d-orbitals, which makes the picture more complex.

Analogous complexes with the $(\mathbf{5})Mn^{III}$- and $(\mathbf{5})Fe^{III}$-units have been synthesized [91]. The X-ray structure of $[(\mathbf{5})Mn^{III}(L^{14})_3Mn^{II}](ClO_4)_2$ has already been discussed in Section 6.4. The structures of $[(\mathbf{5})Fe^{III}(L^{14})_3Mn^{II}](ClO_4)_2$ and $[(\mathbf{5})Fe^{III}(L^{14})_3Ni^{II}](ClO_4)_2$ are shown in Fig. 26.

The structures of all compounds $[(\mathbf{5})M^{III}(L^{14})M^{II}](ClO_4)_2$ are very similar and do not deserve any special discussion. But these compounds are ideally suited for investigation of exchange interactions as a function of d^n-electronic configurations. The exchange parameters are tabulated in Table 2.

Dominant exchange paths are schematically represented for the Mn^{III}- and Fe^{III}-compounds in Scheme 10.

It is obvious from the above scheme that for the Fe(III) compounds, the antiferromagnetic path involving $2e||sp^2||2e$ interactions dominates over all other interactions, resulting in overall antiferromagnetic interactions for all three compounds. On the other hand, for

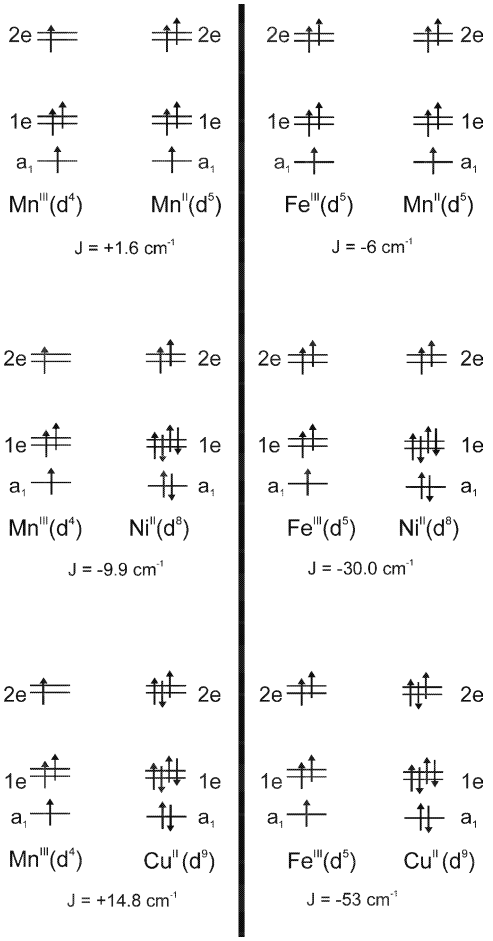

Scheme 10.

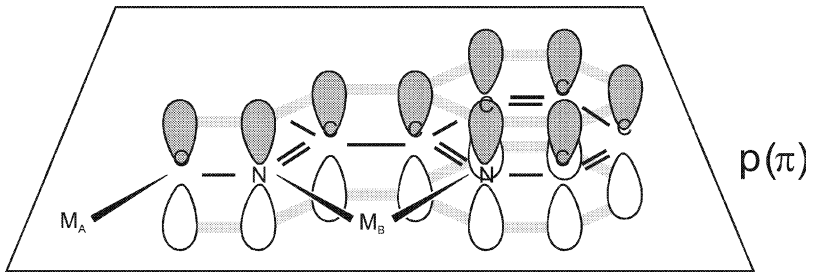

Fig. 27. π-Superexchange path involving the π-system of pyridinealdoxime ligand, $[L^{14}]^-$.

the Mn(III) compounds both antiferromagnetic and ferromagnetic paths (involving $2e \perp a_1$) are important in determining the strength of overall exchange interactions. Thus the overall exchange interaction swings from ferromagnetic to antiferromagnetic and again to ferromagnetic.

The π-conjugated system (Fig. 27) of the planar pyridinealdoximato ligand, delocalized over the bridging groups and perpendicular to the plane of the oxime ligands, appears also to have a role, although small, in tuning the exchange interactions in this series of compounds.

7.2. Trinuclear complexes

As ferromagnetic interactions can be expected for a molecule containing Cr(III) and Cu(II) ions due to orthogonality of their magnetic orbitals, an oximate-bridged trinuclear $Cr^{III}Cu^{II}Cr^{III}$ complex, $[(Salen)Cr^{III}(\mu\text{-}L^1_2Cu^{II})Cr^{III}(Salen)]$, was synthesized by reacting $[Cr(Salen)(H_2O)_2]NO_3$ and $[Cu(HL^1)_2]$ in presence of ethyl orthoformate and triethylamine [105]. The structure **14** containing a bis(dimethylglyoximato)copper(II) $[Cu(L^1)_2]^{2-}$ as a bridging ligand has been proposed.

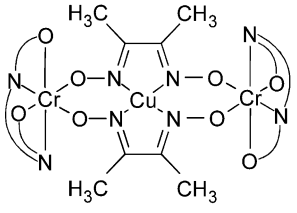

14

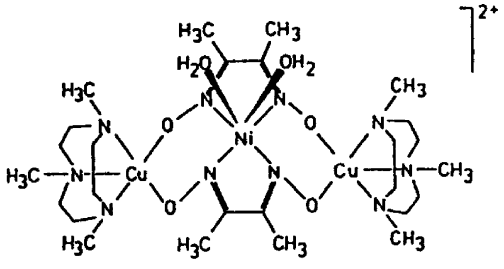

15

Indeed, the spin orientation has been found to be ferromagnetic with $J = +13.0\ cm^{-1}$. This compound possesses an irregular spin ladder as is expected for trinuclear complexes of the type $M_AM_BM_A$ with a spin correlation $2S_A > (S_B + 1/2)$. Similar bis(dimethylglyoximato)-metalates, viz. $[Ni^{II}(L^1)_2]^{2-}$ and $[Pd^{II}(L^1)_2]^{2-}$, which are diamagnetic, have been used [11] to determine the exchange interaction between two copper(II) centers separated by an estimated distance of ~7.6 Å. A complete X-ray structure determination of $[(\mathbf{5})_2Cu^{II}_2(L^1)_2Ni^{II}](ClO_4)_2 \cdot 2H_2O$ was not possible because of crystal disorder, but a qualitative investigation showed that two water molecules are directly attached to the nickel center in a cis-planar fashion yielding a six-coordinate compound that should be formulated as $[(\mathbf{5})Cu(\mu\text{-}\{(L^1)_2Ni(cis\text{-}OH_2)_2\}Cu(\mathbf{5})](ClO_4)_2$. It has also been found that the three metal centers do not lie in a plane, but a bent structure is attained, as shown in **15**. Attempts to fit the magnetic data with spin systems $S_1 = S_3 = S_{Cu} = 1/2$ and $S_2 = S_{Ni} = 1$ were unsuccessful, but a very good quality fit was obtained by considering $S_1 = S_3 = S_{Cu} = 1/2$ and $S_2 = S_{Ni} = 0$ yielding $J = -2.6\ cm^{-1}$. The diamagnetism of the $[Ni(L^1)_2(OH_2)_2]^{2-}$ ion (C_{2v} or cis-planar) means that the in-plane field of the nitrogen atoms is much stronger than the cis-axial perturbations from the oxygen atoms of the water ligands to produce a singlet ground state for Ni(II).

Interestingly, for the compound $[(\mathbf{5})_2Cu^{II}_2(L^1)_2\text{-}Pd^{II}](ClO_4)_2$ [11] with a Cu···Cu distance of ca. ≈7.6 Å a medium-strong antiferromagnetic interaction with $J = -36\ cm^{-1}$ has been reported. The following struc-

ture with the square-planar $[Pd(L^1)_2]^{2-}$ ion (hence $S_{Pd}=0$) bridging two copper ions through its deprotonated oxime oxygen atoms, has been proposed. As a medium-strong coupling was observed, it was tempting for the authors to propose a nearly coplanar trinuclear skeleton **16**.

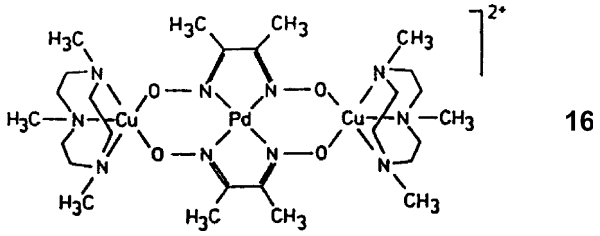

16

The first report of a coordinated complex, in which a diamagnetic metal mediates a ferromagnetic interaction between paramagnetic metal centers as a result of the strict orthogonality of their magnetic orbitals, has recently been documented by synthesizing the heterotrinuclear $Cu^{II}Zn^{II}Cu^{II}$ complex, $[Cu_2Zn(HL^1)_2(L^1)_2(H_2O)]\cdot 0.5H_2L^1\cdot H_2O$ [110]. The structure consists of a chain of neutral $[Cu_2Zn(HL^1)_2(L^1)_2(H_2O)]$ trinuclear units and noncoordinated H_2L^1 and water molecules. The Zn(II) ion is in distorted trigonal pyramidal ZnO_5-environment, whereas the Cu(II) ions adopt a distorted square pyramidal arrangement CuN_4O. Both magnetic susceptibility data and the field dependence of the magnetization at 2.0 K are consistent with a quintet ground state as a result of two exchange pathways via the diamagnetic zinc(II) ion and the out-of-plane double-oximato bridge between the copper(II) ions. Ferromagnetic coupling constants of $J=+1.95\ cm^{-1}$ with Zn(II) as the mediator and of $J'=+2.65\ cm^{-1}$ between the two neighbouring Cu(II) centers within the hexameric $(CuZnCu)_2$ unit was reported. The main orthogonal superexchange pathway J is given in Scheme 11.

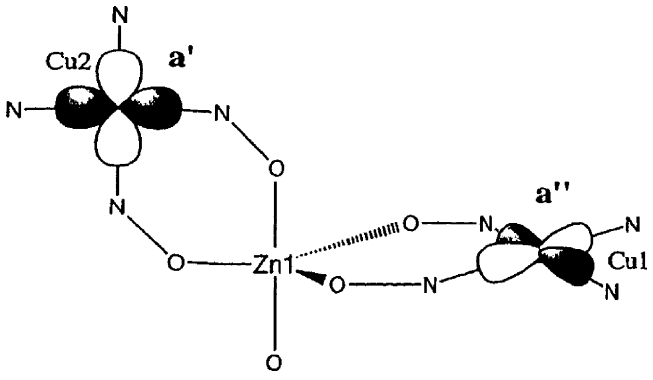

Scheme 11.

Another type of trinuclear compounds $M_AM_BM_A$ was obtained by using the modules $[M_B^{II}(dioxime)_3]^{4-}$ where $M_B=Zn(II)$, Cu(II), Ni(II), Fe(II), Mn(II) as bridging ligands.

Thus cations like

$[(\mathbf{5})Fe^{III}\{\mu\text{-}(dioxime)_3M^{II}\}Fe^{III}(\mathbf{5})]^{2+}$,
$[(\mathbf{5})Mn^{III}\{\mu\text{-}(dioxime)_3M^{II}\}Mn^{III}(\mathbf{5})]^{2+}$,
$[(\mathbf{5})Mn^{IV}\{\mu\text{-}(dioxime)_3M^{II}\}Mn^{IV}(\mathbf{5})]^{4+}$, and
$[(\mathbf{5})Cr^{III}\{\mu\text{-}(dioxime)_3M^{II}\}Cr^{III}(\mathbf{5})]^{2+}$

were isolated as a novel family for investigating the exchange interactions as a function of d^n-electron configurations. The compounds will be denoted by the metal centers only. We will discuss here two compounds of dimethylglyoxime (H_2L^1) with the Fe(III), Mn(III), Cr(III) and of nioxime (H_2L^{16}) with the Mn(IV) centers. We will omit in all cases the macrocyclic amine **5** as terminal ligands. The structures of $Cr^{III}Zn^{II}(L^1)_3Cr^{III}$ [29,111], $Mn^{III}Zn^{II}(L^1)_3Mn^{III}$ [94,112], $Mn^{IV}Zn^{II}(L^{16})_3Mn^{IV}$ [113], $Fe^{III}Zn^{II}(L^1)_3Fe^{III}$ [114,115,122] have been solved. The structure of the $Fe^{III}Zn^{II}(L^1)_3Fe^{III}$ species is shown in Fig. 28 as an archetype of the zinc-containing trinuclear complexes. The Fe(1)Zn(1)Fe(1a) unit is exactly linear with an angle of

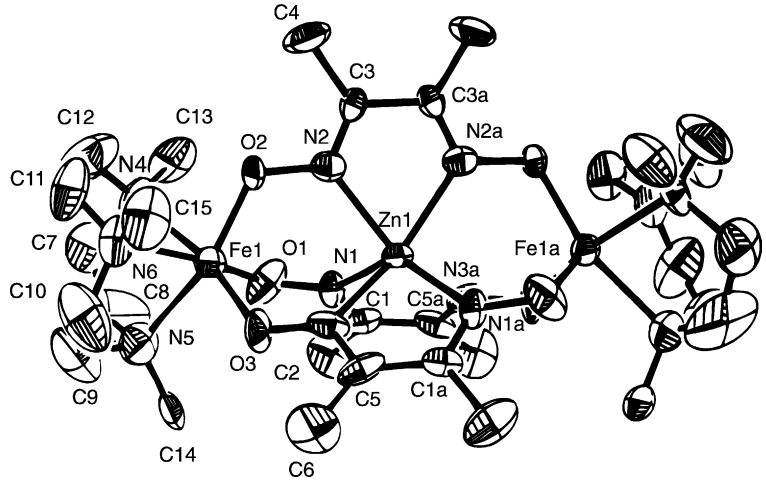

Fig. 28. Molecular structure of the linear $Fe^{III}Zn^{II}Fe^{III}$ core in $[(\mathbf{5})_2Fe_2^{III}(L^1)_3Zn^{II}]^{2+}$. Reproduced with permission from Ref. [122].

179.9(1)°. A $[Zn(L^1)_3]^{4-}$ anion bridges two high-spin Fe(III) through its deprotonated oxime oxygen with an Fe···Zn separation of 3.530(4) Å.

The iron coordination geometry is distorted octahedral FeN_3O_3 with three nitrogen atoms from the facially coordinated tridentate macrocyclic amine and three oxygen atoms from three oximate groups. The six imine nitrogen atoms are arranged around the Zn(II) center with a twist angle of 9.3°, thus yielding a nearly trigonal prismatic central ZnN_6 core. An *intra*molecular Fe(1)···Fe(1a) separation of 7.059(4) Å has been found.

For all of the above zinc-containing compounds, in which the terminal metal ions are separated by a large distance of ca. 7.0 Å, an antiferromagnetic interaction has been observed showing the efficiency of the oximato-bridge in transmitting exchange interactions. The strength of the antiferromagnetic interactions are in the following order: $Mn^{IV}(L^{16})_3ZnMn^{IV}$ ($J = -20.6$ cm^{-1}) > $Cr^{III}(L^1)_3ZnCr^{III}$ ($J = -4.4$ cm^{-1}) > $Fe^{III}(L^1)_3ZnFe^{III}$ ($J = -3.0$ cm^{-1}) > $Mn^{III}(L^1)_3ZnMn^{III}$ ($J = -0.4$ cm^{-1}). The evaluated antiferromagnetic coupling ($J = -20.6$ cm^{-1}) between the terminal manganese(IV) centers ($S_{Mn} = 3/2$) separated by a distance of 6.97 Å is significantly stronger than that prevailing in isoelectronic $Cr^{III}Zn^{II}Cr^{III}$ ($J = -4.4$ cm^{-1}), [111] which is attributable to the higher charge on Mn(IV) than that on the Cr(III) center. Thus, the higher covalent character of the Mn(IV)–ligand bond leads to stronger electronic interactions. There is also another aspect in which the Mn(IV)-compound differs from the other three. The twist angles ϕ of the ZnN_6 are 5.5° [Mn(IV)] < 7° [Cr(III)] < 8.4° [Mn(III)] < 9.3° [Fe(III)].

The π-conjugated system of the oxime ligand, delocalized over the whole bridging groups and perpendicular to the plane of the oxime ligand, appears to provide the dominant antiferromagnetic interaction between the terminal metal ions, separated by as much as ≈7 Å (Scheme 12).

It appears that the distortion of the environment of the central metal ion from a trigonal prismatic arrangement of the ligands toward an octahedron acts as a barrier toward the spin coupling between the terminal metal ions, as a result of inefficient interaction between the orbitals of the oxime network and the terminal ions. In fact, the terminal spins of 3/2 in an analogous $Cr^{III}Fe^{II}$(low spin)Cr^{III} [29] are non-interacting, with the low spin Fe^{II} exhibiting the greatest twist angle of 34.8°.

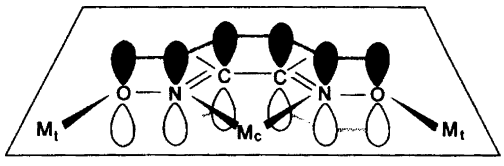

Scheme 12.

The first structurally characterized compound of this novel exchange-coupled family is $[(\mathbf{5})_2Fe^{III}_2(L^1)_3Cu^{II}](ClO_4)_2$ [10], whose structure is shown in Fig. 29. The $[Cu(L^1)_3]^{4-}$ anion bridges the two high-spin ferric ions through its deprotonated oxime oxygens with a Fe···Cu separation of 3.58 Å. The Cu–N distances varying in the range 1.983(5)–2.523(6) Å show that the resultant coordination sphere around the Cu(II) is strongly distorted. The magnetic interac-

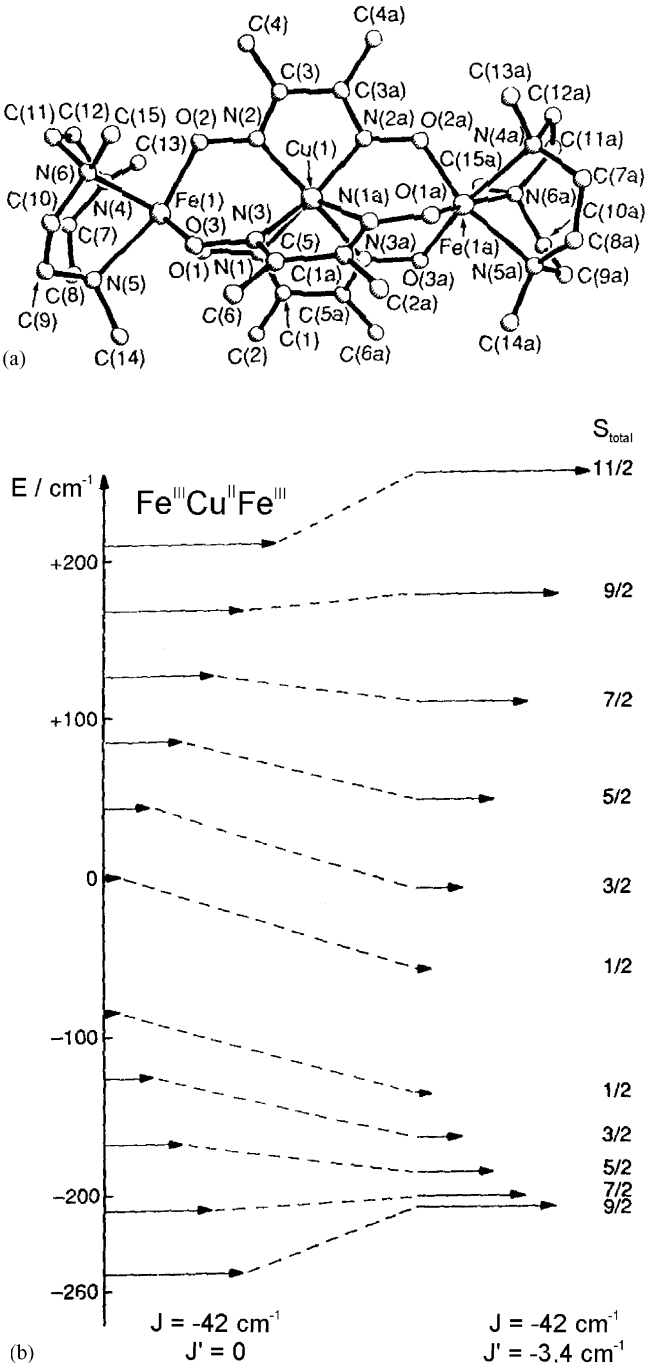

Fig. 29. Molecular structure of the $Fe^{III}Cu^{II}Fe^{III}$ core present in $[(\mathbf{5})_2Fe^{III}_2(L^1)_3Cu^{II}]^{2+}$. Energy ladder for the $Fe^{III}Cu^{II}Fe^{III}$ is shown on the right-hand side. Reproduced with permission from Ref. [10].

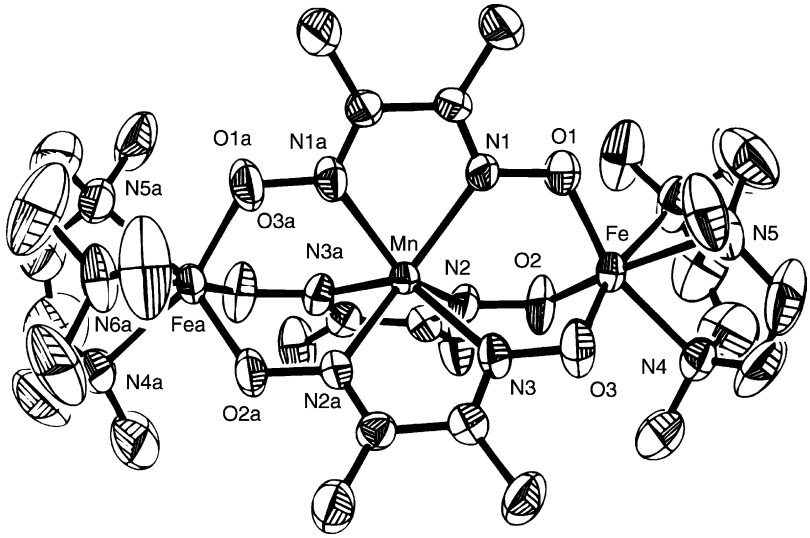

Fig. 30. An ORTEP view of the species $Fe^{III}Mn^{II}Fe^{III}$ in $[(\mathbf{5})_2Fe_2^{III}(L^1)_3Mn^{II}]^{2+}$. Reproduced with permission from Refs. [84,122].

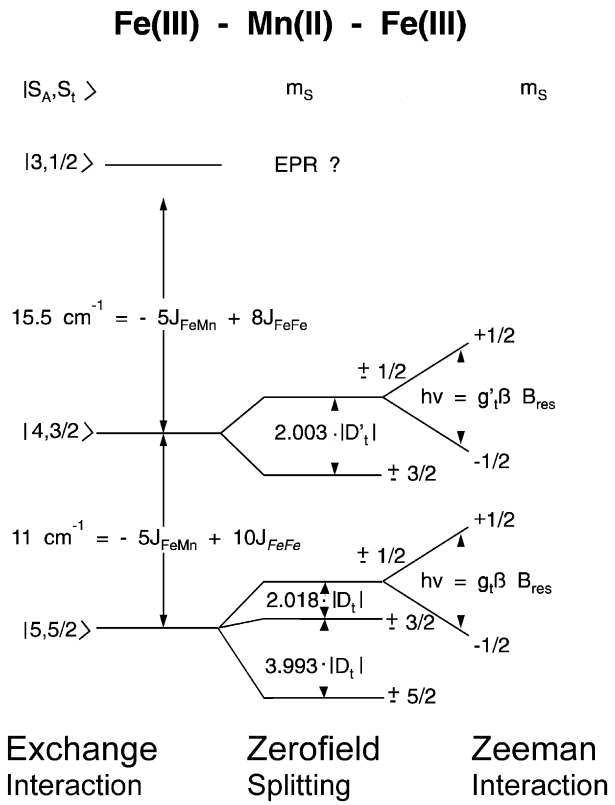

$$D_t = (26D_{Fe} + 15D_{Mn}) / 21 \qquad D'_t = (22D_{Fe} + 14D_{Mn}) / 21$$

$$g_t = (12g_{Fe} - 5g_{Mn}) / 7 \qquad g'_t = (2g_{Fe} - g_{Mn})$$

Fig. 31. The low-lying energy states resulting from exchange and zero-field interactions in $Fe^{III}Mn^{II}Fe^{III}$. Reproduced with permission from Ref. [122].

tion between high-spin Fe(III) and Cu(II) has been evaluated to be antiferromagnetic ($J = -42$ cm^{-1}). Mössbauer and EPR data [116] consistently reveal that the exchange interaction between ferric and cupric ions enforces a total intramolecular spin of $S_{tot} = S_{Fe(1)} - S_{Cu} + S_{Fe(2)} = 5/2 - 1/2 + 5/2 = 9/2$. A schematic energy ladder is also shown in Fig. 29. To emphasize the influence of exchange interactions between the terminal Fe(III) centers (J') on the overall energy ladder, two energy ladders with and without J' are shown. With increasing energy the total spin S_t diminishes, reaches the value of 1/2 and then increases to 11/2 for the most excited state. Thus, an irregular spin-state results [117]. Consequently, a minimum in the μ_{eff} versus T plot is expected, but was not observed due to comparatively strong coupling, which moves the minimum to a much higher temperature than the experimental temperature.

The magnetic properties of $[(\mathbf{5})_2Fe^{III}_2(L^1)_3Mn^{II}](ClO_4)_2$ have been studied in depth by magnetic susceptibility, EPR, and Mössbauer measurements [114,118,122]; the metal centers are in high-spin states. The X-ray structure [84,122], shown in Fig. 30, shows as expected a linear arrangement of three metal ions with distances Fe···Mn and Fe···Fe of 3.52 and 7.04 Å.

Magnetic susceptibility data show antiferromagnetic coupling between the metal centers with $J_{FeMn} = -6.7$ and $J_{FeFe} = -2.3$ cm^{-1}. Thus the ground state is with $S_{total} = 5/2$. The analysis of variable-temperature EPR spectra yields the zero-field parameter $D_{5/2} = (-0.9 \pm 0.1)$ cm^{-1} and rhombicity $E_{5/2}/D_{5/2} \approx 0.03$. The negative value for $D_{5/2}$ indicates that the Kramers doublet $|+1/2\rangle$ lies highest within the $S_t = 5/2$ multiplet. Magnetically split Mössbauer spectra were recorded at 1.5 K under various applied fields. The spin-Hamiltonian analysis of these spectra yields isotropic magnetic hyperfine coupling with $A_{total}/(g_N\mu_N) = -18.5$ T. The corresponding local component A_{Fe} is related to A_{total} via spin-projection: $A_{total} = (6/7)A_{Fe}$. Thus the resulting $A_{Fe}/(g_N\mu_N) = -21.6$ T is in agreement with the standard values of ferric high-spin complexes. A scheme for the low-lying energy states with their splittings caused by exchange and zero-field interactions is shown in Fig. 31.

The antiferromagnetic interaction between the Fe(III) and Ni(II) centers in $[(\mathbf{5})_2Fe^{III}_2(L_1)_3Ni^{II}](ClO_4)_2$ [119] was $J_{FeNi} = -32$ cm^{-1}. The spin-level structure is characterized by the ferromagnetic-like polarization of high local spins with a ground state of $S_t = 5/2 - 1 + 5/2 = 4$. The ordering of energy levels follows from the fact that the Fe(III) ($S_{Fe} = 5/2$) magnetic moments are larger than those of Ni(II) ($S_{Ni} = 1$). That the level ordering is a result of the mutual influence of J_{FeNi} and J_{FeFe} has been clearly shown. Thus the energy difference between the ground state $|S^* = 5,\ S_t = 4\rangle$ and the next upper-lying level $|S^* = 4,\ S_t = 3\rangle$ of 64 cm^{-1} becomes reduced to 14 cm^{-1} in $Fe^{III}Ni^{II}Fe^{III}$ by the effect of J_{FeFe} on the energy splittings. Thus a situation may arise in which the influence of terminal-interactions (J_{FeFe} or J_{13}) on the neighbouring interactions (J_{FeM} or $J_{12} = J_{23}$) alters the expected ground state. Such a ground-state variability has been observed for various trinuclear oximato-bridged complexes and will be discussed later.

With increasing number of unpaired electrons, i.e. the order Cu(II) > Ni(II) > Mn(II), the strength of the neighbouring antiferromagnetic interactions J_{FeM} decreases. The dominant σ path responsible for the antiferromagnetic interaction is

$$d_{x^2-y^2}(Fe^{III})||\sigma_{NO}(sp2)||d'_{x^2-y^2}(M^{II})$$

which is depicted in Scheme 13.

The values of the interaction parameter J, and some relevant distances together with the ground state spins for all compounds with the general formulae

$[(\mathbf{5})M^{III}_A\{(L^1)_3M^{II}_B\}M^{III}_A(\mathbf{5})](ClO_4)_2$,
$[(\mathbf{5})Mn^{IV}\{(L^1)_3M^{II}_B\}Mn^{IV}(\mathbf{5})](ClO_4)_4$ and
$[(\mathbf{5})Mn^{IV}\{(L^{16})_3M^{II}_B\}M^{II}_B\}Mn^{IV}(\mathbf{5})](ClO_4)_4$

are summarized in Table 4.

An inspection of Table 4 draws our attention at least to the following points:

1) A comparison of the complexes containing a diamagnetic ion as the central species clearly indicates the participation of the central metal ion in the transmission of the antiferromagnetic exchange interaction between the terminal paramagnetic ions.
2) When the central ion (M_B) with a zero local spin is present in the $M_AM_BM_A$-type complexes, a noticeable antiferromagnetic interaction between the terminal spin carriers separated by a distance of ~7 Å is observed. In this regard the compound $Mn^{IV}(L^{16})_3Zn^{II}Mn^{IV}$ [113] is remarkable, as the presence of intramolecular antiferromagnetic exchange coupling of considerable magnitude over a distance of 6.97 Å is observed ($J \approx -20$ cm^{-1}). The X-band EPR data of the compound in CH_3CN in the temperature range 20–70 K were quantitatively analyzed considering that the spectra originate from the excited quintet state ($S_t = 2$) to evaluate $J = (-16.5 \pm 3.5)$ cm^{-1}, which is in agreement with the susceptibility data. Below 20 K there is no EPR signal demonstrating the diamagnetic nature of the

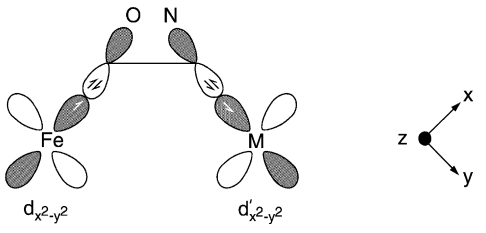

Scheme 13.

Table 4
Exchange parameters for the linear trinuclear tris(oximato)-bridged complexes of Fe(III), Mn(III), Mn(IV) and Cr(III), in which the end-capping ligands are **5**

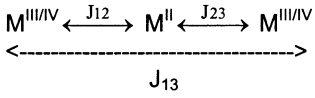

$H = .2J(\hat{S}_1 \bullet \hat{S}_2 + \hat{S}_2 \bullet \hat{S}_3) - 2J_{13}(\hat{S}_1 \bullet \hat{S}_3)$

$J = J_{12} = J_{23}$

Complex	Spin system	J (cm^{-1})	$M^{III/IV}\cdots M^{II}$ (Å)	J_{13} (cm^{-1})	$M^{III/IV}\cdots M^{III/IV}$ (Å)	Ground state(s)	References
$Fe^{III}Zn^{II}Fe^{III}$	$^5/_2\ 0\ ^5/_2$	–	3.53	−3.40	7.06	$S_t = 0$	[10,114,122]
$Fe^{III}Cu^{II}Fe^{III}$	$^5/_2\ ^1/_2\ ^5/_2$	−42.0	3.58	−3.40	7.08	$S_t = 9/2$	[10]
$Fe^{III}Ni^{II}Fe^{III}$	$^5/_2\ 1\ ^5/_2$	−32.0	3.49	−5.0	6.98	$S_t = 8/2$	[119]
$Fe^{III}Fe^{II}$(l.s.)Fe^{III}	$^5/_2\ 0\ ^5/_2$	–	–	−4.4	–	$S_t = 0$	[10]
$Fe^{III}Mn^{II}Fe^{III}$	$^5/_2\ ^5/_2\ ^5/_2$	−6.7	3.52	−2.3	7.04	$S_t = 5/2$	[115,118,122]
$Mn^{III}Zn^{II}Mn^{III}$	$^4/_2\ 0\ ^4/_2$	–	3.57	−0.4	7.13	$S_t = 0$	[94,112]
$Mn^{III}Cu^{II}Mn^{III}$	$^4/_2\ ^1/_2\ ^4/_2$	−63.1	3.58	−2.8	7.11	$S_t = 7/2$	[94]
$Mn^{III}Ni^{II}Mn^{III}$	$^4/_2\ 1\ ^4/_2$	−5.3	–	+2.7	–	$S_t = 6/2$	[94]
$Mn^{III}Mn^{II}Mn^{III}$	$^4/_2\ ^5/_2\ ^4/_2$	+4.7	3.57	−3.0	7.14	$S_t = 13/2,\ 11/2$ ($\Delta E = 1\ cm^{-1}$)	[94]
$Mn^{III}Zn^{II}Mn^{III}$ *	$^4/_2\ 0\ ^4/_2$	–	–	−2.4	–	$S_t = 0$	[113]
$Mn^{III}Cu^{II}Mn^{III}$ *	$^4/_2\ ^1/_2\ ^4/_2$	−70.0	–	−3.9	–	$S_t = 7/2$	[113]
$Mn^{III}Mn^{II}Mn^{III}$ *	$^4/_2\ ^5/_2\ ^4/_2$	+4.7	–	−3.4	–	$S_t = 11/2$	[113]
$Mn^{IV}Zn^{II}Mn^{IV}$	$^3/_2\ 0\ ^3/_2$	–	–	−19.2	–	$S_t = 0$	[94]
$Mn^{IV}Cu^{II}Mn^{IV}$	$^3/_2\ ^1/_2\ ^3/_2$	+72.7	–	−25.0	–	$S_t = 3/2$	[94]
$Mn^{IV}Ni^{II}Mn^{IV}$	$^3/_2\ 1\ ^3/_2$	+19.2	–	−10.1	–	$S_t = 2,3$	[94]
$Mn^{IV}Mn^{II}Mn^{IV}$	$^3/_2\ ^5/_2\ ^3/_2$	+19.6	–	−19.2	–	$S_t = 9/2$	[94]
$Mn^{IV}Zn^{II}Mn^{IV}$ *	$^3/_2\ 0\ ^3/_2$	–	3.49	−20.6	6.97	$S_t = 0$	[113]
$Mn^{IV}Cu^{II}Mn^{IV}$ *	$^3/_2\ ^1/_2\ ^3/_2$	+50.1	3.54	−17.7	7.06	$S_t = 3/2$	[113]
$Mn^{IV}Mn^{II}Mn^{IV}$ *	$^3/_2\ ^5/_2\ ^3/_2$	+25.2	–	−25.7	–	$S_t = 9/2$	[113]
$Cr^{III}(H^+)_2Cr^{III}$	$^3/_2\ 0\ ^3/_2$	–	–	−4.7	7.27	$S_t = 0$	[98]
$Cr^{III}Li^{I}Cr^{III}$	$^3/_2\ 0\ ^3/_2$	–	–	−5.8	–	$S_t = 0$	[29]
$Cr^{III}Co^{III}Cr^{III}$	$^3/_2\ 0\ ^3/_2$	–	–	−0.3	–	$S_t = 0$	[29]
$Cr^{III}Fe^{II}$(l.s.)Cr^{III}	$^3/_2\ 0\ ^3/_2$	–	3.47	0	6.93	$S_t = 3/2,\ 3/2$	[29]
$Cr^{III}Zn^{II}Cr^{III}$	$^3/_2\ 0\ ^3/_2$	–	3.57	−4.4	7.14	$S_t = 0$	[111]
$Cr^{III}Cu^{II}Cr^{III}$	$^3/_2\ ^1/_2\ ^3/_2$	+18.5	3.58	−7.0	7.16	$S_t = 3/2$	[29]
$Cr^{III}Ni^{II}Cr^{III}$	$^3/_2\ 1\ ^3/_2$	−0.7	3.53	−1.8	7.06	S_t = mixed states	[29]
$Cr^{III}Fe^{III}$(l.s.)Cr^{III}	$^3/_2\ ^1/_2\ ^3/_2$	−15.7	–	−3.0	–	S_t = mixed states	[29]
$Cr^{III}Mn^{II}Cr^{III}$	$^3/_2\ ^5/_2\ ^3/_2$	+4.5	–	−11.5(?)	–	$S_t = 7/2,\ 5/2$	[29]

* The bridging oxime is nioxime, H_2L^{16}.

ground state. The EPR spectra in CH_3CN solution also demonstrates unambiguously the intramolecular nature of the exchange interaction.

3) For the $Mn^{IV}Cu^{II}Mn^{IV}$ complexes, both exchange interactions J and J_{13} are relatively strong and J is ferromagnetic. The relatively strong coupling J_{13} has a profound influence on the structure of the spin ladder, yielding a ground state with $S_t = 3/2$, which is otherwise an 'excited state'. Completely parallel spin alignment leading to an $S_t = 7/2$ ground state is inhibited by the competing antiferromagnetic coupling between the terminal Mn(IV) centers. The ground state $S_t = 3/2$ for the compound $Mn^{IV}(L^{16})Cu^{II}Mn^{IV}$ [113] is well separated and lies 14.6 cm^{-1} below the first excited state with $S_t = 1/2$ and 20.9 cm^{-1} below the second excited state with $S_t = 5/2$. The ground state $S_t = 3/2$ obtained from the susceptibility data was further verified by the isothermal magnetization measurements at 5 K in applied fields up to 5 T for both $Mn^{IV}Cu^{II}Mn^{II}$ compounds, listed in Table 4.

Two different exchange interactions are operative in these linear oximato-bridged trinuclear complexes. *The assumption occasionally made that no coupling prevails between the terminal ions may yield a wrong spin ground state*.

The trend in the sign and the magnitude of the neighbouring spin coupling has been qualitatively rationalized [29] in the case of Cr(III) complexes on the basis of the symmetry of the bridge-network $Cr(O–N)_3M$ as a whole. The $Cr(O–N)_3M$ heterobimetallic unit has an idealized D_{3h} symmetry. The five metal d orbitals transform in D_{3h} symmetry as $a_1'(d_{z^2})$, $e'(d_{x^2-y^2}, d_{xy})$ and $e'(d_{xz}, d_{yz})$. Thus the following predominant exchange pathways have been proposed for the Cr(III)–M pair.

$a_1'(d_{z^2}) \| a_1'(d_{z^2})$ antiparallel (1)

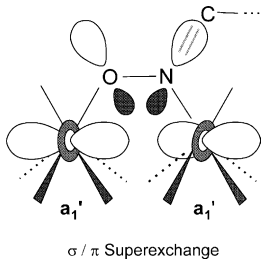

Scheme 14.

$a_1'(d_{z^2}) \perp e'(d_{x^2-y^2},\ d_{xy})$ parallel (2)

$a_1'(d_{z^2}) \perp e'(d_{xz},\ d_{yz})$ parallel (3)

$e'(d_{x^2-y^2},\ d_{xy}) \| e'(d_{x^2-y^2},\ d_{xy})$ antiparallel (4)

$e''(d_{xz},\ d_{yz}) \| e''(d_{xz},\ d_{yz})$ antiparallel (5)

The $a_1'a_1'$ overlap, shown in Scheme 14, is of both σ and π-character.

Recently a rational assembly of a series of exchange coupled linear heterotrinuclear complexes of the type $M_AM_BM_C$ based on the strategy of using 'metal oximates' as building blocks has been reported [27,31,120]. Thus complexes $[(\mathbf{5})M_A(L_{ox})M_BM_C]^{3+}$, where M_A = Fe(III) or Co(III) is facially coordinated to three nitrogen donors of the macrocyclic amine **5** and M_B = Cu(II), Ni(II) or Mn(II) and M_C = Cu(II) or Ni(II) are embedded in the asymmetric dicompartmental imine-oxime ligand H_4L_{ox} **17**.

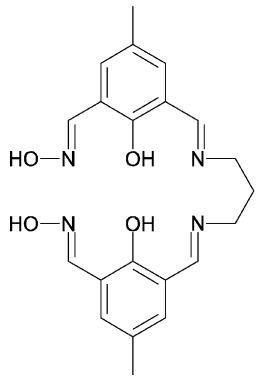

$= H_4L_{ox}$ **17**

The first compound synthesized in this series $M_AM_BM_C$ is the $Fe^{III}Cu^{II}Ni^{II}$ complex, $[(\mathbf{5})Fe^{III}(Cl)Cu^{II}(CH_3OH)(L_{ox})Ni^{II}(CH_3OH)_2](ClO_4)_2$ [27]. The structure of the dication is shown in Fig. 32.

The Fe–Cu–Ni skeleton is almost planar (174°) and intramolecular separations between the metal centers are Fe···Cu 3.695, Cu···Ni 3.087 and Fe···Ni 6.772 Å. Fig. 33 shows the plots of μ_{eff} versus T for the compounds $Fe^{III}Cu^{II}Ni^{II}$, its topological isomer Fe^{III}-$Ni^{II}Cu^{II}$ and Co^{III}(l.s.)$Cu^{II}Ni^{II}$.

The variable-temperature magnetic moments reveal a ground state $S_t = 3$, also confirmed by the magnetization measurements, for the compound $Fe^{III}Cu^{II}Ni^{II}$. The magnetic interactions operating in this type of linear trinuclear structure result in a ground state of high spin multiplicity, although the nearest neighbour spin alignments are antiparallel. Isoelectronic $Fe^{III}Cu^{II}$-Ni^{II} and $Fe^{III}Ni^{II}Cu^{II}$ demonstrate the strong influence of topological features on the magnetochemical properties.

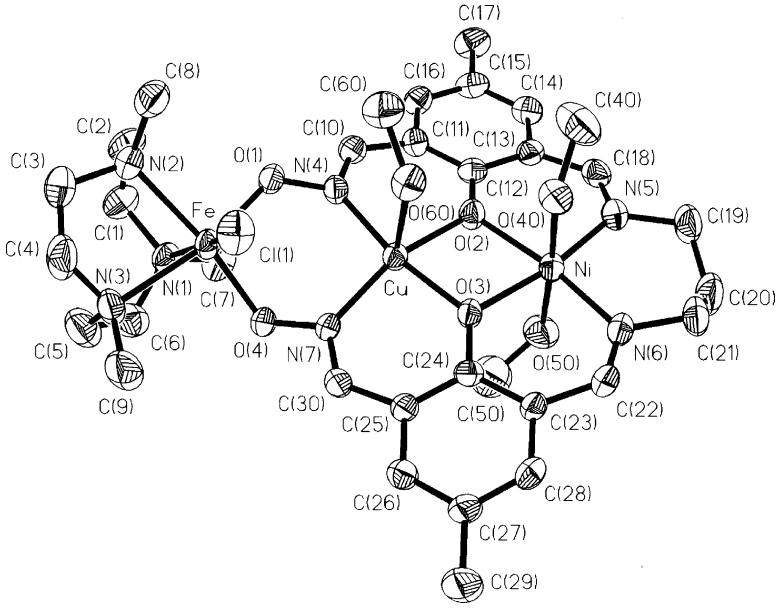

Fig. 32. Structure of the $Fe^{III}Cu^{II}Ni^{II}$ species in the dication $[(\mathbf{5})Fe^{III}(Cl)Cu^{II}(CH_3OH)(L_{ox})Ni^{II}(CH_3OH)_2]^{2+}$. Reproduced with permission from Ref. [31].

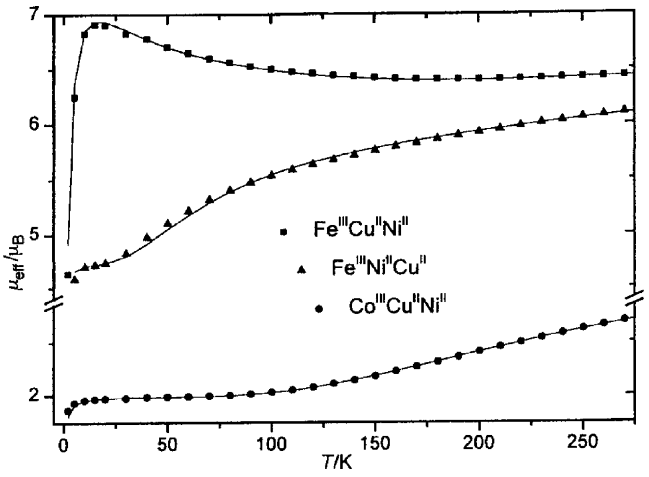

Fig. 33. Plots of μ_{eff} vs. T for $Fe^{III}Cu^{II}Ni^{II}$, $Fe^{III}Ni^{II}Cu^{II}$ and $Co^{III}Cu^{II}Ni^{II}$. The solid lines represent the simulation of the experimental data. Reproduced with permission from Ref. [31].

In contrast to the compound $Fe^{III}Cu^{II}Ni^{II}$ where the magnetic interactions result in a ground state of high-spin multiplicity ($S_t = 6/2$), the linear trinuclear structure $Fe^{III}Ni^{II}Cu^{II}$ yields an $S_t = 4/2$ ground state resulting also from an antiparallel spin alignment. As a direct consequence, the energy for $Fe^{III}Ni^{II}Cu^{II}$ is very similar to that of the isoelectronic $Fe^{III}Cu^{II}Ni^{II}$, but with *inverted* ground and first excited states, as shown in Fig. 34.

Another compound with the composition $[(\mathbf{5})Fe^{III}(NCS)Ni^{II}(H_2O)(NCS)(L_{ox})Ni^{II}(NCS)(H_2O)]$ has also been structurally characterized [27]. Simulated J-parameters for all compounds synthesized till to date are summarized in Table 5. For the series $M_AM_BM_C$, there was no necessity to consider the interactions between the terminal paramagnetic ions, and evaluated ground states were confirmed by magnetization measurements at a high field (7 T). This is in contrast with the behaviour of the series $M_AM_BM_A$, where the interactions between the terminal ions play a very important role in determining the ground state.

Following the Goodenough–Kanamori rules a qualitative rationalization for the exchange paths prevailing between neighbouring and terminal spin carriers in these heterotrinuclear complexes has been presented [27]. This interpretation implies the *predominance* of σ interactions over the insignificant π interactions.

Treatment of the heterotrinuclear complex $Fe^{III}Cu^{II}Ni^{II}$ with an excess of azide results in a bis(heterodnuclear) complex $[\{Cu^{II}(HL_{ox})Ni^{II}(N_3)\}_2]$, which can also be prepared in a step-wise synthesis. Although the compound is a tetranuclear species in the solid state and present as dinuclear units in the presence of a solvent like DMF, we are discussing this compound in this section because of its core [CuNi] present also in other trinuclear complexes. The molecular structure of the $[Cu^{II}Ni^{II}]_2$ is shown in Fig. 35.

The compound shows a centrosymmetric tetranuclear structure $[CuNi]_2$ with both nickel centers having pseudooctahedral geometry NiN_3O_3, whereas both

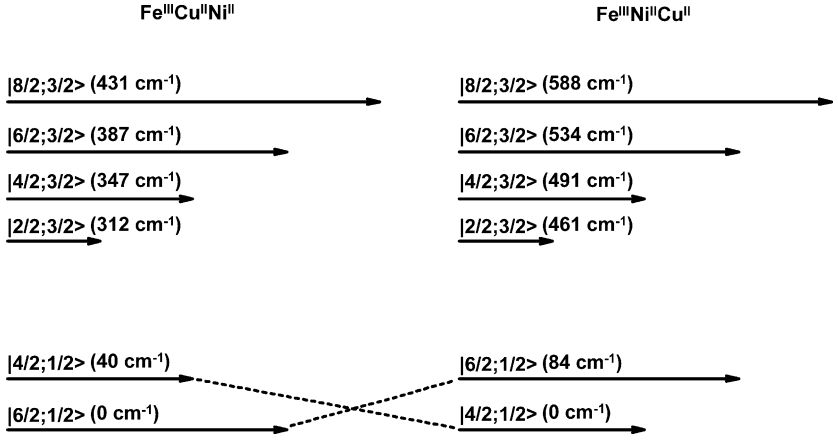

Fig. 34. Low-lying energy levels for $Fe^{III}Ni^{II}Cu^{II}$ and $Fe^{III}Cu^{II}Ni^{II}$. Reproduced with permission from Ref. [27].

Table 5
Magnetic properties of the heterotrinuclear complexes ($M_AM_BM_C$), $H = -2J_{AB}(S_A \cdot S_B) - 2J_{BC}(S_B \cdot S_C)$

Compound $[M_AM_BM_C]$ *	J_{AB}/cm^{-1}	J_{BC}/cm^{-1}	g_A	g_B	g_C	Ground state (S_t)	Reference
$Fe^{III}Cu^{II}Ni^{II}$	−19.8	−118.6	2.0	2.10	2.20	6/2	[27,31,120]
$Fe^{III}Ni^{II}Ni^{II}$	−9.3	−21.4	2.0	2.28	2.28	5/2	[27,31,120]
$Co^{III}Cu^{II}Ni^{II}$	–	−130.2	–	2.24	2.27	1/2	[27,31,120]
$Fe^{III}Cu^{II}Cu^{II}$	−5.0	−395.0	1.98	2.10	2.10	5/2	[27,31,120]
$Fe^{III}Ni^{II}Cu^{II}$	−10.6	−161.5	2.0	2.30	2.10	4/2	[27,31,120]
$Fe^{III}Mn^{II}Cu^{II}$	−12.6	−66.8	2.0	2.00	2.10	1/2	[27,31,120]

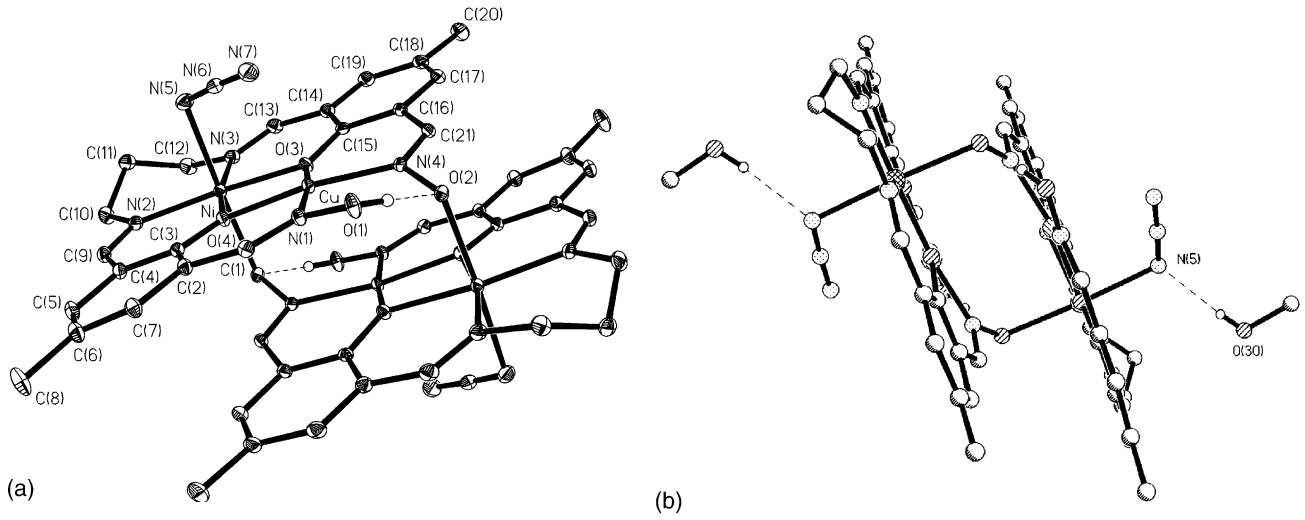

Fig. 35. (a) Molecular structure of $[\{Cu^{II}(HL_{ox})Ni^{II}(N_3)\}_2]$ showing the protonated oximic oxygen; (b) a perspective view of the same structure highlighting the connectivity between the two $Cu^{II}Ni^{II}$ units, together with two solvent methanol molecules. Reproduced with permission from Ref. [120].

Cu^{II} in square-planar CuN_2O_2 stereochemistries. The structure is built up of two heterodinuclear [Cu(H-L_{ox})Ni(N_3)] units, which are held together by two deprotonated oxime oxygens. The azide ions are bound only to nickel ions. In this regard this bis(heterodinuclear) complex differs from the similar reported complex [121]. The Cu···Ni separation of 3.085 Å is very similar to that of other oxime-bridged CuNi-complexes described in this section. Simulation of the magnetic data yields $J = -114.9$ cm^{-1}, $J' = +0.96$ cm^{-1}, where J corresponds to the coupling between the neighbouring Ni(II) and Cu(II) through the phenolate bridges (*intra*-dimer) and J' to the coupling through the oximato bridges (*inter*-dimer). The spin interactions, J and J', are shown schematically as J_{AF} and J_F in Fig. 36. Ferromagnetic coupling through oximato bridges is not very common.

A similar situation, i.e. ferromagnetic *inter*-dimer coupling has also been described for the compound $[Cu^{II}Mn^{II}]_2$ with an $S_t = 4$ ground state arising from the interaction between two $S = 2$ spin states, which again results from the antiferromagnetic *intra*-dimer interaction between the Cu(II) and Mn(II) center [108].

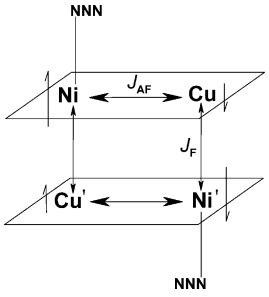

Fig. 36. Schematic representation of the interactions J_{AF} and J_F between the two hetero-dimeric units $Cu^{II}Ni^{II}$ in $[\{Cu^{II}(H-L_{ox})Ni^{II}(N_3)\}_2]$. Reproduced with permission from Ref. [120].

The EPR spectrum of $[Cu^{II}(HL_{ox})Ni^{II}(N_3)]_2$ in DMF at 10 K (Fig. 37) exhibiting copper hyperfine structure in the high field regions (*inverted* g-values, $g_{\|} < g_{\perp}$) clearly indicates that the unpaired electron in the ground state resides on the molecular orbital of d_{z^2} character comprising d_{z^2}(Cu) and d_{z^2}(Ni) and is delocalized over the [CuNi] core.

Summarily, the strength of the coupling described in this section between Cu(II) and Ni(II) centers belong to the upper end of the range observed (Tables 5 and 2). The small increase in $|J_{CuNi}|$ from 114.9 to 130.2 cm^{-1} in $Co^{III}Cu^{II}Ni^{II}$ has been attributed to the more distorted geometry (nonlinear CoCuNi skeleton) of the latter.

The mechanism of leading phenomenon of isotropic exchange for the $Cu^{II}Ni^{II}$ pairs is now understood [4,5]. The net exchange is composed of two competing individual antiferro- and ferro-magnetic exchanges,

$$J[d_{x^2-y^2}(Cu) \leftrightarrow d_{x^2-y^2}(Ni)] \text{ and } J[d_{x^2-y^2}(Cu) \leftrightarrow d_{z^2}(Ni)]$$

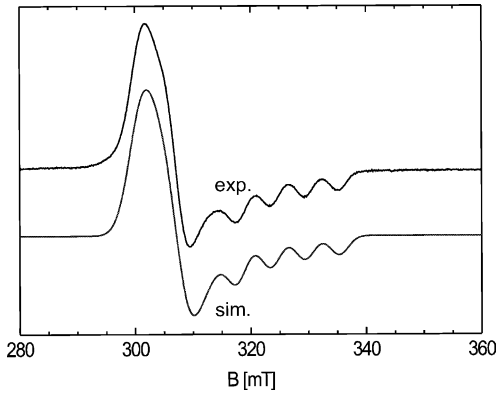

Fig. 37. X-band EPR spectrum of $[Cu^{II}(HL_{ox})Ni^{II}(N_3)]_2$ in DMF at 10 K, together with the simulated spectrum. Reproduced with permission from Ref. [120].

The dominant pathway $d_{x^2-y^2}/d_{x^2-y^2}$ is antiferromagnetic, while the pathway $d_{x^2-y^2}/d_{z^2}$ involving orthogonal magnetic orbitals is weak ferromagnetic, thus resulting in a significant overall antiferromagnetic interaction for all reported [$Cu^{II}Ni^{II}$] complexes, irrespective of the bridging ligands.

7.3. Tetranuclear complexes

The oxime-bridged heterometallic tetranuclear complexes reported until now are of two types:

i) Linear $M_AM_BM_BM_A$ type containing the dinucleating oxime, $[L^{30}]^{3-}$, with the composition

$[(\mathbf{5})_2Fe^{III}_2(\mu_2\text{-}OOC\cdot CH_3)_2(L^{30})_2(CH_3OH)_2Ni^{II}_2] \times (BF_4)_2$ [30]

and its manganese(III) analog

$[(\mathbf{5})_2Mn^{III}_2(\mu_2\text{-}OOC\cdot CH_3)_2(L^{30})_2(CH_3OH)_2Ni^{II}_2] \times (BF_4)_2$ [89, 122].

A similar $Fe^{III}Fe^{II}Fe^{II}Fe^{III}$ species has been described in Section 6.3.

ii) Butterfly structures with the cores $[(M_A)_2(\mu_3\text{-}O)_2(M_B)_2]^{8+}$. Similar homometallic butterfly cores have been described in Sections 6.3 and 6.4. The cores $[Cr^{III}_2(\mu_3\text{-}O)_2Fe^{III}_2]^{8+}$ [69], $[Cr^{III}_2(\mu_3\text{-}O)_2Mn^{III}_2]$ [32] and $[Fe^{III}_2(\mu_3\text{-}O)_2Mn^{III}_2]$ [79,122] with the oxime $[L^{27}]^{2-}$ are known.

Two isostructural mixed metal complexes of the dinucleating ligand H_3L^{30} have been reported, both of which incorporate the $[Ni_2(L^{30})_2]^{2-}$ core. The first example $[(\mathbf{5})_2Fe^{III}_2(\mu_2\text{-}OOC\cdot CH_3)_2(L^{30})_2(CH_3OH)_2Ni^{II}_2](BF_4)_2$ [30] was prepared by the reaction of (**5**)$FeCl_3$ with $Ni(CH_3COO)_2\cdot 4H_2O$ and H_3L^{30} in methanol, followed by precipitation of the product with tetrafluoroborate. The second example is prepred in an analogous fashion, but replacing (**5**)$FeCl_3$ with [(**5**)$MnCl_3$]. The two compounds are isostructural and the structure of the manganese complex is shown in Fig. 38.

Due to static Jahn–Teller effect of Mn(III) (d^4 high spin) the Mn–O3 (acetate) and its *trans* disposed Mn–N3 bonds are significantly longer than the other equatorial bonds. The manganese center is in an axially elongated octahedral coordination with the unoccupied

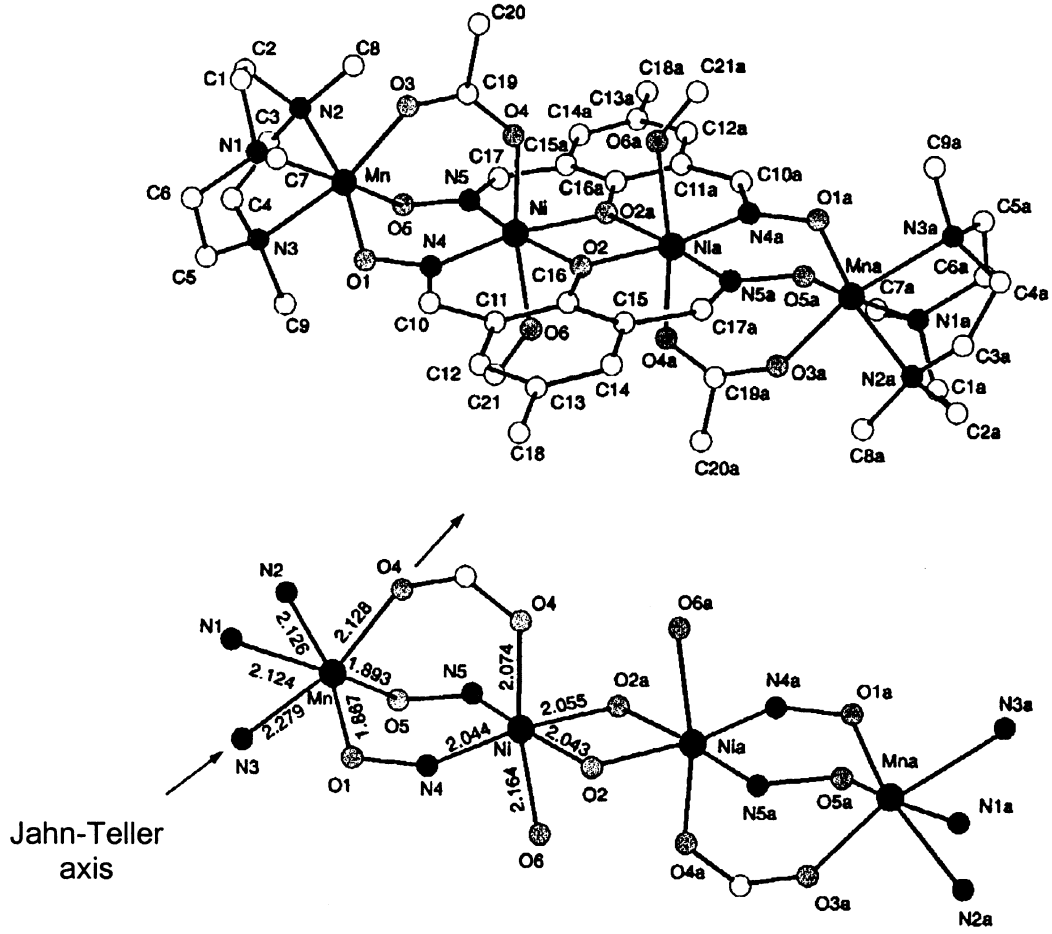

Fig. 38. Structure of the cation $[(\mathbf{5})_2Mn^{III}_2(L^{30})_2(\mu_2\text{-}OOC\cdot CH_3)_2(CH_3OH)_2Ni^{II}_2]^+$ and a view of the first coordination spheres of the metal ions in $Mn^{III}Ni^{II}Ni^{II}Mn^{III}$. Reproduced with permission from Refs. [89,122].

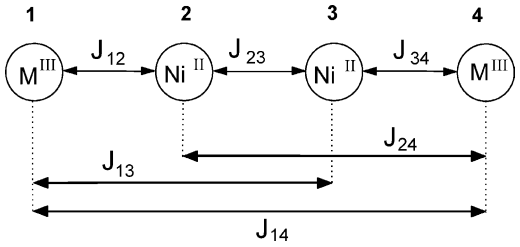

Scheme 15.

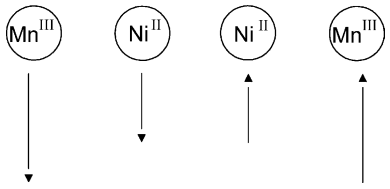

Scheme 16.

$d_{x^2-y^2}$ orbital, which is pointing towards the oxime ligands. The nickel centers adopt distorted octahedral environment; an acetate ion acts, together with two oxime N–O groups, as a bridging ligand between the terminal manganese(III) and the central nickel(II) centers. The central phenoxide bridging unit Ni(1)O(2)Ni(1a)O(2a) forms an exact plane with a center of inversion. The Mn–Ni–Ni–Mn skeleton is not perfectly linear; the angle Mn–Ni–Ni(a) is 166.6°. The magnetic analysis was carried out using the model shown in Scheme 15.

In this model J_{ik} represents the exchange interaction between the ith and kth paramagnetic ions. Preliminary simulation of the experimental data yields: $J_{12} = J_{34} = +4.3\ cm^{-1}$, $J_{13} = J_{24} = +1.6\ cm^{-1}$, $J_{23} = -13.6\ cm^{-1}$, $J_{14} = -0.4\ cm^{-1}$, $g_{Ni} = 2.58$, $g_{Fe} = 2.0$, $D_{Mn} = 0$, $D_{Ni} = 0$. The g_{Ni}-value is physically not meaningful. Nevertheless, the spin orientations in the complex have been established and are shown in Scheme 16.

That the compound $Mn^{III}Ni^{II}Ni^{II}Mn^{III}$ has an extremely complicated low-lying magnetic structure with a non-diamagnetic ground state, which is not well separated from the upper-lying states, is in full conformity with the non-zero magnetic moment of 3.48 μ_B at 2.0 K.

On the other hand, the best fit of the experimental data for the compound $Fe^{III}Ni^{II}Ni^{II}Fe^{III}$ [30] yields $J_{12} = J_{34} = -6.8\ cm^{-1}$, $J_{13} = J_{24} = -3.2\ cm^{-1}$, $J_{23} = -7.7\ cm^{-1}$, $J_{14} = -1.8\ cm^{-1}$, $D_{Ni} = -3.90\ cm^{-1}$, $g_{Ni} = 2.21$ (fixed), $g_{Fe} = 2.00$ (fixed), $D_{Fe} = 0$ (fixed). The evaluated value of the zero-field splitting parameter D_{Ni} agrees with the non-zero magnetic moment of 2.05 μ_B at 2.0 K, which indicates a non-diamagnetic ground state with a complicated low-lying magnetic structure. The fitting of the susceptibility data does not provide the most accurate means of determining D values. The exchange interaction between the neighbouring Fe(III) and Ni(II) ions $J_{12} = J_{34} = -6.8\ cm^{-1}$ is appreciably weaker than that in the trinuclear $Fe^{III}Ni^{II}Fe^{III}$ complex ($J = -32\ cm^{-1}$) [119] described in Section 7.2, although the Fe···Ni separations are the same 3.50 Å, but there are *three* –N–O bridging ligands in the trinuclear complex.

Scheme 17 shows the important exchange pathways operating in the $Ni_2(phenoxo)_2$ core. It is evident from the scheme that the dominant exchange pathway for the core is the symmetry-allowed $b_1(d_{xy})||p(O)||b_1(d_{xy})$ (using Ginsberg's symbols in idealized C_{2v} symmetry) σ-superexchange pathway.

The sign of the neighbouring spin-couplings, which are different in Fe(III)- and Mn(III), can be qualitatively rationalized on the basis of the symmetry of the bridge-network M(III)(O–N)$_2$Ni(II) as a whole. Considering the xy-plane as the paper plane, the electron distribution in different d-orbitals are shown below:

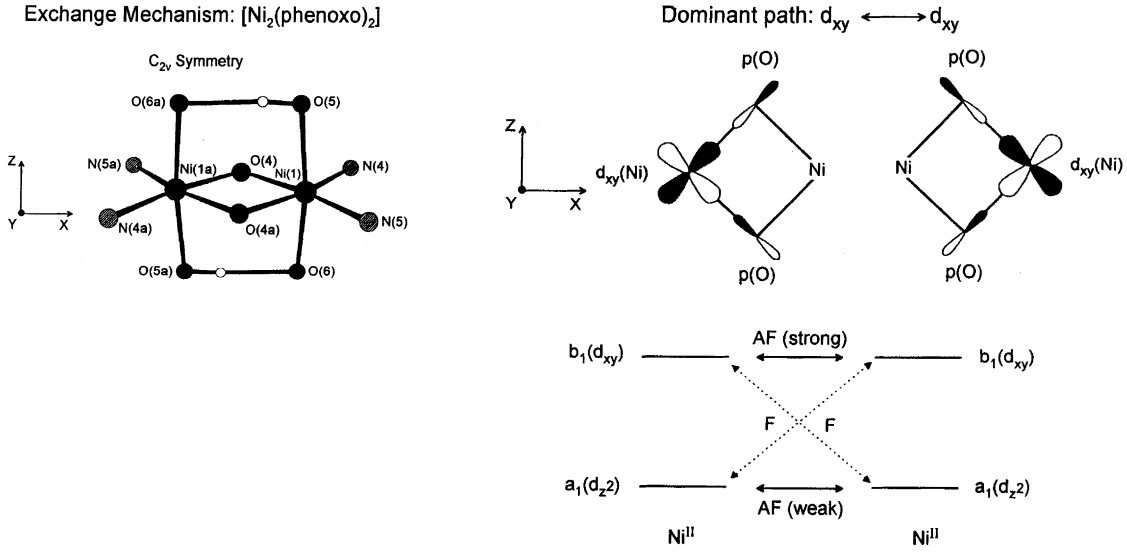

Scheme 17.

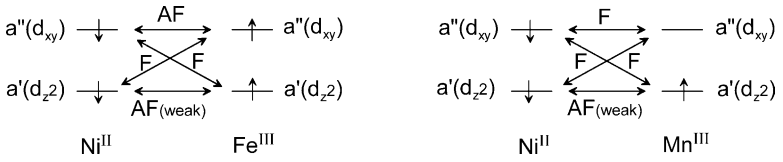

Scheme 18.

	t_{2g}-parentage	e_g-parentage
$Ni^{II}(d^8)$	$(d_{x^2-y^2})^2(d_{xz})^2(d_{yz})^2$	$(d_{z^2})^1(d_{xy})^1$
$Fe^{III}(d^5$h.s.)	$(d_{x^2-y^2})^1(d_{xz})^1(d_{yz})^1$	$(d_{z^2})^1(d_{xy})^1$
$Mn^{III}(d^4$h.s.)	$(d_{x^2-y^2})^1(d_{xz})^1(d_{yz})^1$	$(d_{z^2})^1(d_{xy})^0$

In C_s symmetry the d_z^2 and d_{xy} orbitals transform as a′ and a″, respectively. Thus the following predominant exchange pathways can be envisaged for the M(III)–Ni(II) pair, present in the Fe(III)Ni(II)Ni(II)Fe(III) and Mn(III)Ni(II)Ni(II)Mn(III) complexes. That the dominant superexchange pathway, which determines the sign of J, is $a''(d_{xy})\leftrightarrow a''(d_{xy})$ for both cases, is evident from Scheme 18.

Three different heterotetranuclear butterfly cores are known, viz. $[Cr_2^{III}(\mu_3\text{-}O)_2Fe_2^{III}]^{8+}$ [69], $[Cr_2^{III}(\mu_3\text{-}O)_2Mn_2^{III}]^{8+}$ [70] and $[Fe_2^{III}(\mu_3\text{-}O)_2Mn_2^{III}]^{8+}$ [79,122]. The structure of the compounds are very similar and the structure of the $[Fe_2^{III}(\mu_3\text{-}O)_2Mn_2^{III}]^{8+}$ core is discussed here. The compounds with the composition $[(\mathbf{5})_2Fe_2^{III}(\mu_3\text{-}O)_2(\mu_2\text{-carboxylate})_3(L^{27})_2Mn_2^{III}]ClO_4$ with μ_2-carboxylate = acetate, diphenylglycolate and benzoate have been structurally characterized and as an archetype the structure with the acetate bridging ligands is shown in Fig. 39.

The metal centers in the core $Fe_2^{III}(\mu_3\text{-}O)_2Mn_2^{III}$ are disposed in a butterfly arrangement. The structure can thus be considered as two $FeMn_2O$ triangular units joined by edge-sharing with a dihedral angle of 145.1° (compare Scheme 2). That the 'body' metal ions are Jahn–Teller distorted, high-spin d^4Mn(III) ions is clearly shown by the X-ray structure; the axially elongated sites are occupied by the carboxylate oxygen atoms of acetate. Considering a two-J model used in Section 6.3, the magnetic data for these three complexes were analyzed and the following parameters were evaluated by simulation of the experimental susceptibility data.

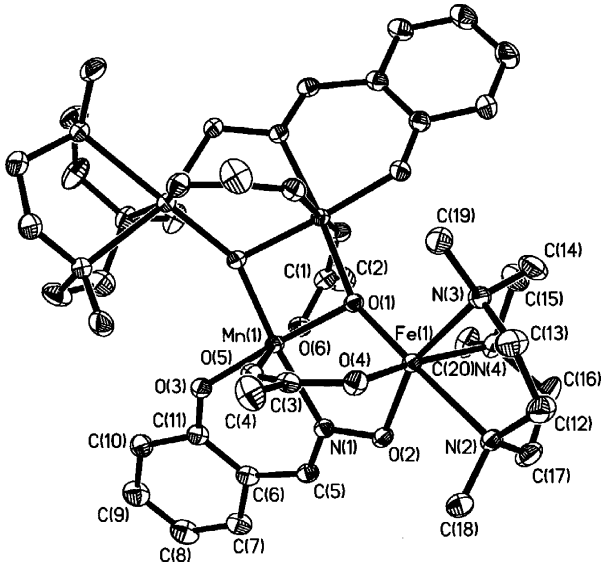

Fig. 39. Structure of the butterfly core $[Fe_2^{III}(\mu_3\text{-}O)_2Mn^{III}]$ in $[(\mathbf{5})_2Fe_2^{III}(\mu_3\text{-}O)_2(\mu_2\text{-}OOC\cdot CH_3)_3(L^{27})_2Mn_2^{III}]^+$. Reproduced with permission from Refs. [79,122].

Fe_2Mn_2-acetate:	$J_{wb} = -25.2\ cm^{-1}$
spin ground state	$J_{bb} = -35.1\ cm^{-1}$
$S_t = 1$	$\langle g \rangle = 2.05$ (fixed)
	$D = -0.38$
Fe_2Mn_2-diphenylglycolate:	$J_{wb} = -22.3\ cm^{-1}$
spin ground state	$J_{bb} = -31.6\ cm^{-1}$
$S_t = 1$	$\langle g \rangle = 2.0$ (fixed)
	$D = 0$
Fe_2Mn_2-benzoate:	$J_{wb} = -19.4\ cm^{-1}$
spin ground state	$J_{bb} = -28.9\ cm^{-1}$
$S_t = 2,1$	$\langle g \rangle = 2.09$
	$D = 0$

Now, it would be proper at this place to make a comparison of the magnetic properties of the cores $[Fe_4O_2]^{8+}$, $[Mn_4O_2]^{8+}$ and $[Fe_2Mn_2O_2]^{8+}$. The temperature dependence of the magnetic susceptibility unambiguously reveals a non-degenerate $S_t = 0$ ground state, well isolated in energy, for the $[Fe_4O_2]^{8+}$ core, not only for the *acetate*, but also for the *diphenylglycolate* and *triphenylacetate* as the bridging carboxylate groups. On the other hand, for the $[Mn_4O_2]^{8+}$ core, the ground state is established to be $S_t = 3$ from the magnetic susceptibility as well as from the field-dependent (0.5–7.0 T) magnetization measurements at 2 K for various bridging carboxylates, viz. acetate, diphenylglycolate, benzoate etc. On the contrary, the triplet ground state ($S_t = 1$, $|1,4,5\rangle$) for the acetate bridged $[Fe_2Mn_2(\mu_3\text{-}O)_2(CH_3COO)_3]^{5+}$ core has components S_{Mn} and S_{Fe} values of 4 and 5, respectively, and the overall favoured spin alignment is shown with the exchange coupling constants in Scheme 19.

The first excited spin-quintet state $|2,3,5\rangle$ is placed 22 cm^{-1} above the ground state $|1,4,5\rangle$. The energy difference between the lowest two states is $\Delta E = 26 \pm 6$ cm^{-1} from the EPR measurements (5–50 K), thus confirming the results of the susceptibility data. Although the intrinsic interaction between the 'body'

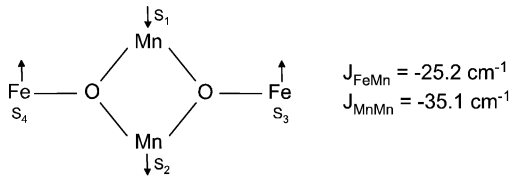

Scheme 19.

manganese ions of the butterfly is antiparallel in nature, there is frustration in the spin alignment associated with the two manganese ions, causing the alignment to be parallel. The ground state for the *benzoate* complex is degenerate with $S_t = 2$ and 1. This ground-state variability may be a result of the spin frustration. The ground state is particularly sensitive to the relative magnitudes of the competing interactions and the spin of the ground state adopts an intermediate value rather than the lowest value that might be anticipated for an antiferromagnetically coupled system.

The compound with the butterfly core $[Cr_2^{III}(\mu_3\text{-}O)_2\text{-}Mn_2^{III}]$ [70] contains six-coordinated CrN_3O_3, chromium(III) ions representing the wing-tips, and *five-coordinated* $MnNO_4$, high-spin manganese(III) ions as the 'body' ions. The magnetic susceptibility measurements revealed a diamagnetic ($S_t = 0$) ground state with antiferromagnetic exchange interactions $J_{CrMn} = -11.7$ cm^{-1} and $J_{MnMn} = -13.0$ cm^{-1}. The ground state is separated from the first excited state by an energy gap of 15.8 cm^{-1}. The ground state $S_t = 0$ results from the coupling of $S_{Cr} = 3$ and $S_{Mn} = 3$ subspins. On the contrary, the compound with the core $[Cr_2^{III}(\mu_3\text{-}O)_2Fe_2^{III}]$ [69], which is isostructural but not isoelectronic with the above discussed $[Cr_2^{III}(\mu_3\text{-}O)_2\text{-}Mn_2^{III}]$ core, has a non-diamagnetic ($S_t \neq 0$) ground state and the low-lying magnetic states of the compound are very complicated. The interaction J_{CrFe} ($= -7.5$ cm^{-1}) does not dominate over the other J_{FeFe} ($= -5.3$ cm^{-1}), thus the intrinsic character of the J_{FeFe} cannot be totally ignored, resulting in *spin frustration*.

7.4. Miscellaneous

The compound $Mn^{II}\{Cu^{II}(L)\}(H_2O)_4$, where H_4L is *N*,*N*′-bis[2-hydroxyiminomethyl)phenyl]oxamide, is proposed to have a polymeric structure extended by the dioximate–Mn^{II}–dioximate linkage [123]. It is a weak ferromagnet ($T_c = 5.5$ K) exhibiting a weak antiferromagnetic interaction between the ferrimagnetic chains.

Two dinuclear ($Cu^{II}Gd^{III}$) complexes (Fig. 40) with a μ-phenolato–μ-oximato linkage deriving from a polydentate asymmetrical oxime/Schiff base ligand have recently been structurally and magnetochemically characterized [124]. The bridging network is not planar.

The complex with the larger diamino chain unexpectedly exhibits an antiferromagnetic interaction, although

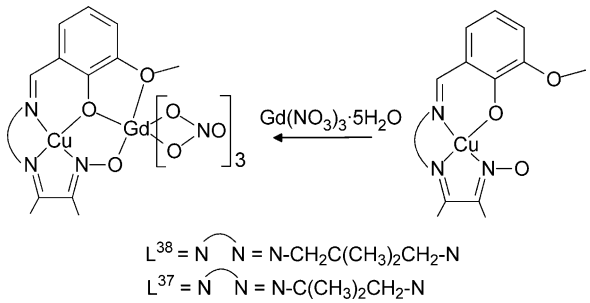

Fig. 40. Schematic representations of the structures of two $Cu^{II}Gd^{III}$-complexes together with their precursors mononuclear copper(II) complexes. Reproduced with permission from Ref. [124].

very weak $J \approx -1$ cm^{-1}. For the other complex the interaction is ferromagnetic as expected, $J \approx +7.0$ cm^{-1}. The same group has also described the structures and magnetic properties of trinuclear complexes with μ-phenolato–μ-oximato Cu^{II}–Gd^{III}–Cu^{II} cores [125]. The resulting Cu(O,N–O)Gd networks are not planar. Both the 'usual' ferromagnetic and 'unusual' antiferromagnetic interactions have been observed for the CuGd-pairs with the ligands HL^{34}, H_2L^{37}–H_2L^{39}. A relationship of the magnetic properties for the [CuGd] pairs with the bending of the bridging network has been invoked.

Three compounds with the composition $[Mn^{III}Cu^{II}\text{-}(L^1)_2(RCOO)\cdot(H_2O)_2]_n$, where R = CH_3, C_2H_5 and C_6H_5 have been described as ferromagnetic Mn(III)Cu(II) alternating linear chains [126]. The EXAFS data are consistent with a distorted octahedral environment for both divalent copper and trivalent manganese centers. The $\chi_M \cdot T$ data down to ~30 K was fitted with the formula appropriate to one-dimensional $S_{Mn} = 2$ and $S_{Cu} = 1/2$ ferromagnet with $g_{Mn} = 2.0$, $g_{Cu} = 2.21$ and $J = +26$ cm^{-1}. The ferromagnetic nature of the interaction is attributable to the orthogonality of the respective magnetic orbitals. The maximum of χ_M at 12 K for applied fields lower than 4000 G is due to a long-range antiferromagnetic ordering of the ferromagnetic chains. This maximum broadens as the field is increased and finally disappears for $H > 4000$ G demonstrating that a field-induced transition from an antiferromagnetic to a ferromagnetic ground state occurs. Thus the compound **18** exhibits a metamagnetic behaviour.

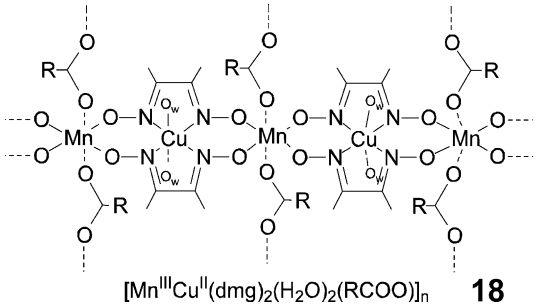

18

If the ligand H_2L^1 is replaced by H_2L^{16}, then the oximato-bridged $[Mn^{III}Cu^{II}(L^{16})(CH_3COO)(H_2O)_2]_n$ chain exhibits a long-range ferromagnetic ordering with $T_c = 9$ K [127]. An iron(III)-containing compound $[Fe^{III}Cu^{II}(L^{16})(H_2O)_2(CH_3COO)]_n$ described in the same paper is a ferrimagnet and orders antiferromagnetically at 7.5 K.

8. Conclusion and perspective

In the last few years, the idea of synthesizing polymetallic complexes involving 'metal-oximates' as building blocks has become quite popular. In general, most approaches taken thus far involve facile chemistry available for the synthesis of oximes and the wide variety of starting materials available. In the near future new chemistry is expected to be developed that enables chemists to be able to synthesize a wide variety of ligands possessing the versatility of functioning both as bridging and multimetal-nucleating group. A step forward in this direction has already been done by the introduction of the polydinucleating oxime ligand H_3L^{30} and H_3L^{31}. The ultimate goal obviously is the development of the area of molecular magnetism.

The oxime moiety ($-C(R)=NO^-$) combined with a coordination site for a metal ion, represents a bridge between coordination complexes and supramolecular assembly. Since hydrogen bonding is presently one of the best known strategies to build supramolecular arrays in a controlled way, it is of utmost importance to understand the mechanism of exchange interactions mediated by hydrogen bonding in conjunction with oxime ligands, which are well-known for their hydrogen-bonding capabilities. In this regard exchange-coupled polymetallic complexes with hydrogen-bonded oximates are highly desirable.

Recently, coordination compounds of some non-innocent ligands, which facilitate easy generation of organic radicals in presence of air, have been described [128,129]. Incorporation of such functionalities in oxime-ligands would increase the paramagnetic nuclearity of the complexes exhibiting unusual magnetic properties. Thus, larger polyparamagnetic assemblies are expected to be synthesized through modular techniques by choosing suitable ligands.

Oximato groups ($=N-O^-$) can mediate exchange interactions of varying range, weak and moderate ferromagnetic to strong antiferromagnetic. A problem concerning such exchange coupled systems is the unavailability of isostructural polynuclear complexes with varying d^n electron configurations. Investigations of a series of isostructural polynuclear complexes are more informative in comparison to those comprising singly isolated exchange-coupled clusters only. Although most of the compounds discussed in this article have been structurally characterized, little can be said about the magneto-structural trends. In the light of the present state of knowledge the strategy of 'irregular spin-state structure' resulting from a particular spin topology is more effective in obtaining 'high spin' molecules than the common strategy of obtaining ferromagnetically coupled systems through involvement of symmetry-related strict orthogonality of the magnetic orbitals of the interacting metal centers. It is now clear that a small perturbation may have a dramatic effect on the ground state and may lead to ground-state variability. This observation is potentially relevant for generating magnetic materials with predictable and controllable properties.

The continuous development of exchange coupled heterometallic systems started with an aim of understanding interactions between two magnetic ions. The number of papers cited testify to the uninterrupted interest in this area of chemistry, they have narrowed the gap prevailing so long in the area of coordination chemistry involving exchange-coupled metal oximates. Of particular interest is the small but significant effect of bridging ligands like carboxylato anions for cooperation with the ancillary ligand, viz. the oxime-ligands, to build-up high-nuclearity metal clusters.

Additionally, in traversing the first-row d-block elements we have noticed that paramagnetic Ti- and V-oximates remain relatively unexplored, probably because of difficulties in synthesis and stability. Clearly, these aspects need to be further experimentally explored.

Acknowledgements

Continuous and generous financial support of our work by the Max-Planck Society, the Deutsche Forschungsgemeinschaft, the Fonds der Chemischen Industrie is thankfully acknowledged. I wish to express my deepest gratitude to the colleagues and students whose names appear in the references for their enthusiasm and invaluable contributions. Hearty thanks are due to Professor Dr K. Wieghardt for his continuous interest. Skilful technical assistance of H. Schucht, R. Wagner, U. Pieper, A. Goebels and M. Winter (Bochum) is thankfully acknowledged. Last, but not least, I highly appreciate the help of T. Montenbruck and B. Deckers for the electronic manuscript preparation.

References

[1] See for example: R.H. Holm, E.I. Solomon (Guest Editors), Chem. Rev. 96 (1996) no. 7;
A.L. Feig, S.J. Lippard, Chem. Rev. 94 (1994) 759;
L. Que, A.E. True, Prog. Inorg. Chem. 38 (1990) 98;
S.J. Lippard, J.M. Berg, Principles of Bioinorganic Chemistry, University Science Books, Mill Valley, CF, 1994;

W. Kaim, B. Schwederski, Bioanorganische Chemie, B.G. Teubner, Stuttgart, 1991; Bioinorganic Chemistry of Copper, eds. K.D. Karlin, Z. Tyeklár, Chapman & Hall, New York, 1993; Mechanistic Bioinorganic Chemistry, eds. H. Holden Thorp, V.L. Pecoraro, American Chemical Society, Washington, 1995.
[2] R.D. Willett, D. Gatteschi, O. Kahn (Eds.), Magneto-Structural Correlations in Exchange Coupled Systems, Kluwer Academic Publishers, Dordrecht, 1985.
[3] D. Gatteschi, O. Kahn, J.S. Miller, F. Palacio (Eds.), Magnetic Molecular Materials, Kluwer Academic Publishers, Dordrecht, 1991.
[4] O. Kahn, Molecular Magnetism, VCH-Verlagsgesellschaft, Weinheim, 1993.
[5] O. Kahn, Adv. Inorg. Chem. 43 (1995) 179.
[6] K.S. Murray, Adv. Inorg. Chem. 43 (1995) 261.
[7] C.J. O'Connor (ed.), Research Frontiers in Magnetochemistry, World Scientific, Singapore, 1993.
[8] (a) S.J. Gruber, C.M. Harris, E. Sinn, J. Inorg. Nucl. Chem. 30 (1968) 1805;
(b) J. Selbin, L. Ganguly, J. Inorg. Nucl. Chem. Lett. 5 (1969) 815;
(c) C.B. Singh, B. Sahoo, J. Inorg. Nucl. Chem. 36 (1974) 1259;
(d) R.L. Linkvedt, L.S. Kramer, G. Ranger, P.W. Corfield, M.D. Glick, Inorg. Chem. 22 (1983) 3580;
(e) S. Pal, R. Mukherjee, M. Tomas, L.R. Falvello, A. Chakravorty, Inorg. Chem. 25 (1986) 200.
[9] D. Luneau, H. Oshio, H. Okawa, S. Kida, J. Chem. Soc. Dalton Trans. (1990) 2283.
[10] P. Chaudhuri, M. Winter, P. Fleischhauer, W. Haase, U. Flörke, H.-J. Haupt, J. Chem. Soc. Chem. Commun. (1990) 1728.
[11] P. Chaudhuri, M. Winter, B.P.C. Della Védova, E. Bill, A. Trautwein, S. Gehring, P. Fleischhuer, B. Nuber, J. Weiss, Inorg. Chem. 30 (1991) 2148.
[12] D. Luneau, H. Oshio, H. Okawa, S. Kida, Chem. Lett. (1989) 443.
[13] H. Okawa, M. Koikawa, S. Kida, D. Luneau, H. Oshio, J. Chem. Soc. Dalton Trans. (1990) 469.
[14] R. Ruiz, F. Lloret, M. Julve, M.C. Munoz, C. Bois, Inorg. Chim. Acta 219 (1994) 179.
[15] E. Colacio, J.M. Dominguez-Vera, A. Escuer, M. Klinga, R. Kivekäs, A. Romerosa, J. Chem. Soc. Dalton Trans. (1995) 343.
[16] L. Tschugaeff, Chem. Ber. 23 (1890) 1.
[17] A. Chakravorty, Coord. Chem. Rev. 13 (1974) 1.
[18] M.E. Keeney, K. Osseo-Asare, K.A. Woode, Coord. Chem. Rev. 59 (1984) 141.
[19] G.N. Schrauzer, Angew. Chem. Int. Ed. Engl. 15 (1976) 417.
[20] R.C. Mehrotra, in: G. Wilkinson, R.D. Gillard, J.A. McCleverty (Eds.), Comprehensive Coordination Chemistry, vol. 2, Pergamon, Oxford, 1987, p. 269.
[21] V.Y. Kukushkin, A.J.L. Pombeiro, Coord. Chem. Rev. 181 (1999) 147 (and references therein).
[22] (a) D.J. White, P.A. Tasker, A.G. Smith, Coord. Chem. Rev. in press.;
(b) P. Chaudhuri, Proc. Indian Acad. Sci. (Chem. Sci.) 111 (1999) 397.
[23] J.B. Goodenough, J. Phys. Chem. Solids 6 (1958) 287.
[24] J. Kanamori, J. Phys. Chem. Solids 10 (1959) 87.
[25] J.B. Goodenough, Magnetism and the Chemical Bond, Wiley, New York, 1963.
[26] A.P. Ginsberg, Inorg. Chim. Acta Rev. 5 (1971) 45.
[27] (a) C.N. Verani, E. Rentschler, T. Weyhermüller, E. Bill, P. Chaudhuri, J. Chem. Soc. Dalton Trans. (2000) 4263;
(b) C.N. Verani, Dissertation, Bochum, Germany, 2000.
[28] S. Ross, T. Weyhermüller, E. Bill, K. Wieghardt, P. Chaudhuri, Inorg. Chem. 40 (2001) 6656.
[29] D. Burdinski, F. Birkelbach, T. Weyhermüller, U. Flörke, H.-J. Haupt, M. Lengen, A.X. Trautwein, E. Bill, K. Wieghardt, P. Chaudhuri, Inorg. Chem. 37 (1998) 1009 (and references therein).
[30] C. Krebs, M. Winter, T. Weyhermüller, E. Bill, K. Wieghardt, P. Chaudhuri, J. Chem. Soc. Chem. Commun. (1995) 1913.
[31] C.N. Verani, T. Weyhermüller, E. Rentschler, E. Bill, P. Chaudhuri, Chem. Commun. (1998) 2475.
[32] P. Chaudhuri, F. Birkelbach, M. Winter, V. Staemmler, P. Fleischhauer, W. Haase, U. Flörke, H.-J. Haupt, J. Chem. Soc. Dalton Trans. (1994) 2313 (and references therein).
[33] P. Chaudhuri, K. Wieghardt, Prog. Inorg. Chem. 35 (1987) 329.
[34] (a) R. Beckett, R. Colton, B.F. Hoskins, R.L. Martin, D.G. Vince, Aust. J. Chem. 22 (1969) 2527;
(b) R. Beckett, B.F. Hoskins, J. Chem. Soc. Dalton Trans. (1972) 291.
[35] (a) J.A. Bertrand, J.H. Smith, P.G. Eller, Inorg. Chem. 13 (1974) 1649;
(b) J.A. Bertrand, P.G. Eller, Prog. Inorg. Chem. 21 (1976) 29.
[36] W.E. Hatfield, Inorg. Chem. 11 (1972) 216.
[37] A. Vaciago, L. Zamibonelli, J. Chem. Soc. Sect. A (1970) 218.
[38] B. Cervera, R. Ruiz, F. Lloret, M. Julve, J. Cano, J. Faus, C. Bois, J. Mrozinski, J. Chem. Soc. Dalton Trans. (1997) 395.
[39] Y.M. Wang, C.C. Wang, S.L. Wang, C.S. Chung, Acta Crystallogr. Sect. C 46 (1990) 1770.
[40] M. Maekawa, S. Kitagawa, Y. Nakao, S. Sakamoto, A. Yatani, W. Mori, S. Kashino, M. Munakata, Inorg. Chim. Acta 293 (1999) 20.
[41] J.A. Bertrand, J.H. Smith, D.G. VanDerveer, Inorg. Chem. 16 (1977) 1477.
[42] R.J. Butcher, C.J. O'Connor, E. Sinn, Inorg. Chem. 18 (1979) 1913.
[43] (a) G.A. Nicholson, C.R. Lazarus, B.J. McCormick, Inorg. Chem. 19 (1980) 192;
(b) G.A. Nicholson, J.L. Petersen, B.J. McCormick, Inorg. Chem. 19 (1980) 195.
[44] M. Näsäkkälä, H. Saarinen, J. Korvenranta, E. Näsäkkälä, Acta Chem. Scand. 35A (1981) 569.
[45] F. Abraham, J.M. Capon, G. Nowogrocki, S. Suer, C. Bremard, Polyhedron 4 (1985) 1761.
[46] D. Luneau, H. Oshio, H. Okawa, M. Koikawa, S. Kida, Bull. Chem. Soc. Jpn. 63 (1990) 2212.
[47] K. Matsumoto, S. Ooi, W. Mori, Y. Nakao, J. Chem. Soc. Dalton Trans. (1990) 3117.
[48] R. Ruiz, J. Sanz, B. Cervera, F. Lloret, M. Julve, C. Bois, J. Faus, M.C. Munoz, J. Chem. Soc. Dalton Trans. (1993) 1623.
[49] R. Ruiz, J. Sanz, F. Lloret, M. Julve, J. Faus, C. Bois, M.C. Munoz, J. Chem. Soc. Dalton Trans. (1993) 3035.
[50] F. Birkelbach, M. Winter, U. Flörke, H.-J. Haupt, C. Butzlaff, M. Lengen, E. Bill, A.X. Trautwein, K. Wieghardt, P. Chaudhuri, Inorg. Chem. 33 (1994) 3990.
[51] T.K. Paine, P. Chaudhuri, unpublished results.
[52] P. Chaudhuri, M. Winter, U. Flörke, H.-J. Haupt, Inorg. Chim. Acta 232 (1995) 125.
[53] P. Chaudhuri, T. Weyhermüller, unpublished results.
[54] J.M. Dominguez-Vera, E. Colacio, A. Escuer, M. Klinga, R. Kivekäs, A. Romerosa, Polyhedron 16 (1997) 281.
[55] F. Akagi, Y. Nakao, K. Matsumoto, S. Takamizawa, W. Mori, S. Suzuki, Chem. Lett. (1997) 181.
[56] T.Y. Sliva, A. Dobosz, L. Jerzykiewicz, A. Karaczyn, A.M. Moreeuw, J. Swiatek-Kozlowska, T. Glowiak, H. Kozlowski, J. Chem. Soc. Dalton Trans. (1998) 1863.
[57] R. Ruiz, F. Lloret, M. Julve, J. Faus, M.C. Munoz, X. Solans, Inorg. Chim. Acta 268 (1998) 263.
[58] S. Sakamoto, A. Yatani, K. Kimura, M. Fujii, Y. Nakao, S. Kashino, M. Kinoshita, W. Mori, Bull. Chem. Soc. Jpn. 74 (2001) 2375.

[59] J.W. Fraser, G.R. Hedwig, H.K.J. Powell, W.T. Robinson, Aust. J. Chem. 25 (1972) 747.
[60] Y. Agnus, R. Louis, R. Jesser, R. Weiss, Inorg. Nucl. Chem. Lett. 12 (1976) 455.
[61] (a) J. Faus, F. Lloret, M. Julve, J.M. Clemente-Juan, M. Munoz, X. Solans, M. Font-Bardía, Angew. Chem. 108 (1996) 1591;
(b) J. Faus, F. Lloret, M. Julve, J.M. Clemente-Juan, M. Munoz, X. Solans, M. Font-Bardía, Angew. Chem. Int. Ed. Engl. 35 (1996) 1485.
[62] V.V. Pavlishchuk, S.V. Kolotilov, A.W. Addison, M.J. Prushan, R.J. Butcher, L.K. Thompson, Inorg. Chem. 38 (1999) 1759.
[63] V.V. Pavlishchuk, S.V. Kolotilov, A.W. Addison, M.J. Prushan, D. Schollmeyer, L.K. Thompson, E.A. Goreshnik, Angew. Chem. Int. Ed. Engl. 40 (2001) 4734.
[64] J.M. McCusker, J.B. Vincent, E.A. Schmitt, M.L. Mino, K. Shin, D.K. Coggin, P.M. Hagen, J.C. Huffman, G. Christou, D.N. Hendrickson, J. Am. Chem. Soc. 113 (1991) 3012.
[65] J.B. Vincent, C. Christmas, H.R. Chang, Q. Li, P.D. Boyd, J.C. Huffman, D.N. Hendrickson, G. Christou, J. Am. Chem. Soc. 111 (1989) 2086.
[66] A. Bino, R. Chayat, E. Pedersen, A. Schneider, Inorg. Chem. 30 (1991) 856.
[67] S.L. Castro, Z. Sun, C.M. Grant, J.C. Bollinger, D.N. Hendrickson, G. Christou, J. Am. Chem. Soc. 120 (1988) 2365.
[68] P. Chaudhuri, M. Winter, P. Fleischhauer, W. Haase, U. Flörke, H.-J. Haupt, Inorg. Chim. Acta 212 (1993) 241.
[69] P. Chaudhuri, M. Winter, P. Fleischhauer, W. Haase, U. Flörke, H.-J. Haupt, J. Chem. Soc. Chem. Commun. (1993) 566.
[70] P. Chaudhuri, F. Birkelbach, M. Winter, V. Staemmler, P. Fleischhauer, W. Haase, U. Flörke, H.-J. Haupt, J. Chem. Soc. Dalton Trans. (1994) 2313.
[71] M. Orama, H. Saarinen, J. Korvenranta, Acta Chem. Scand. 43 (1989) 407.
[72] H. Saarinen, M. Orama, Acta Chem. Scand. 52 (1998) 1209.
[73] J. Lisowski, P. Starynowicz, A. Jezierski, Z. Siatecki, Polyhedron 15 (1996) 3589.
[74] (a) G. Psomas, C. Dendrinou-Samara, M. Alexiou, A. Tsohos, C.P. Raptopoulou, A. Terzis, D.P. Kessissoglou, Inorg. Chem. 37 (1998) 6556;
(b) G. Psomas, A.J. Stemmler, C. Dendrinou, J.J. Bodwin, M. Schneider, M. Alexiou, J.W. Kampf, D.P. Kessissoglou, V.L. Pecoraro, Inorg. Chem. 40 (2001) 1562 (and references therein).
[75] S. Pal, T. Melton, R. Mukherjee, A.R. Chakravarty, M. Tomas, L.R. Falvello, A. Chakravorty, Inorg. Chem. 24 (1985) 1250.
[76] S. Ross, Dissertation, Bochum, Germany, 1998.
[77] C.N. Verani, E. Bothe, D. Burdinski, T. Weyhermüller, U. Flörke, P. Chaudhuri, Eur. J. Inorg. Chem. (2001) 2161.
[78] J.M. Thorpe, R.L. Beddoes, D. Collison, C.D. Garner, M. Helliwell, J.M. Holmes, P.A. Tasker, Angew. Chem. Int. Ed. 38 (1999) 1119.
[79] P. Chaudhuri, E. Rentschler, F. Birkelbach, C. Krebs, E. Bill, T. Weyhermüller, U. Flörke, Eur. J. Inorg. Chem. (2003) 541.
[80] O. Kahn, Chem. Phys. Lett. 265 (1997) 109.
[81] D. Hendrickson, in: C.J. O'Connor (Ed.), Research Frontiers in Magnetochemistry, World Scientific, Singapore, 1993, p. 87.
[82] E. Bill, C. Krebs, M. Winter, M. Gerdan, A.X. Trautwein, U. Flörke, H.-J. Haupt, P. Chaudhuri, Chem. Eur. J. 3 (1997) 193.
[83] P. Chaudhuri, M. Hess, T. Weyhermüller, E. Bill, H.-J. Haupt, U. Flörke, Inorg. Chem. Commun. 1 (1998) 39.
[84] P. Chaudhuri, U. Flörke, unpublished results.
[85] S.L. Castro, W.E. Streib, J.S. Sun, G. Christou, Inorg. Chem. 35 (1996) 4462.
[86] B.J. Allin, P. Thornton, Inorg. Nucl. Chem. Lett. 9 (1973) 443.
[87] S.L. Castro, Z. Sun, C.M. Grant, J.C. Bollinger, D.N. Hendrickson, G. Christou, J. Am. Chem. Soc. 120 (1998) 2365.
[88] F. Corazza, E. Solari, C. Floriani, A. Chiesi-Villa, C. Guastini, J. Chem. Soc. Chem. Commun. (1986) 1562.
[89] C. Krebs, Dissertation, Bochum, Germany, 1997.
[90] V. Pavlishchuk, F. Birkelbach, T. Weyhermüller, K. Wieghardt, P. Chaudhuri, Inorg. Chem. 41 (2002) 4405.
[91] U. Flörke, M. Winter, S. Ross, P. Chaudhuri, unpublished results.
[92] P. Basu, S. Pal, A. Chakravorty, Inorg. Chem. 27 (1988) 1848.
[93] S. Chattopadhyay, P. Basu, S. Pal, A. Chakravorty, J. Chem. Soc. Dalton Trans. (1990) 3829.
[94] F. Birkelbach, U. Flörke, H.-J. Haupt, C. Butzlaff, A.X. Trautwein, K. Wieghardt, P. Chaudhuri, Inorg. Chem. 37 (1998) 2000.
[95] M.W. Wemple, D.K. Coggin, J.B. Vincent, J.K. McCusker, W.E. Streib, J.C. Huffman, D.N. Hendrickson, G. Christou, J. Chem. Soc. Dalton Trans. (1998) 719.
[96] E. Rentschler, T. Weyhermüller, U. Flörke, P. Chaudhuri, unpublished results.
[97] P. Chaudhuri, M. Hess, E. Rentschler, T. Weyhermüller, U. Flörke, New J. Chem. (1998) 553.
[98] D. Burdinski, F. Birkelbach, M. Gerdan, A.X. Trautwein, K. Wieghardt, P. Chaudhuri, J. Chem. Soc. Chem. Commun. (1995) 963.
[99] D. Gatteschi, L. Pardi, Gazz. Chim. Ital. 123 (1993) 231.
[100] Ö. Bekaroglu, S. Sarisaban, A.R. Korray, M.L. Ziegler, Z. Naturforsch. Teil B 32 (1977) 387.
[101] T. Hirotsu, N. Takagi, J. Sakakibara, S. Kato, M. Seno, J. Chem. Soc. Chem. Commun. (1990) 1631.
[102] F. Kubel, J. Strähle, Z. Naturforsch. Teil B 36 (1981) 441.
[103] I. Vasilevsky, R.E. Stenkamp, E.C. Lingafelter, N.J. Rose, J. Coord. Chem. 19 (1988) 171.
[104] E. Colacio, J.M. Dominguez-Vera, A. Escuer, R. Kivekas, A. Romerosa, Inorg. Chem. 33 (1994) 3914.
[105] Z.J. Zhong, H. Okawa, N. Matsumoto, H. Sakiyama, S. Kida, J. Chem. Soc. Dalton Trans. (1991) 497.
[106] J.-P. Costes, F. Dahan, A. Dupuis, J.-P. Laurent, J. Chem. Soc. Dalton Trans. (1998) 1307.
[107] R. Ruiz, F. Lloret, M. Julve, J. Faus, M.C. Munoz, X. Solans, Inorg. Chim. Acta 213 (1993) 261.
[108] B. Cervera, R. Ruiz, F. Lloret, M. Julve, J. Faus, M.C. Munoz, Y. Journaux, Inorg. Chim. Acta 288 (1999) 57.
[109] J. Cano, A. Rodrígúez-Foreta, P. Alemany, S. Alvarez, E. Ruiz, Chem. Eur. J. 6 (2000) 327.
[110] R. Ruiz, M. Julve, J. Faus, F. Lloret, M.C. Munoz, Y. Journaux, C. Bois, Inorg. Chem. 36 (1997) 3434.
[111] D. Burdinski, E. Bill, F. Birkelbach, K. Wieghardt, P. Chaudhuri, Inorg. Chem. 40 (2001) 1160.
[112] P. Chaudhuri, M. Winter, F. Birkelbach, P. Fleischhauer, W. Haase, U. Flörke, H.-J. Haupt, Inorg. Chem. 30 (1991) 4291.
[113] F. Birkelbach, T. Weyhermüller, M. Lengen, M. Gerdan, A.X. Trautwein, K. Wieghardt, P. Chaudhuri, J. Chem. Soc. Dalton Trans. (1997) 4529.
[114] M. Lengen, Dissertation, Lübeck, Germany, 1994.
[115] P. Chaudhuri, M. Lengen, E. Bill, A.X. Trautwein, U. Flörke, unpublished results.
[116] E. Bill, C. Butzlaff, A.X. Trautwein, H. Winkler, M. Winter, P. Chaudhuri, Hyperfine Interactions 68 (1991) 229.
[117] Y. Pei, Y. Journaux, O. Kahn, Inorg. Chem. 27 (1988) 399.
[118] M. Lengen, E. Bill, C. Butzlaff, A.X. Trautwein, M. Winter, P. Chaudhuri, Hyperfine Interactions 94 (1994) 1849.
[119] P. Chaudhuri, M. Winter, B.P.C. Della Védova, P. Fleischhauer, W. Haase, U. Flörke, H.-J. Haupt, Inorg. Chem. 30 (1991) 4777.
[120] C.N. Verani, E. Rentschler, T. Weyhermüller, E. Bill, P. Chaudhuri, J. Chem. Soc. Dalton Trans. (2000) 251.
[121] J. Ribas, C. Diaz, R. Costa, J. Tercero, X. Solans, M. Font-Bardia, H. Stoeckli-Evans, Inorg. Chem. 37 (1998) 233.
[122] P. Chaudhuri, Habilitationsschrift, Paderborn, 1995.
[123] N. Fukita, M. Ohba, T. Shiga, H. Okawa, Y. Ajiro, J. Chem. Soc. Dalton Trans. (2001) 64.

[124] J.-P. Costes, F. Dahan, A. Dupuis, J.-P. Laurent, Inorg. Chem. 39 (2000) 169.
[125] J.P. Costes, F. Dahan, A. Dupuis, Inorg. Chem. 39 (2000) 5994.
[126] F. Lloret, R. Ruiz, M. Julve, J. Faus, Y. Journaux, I. Castro, M. Verdaguer, Chem. Mater. 4 (1992) 1150.
[127] F. Lloret, R. Ruiz, B. Cervera, I. Castro, M. Julve, J. Faus, J.A. Real, F. Sapina, Y. Journaux, J.C. Colin, M. Verdaguer, J. Chem. Soc. Chem. Commun. (1994) 2615.
[128] C.N. Verani, S. Gallert, E. Bill, T. Weyhermüller, K. Wieghardt, P. Chaudhuri, Chem. Commun. (1999) 1747.
[129] P. Chaudhuri, C.N. Verani, E. Bill, E. Bothe, T. Weyhermüller, K. Wieghardt, J. Am. Chem. Soc. 123 (2001) 2213.
[130] (a) P.F. Ross, R.K. Murmann, E.O. Schlemper, Acta Crystallogr. Sect. B 30 (1974) 1120;
(b) J.E. Young, R.K. Murmann, J. Phys. Chem. 67 (1963) 2647.
[131] F. Lloret, Y. Journaux, M. Julve, Inorg. Chem. 29 (1990) 3967.
[132] S.G. Sreerama, S. Pal, Inorg. Chem. 41 (2002) 4843.